ISSN 0736-5306

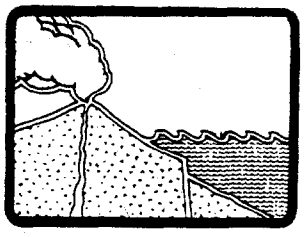

SCIENCE OF TSUNAMI HAZARDS

The International Journal of The Tsunami Society

Volume 9 Number 1 1991

SPECIAL ISSUE

EUROPEAN GEOPHYSICAL SOCIETY 1990 TSUNAMI MEETING 3

TSUNAMI POTENTIAL IN SOUTHERN ITALY 5
Stefano Tinti

NUMERICAL SIMULATION OF SLIDE GENERATED WATER WAVES 15
Carl Harbitz

MODELING OF TSUNAMI GENERATION AND RUN-UP 23
H. I. Bundgaard, I. R. Warren, A. Barnett

A PRELIMINARY EVALUATION OF THE TSUNAMI HAZARDS IN THE MOROCCAN COASTS 31
S. O. El Alami, S. Tinti

A PROPOSAL FOR A NEW CATALOG ON TSUNAMIS IN THE MEDITERRANEAN AREA 39
A. Maramai, C. Gasparini

COASTAL ALGERIAN EARTHQUAKES: A POTENTIAL RISK OF TSUNAMIS IN WESTERN MEDITERRANEAN? 47
A. Yelles Chaouche

THEORETICAL AND EXPERIMENTAL TSUNAMIGENIC MODELS TO STUDY INLAND ACTIVE GEOSTRUCTURES 55
G. Finzi-Contini

NUMERICAL MODEL ON TSUNAMI PROPAGATION 63
Th. V. Karambas, Y. Krestenitis, C. Koutitas

THE IDENTIFICATION OF TSUNAMI DEPOSITS IN COASTAL SEDIMENT SEQUENCES 73
A. G. Dawson, I. D. Foster, S. Shi, D. E. Smith, D. Long

TSUNAMI HAZARD ON THE SPANISH COASTS OF THE IBERIAN PENISULA 83
Maria Lourdes Campos

CUMULATIVE INDEX 91

copyright © 1991
THE TSUNAMI SOCIETY

OBJECTIVE: The Tsunami Society publishes this journal to increase and disseminate knowledge about tsunamis and their hazards.

DISCLAIMER: The Tsunami Society publishes this journal to disseminate information relating to tsunamis. Although these articles have been technically reviewed by peers, The Tsunami Society is not responsible for the veracity of any statement, opinion, or consequences.

EDITORIAL STAFF

T. S. Murty-Technical Editor
Institute of Ocean Sciences
Department of Fisheries and Oceans
Sidney, B.C., Canada

Charles L. Mader - Production Editor
Joint Institute for Marine and Atmospheric Research
University of Hawaii
Honolulu, HI, U.S.A.

George Pararas-Carayannis - Circulation
International Tsunami Information Center
Honolulu, HI, U.S.A.

George D. Curtis - Publisher
Joint Institute for Marine and Atmospheric Research
University of Hawaii
Honolulu, HI, U.S.A.

Submit manuscripts of articles, notes, or letters to:

T. S. Murty Technical Editor
Institute of Ocean Sciences
Department of Fisheries and Oceans
Sidney, B.C., Canada V8L 4B2

If article is accepted for publication the author(s) must submit a camera ready manuscript. A voluntary $50.00 page charge will include 50 reprints.

SUBSCRIPTION INFORMATION: Price per copy $20.00 USA

ISSN 0736-5306

Published by **The Tsunami Society** in Honolulu, Hawaii, U.S.A.

FOREWORD

The European Geophysical Society (EGS) tsunami meeting was held in Copenhagen, Denmark on 27th of April 1990 in the framework of the XV EGS General Assembly (23 - 27 April). It was structured as a workshop jointly organized by the Section I (Solid Earth and Planets) and Section II (Hydrospheres and Atmospheres) of the EGS upon specific request of the EGS Working Group (WG) on tsunamis. The symposium entitled "Tsunami sources around Europe" was convened by Professors C.G.Koutitas (Greece), V.S.Moreira (Portugal) and Dr. I.R.Warren (Denmark).

The importance of the meeting lies in the circumstance that it was the first scientific symposium promoted by the EGS WG on tsunamis since it was constituted in March 1988. Thus the response to this meeting could be taken as a measure of the impact and effect that the promotional activities carried out by the WG have had on the European geophysical community in order to raise attention and interest on the tsunami research. A poor response would have been prejudicial for future activities, whereas a good participation would have been a quite encouraging and promising signal for the development of future research. Considering this crucial point, the symposium was prepared with very special attention and it is a real satisfaction that it was fully successful as regards the number of participants, the variety of the subjects covered and the quality of the presentations. This may be appreciated in reading these proceedings that are published as a special issue of the Science of Tsunami Hazards journal.

The WG expresses full gratitude to Professor T.S.Murty, Technical Editor of the journal, and to the whole Editorial staff for offering the chance to publish the scientific contributions presented at the meeting in a unique issue of a journal that is fundamental for the tsunami research in the world.

Editors of the proceedings are Professor T.S. Murty and Professor S.Tinti. They wish to inform the readers that the papers included in the proceedings underwent a very rapid and expeditious revision process in order to speed up their publication. They remark therefore that neither the journal nor the proceeding editors take any responsability for the content of the papers, that fully pertains to the authors.

In agreement with the resolution of the EGS WG, promoting the organization of specific biannual meetings on tsunamis, the next meeting will take place in Edinburgh, United Kingdom, in 1992 in connection with the XVII EGS General Assembly (6-10 April).

Prof. Stefano Tinti
EGS Tsunami WG Coordinator

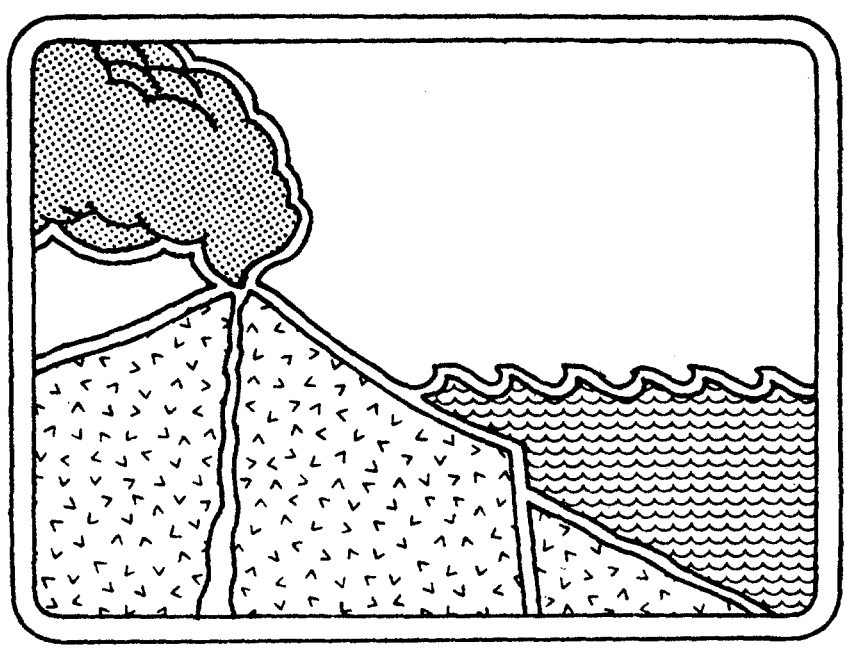

TSUNAMI POTENTIAL IN SOUTHERN ITALY

Stefano Tinti

Università di Bologna, Dipartimento di Fisica,
Settore di Geofisica, Viale Berti Pichat, 8
40127 Bologna, Italy.

ABSTRACT

Existing seismic and tsunami catalogs for Italy show that Italian coasts are the most exposed to tsunami attacks in Central Mediterranean. Tsunamis are mostly of seismic origin, though some events mainly associated with volcanic activity of Etna, of Vesuvius and of Aeolian Islands are reported. Though important, tsunamis are relatively rare events in Italy and therefore statistical methods applied to tsunami compilations alone cannot provide reliable evaluations, due to the small number of the available data. Seismic information, however, may be usefully utilized in order to supplement the tsunami data base. A recent analysis mostly based on studying the seismicity along the Italian coasts showed that the most active tsunamigenic sources are concentrated in Southern Italy, that is in Southern Adriatic (Gargano promontory) and in Southern Calabria and Eastern Sicily. A sophisticated statistical technique is here applied to perform the evaluation of the tsunami potential in both these regions, where the tsunami activity is particularly high and the most disastrous Italian tsunamis occurred. The areas most prone to generate large tsunamis have been identified on the basis of the characteristic features of the seismicity, inferred by means of statistical methods, as well as on the grounds of complementary seismotectonic studies mainly concerning the predominant tectonic style and the earthquake focal mechanism.

INTRODUCTION

Evaluation of tsunami potential is largely accepted to be a fundamental step for any relevant activities aiming at reducing the impact of future events. In spite of this wide recognition, however, a unique definition of tsunami potential cannot be found in the literature, which may originate some confusion and misunderstanding. So, in order to avoid possible misinterpretations, it may be convenient first of all to explain what is meant for tsunami potential in this paper. Here tsunami potential and hazard are taken as synonyms and are both indifferently used to indicate the probability that a tsunami be generated in a given area within a given interval of time. This specific use leads us to concentrate on the generation process. The physical aspects related to tsunami propagation and impact on the coasts are not taken into account here. Their incorporation in the analysis parallelled by the inclusion of studies on the vulnerability of the structures built on the coasts will be a subsequent development of the present research guiding us from tsunami potential to tsunami risk evaluations.

Direct examination of tsunami catalogs is a powerful means to establish tsunami potential in those countries where tsunami rate is relevant and events have been observed and recorded for a period of time sufficiently long, say several decades or centuries. In the Mediterranean, a long tradition of natural and physical sciences enables one to go back more than 2000 years to the ancient times of greek and roman civilitation and even further; but tsunamis are relatively unfrequent and so tsunami catalogs count only a few hundreds of events for the whole Mediterranean basin. Though a quite encouraging revival of interest of the European research on tsunamis involved recently also catalog assembling (see Soloviev, 1990 and Antonopoulos, 1990), nonetheless the total number of tsunamis is not likely to change very much by virtue of the revisions presently underway. Scarcity of data is therefore a problem to face and it is even more pronounced when the attention is restricted to particular areas such as the Western or the Central Mediterranean or to particular subregions such as Southern Italy. In these cases, tsunami compilations cannot provide a data set large enough to allow stable and reliable statistical analyses. One possible way is to extend the analysis to earthquake catalogs, since delineating the features of the seismicity in marine and coastal areas helps to perform evaluations on tsunamigenic earthquake occurrences. A statistical procedure to analyze seismic catalogs with the peculiar purpose of assessing the probability rate of tsunamigenic earthquakes was specifically devised by the author and was applied to evaluate tsunami potential in the sea surrounding Italy (Tinti, 1990). The same method has been successfully applied to the Moroccan coasts, where the number of the known tsunamis is so small that any other method of analysis is practically unproposable (El Alami and Tinti, 1990). The systematic study quoted above on tsunami potential in Italy demonstrated that Southern Italy is the part of the Central Mediterranean with the highest concentration of tsunami activity and with the highest expected number of tsunamis and provided the basic motivation for the present study. A more refined analysis of tsunami potential is applied to two regions, namely Southern Adriatic and Calabria–Eastern Sicily, that were attacked by most of the disastrous tsunamis occurred in Italy.

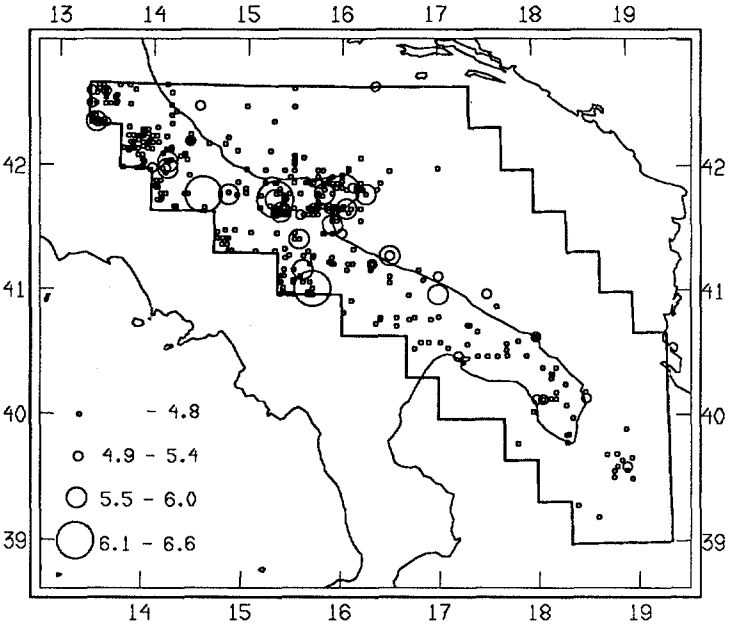

Figure 1. Map of the epicenters for the Southern Adriatic region based on the Italian catalog of earthquakes from the ancient times up to the end of 1982. Events are classed according to the magnitude. Magnitudes are local instrumental magnitudes for recent events or suitably computed macroseismic magnitudes for historical earthquakes (see Tinti et al., 1987).

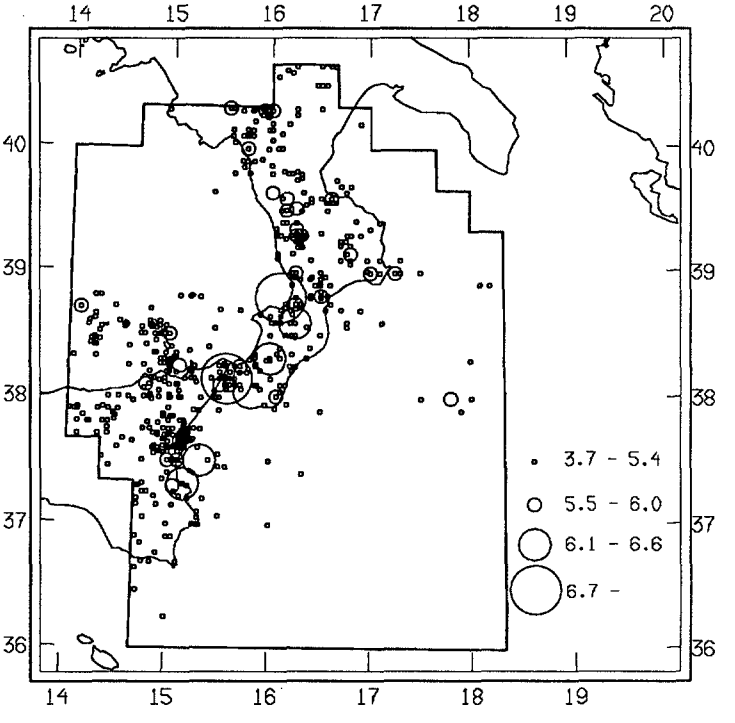

Figure 2. Map of the epicenters for the region including Calabria and Eastern Sicily. The region border is the thick solid line superimposed to the geographical contours. For further details refer to the above Figure 1.

SHORT DESCRIPTION OF THE PROCEDURE

The statistical procedure employed in the present study is fully described elsewhere (Tinti,1990). Here only the salient points will be very briefly outlined to favour the understanding of the reader. The tsunami catalog used is that assembled by Caputo and Faita (1984), updated a few years later by Bedosti and Caputo (1986). Results of recent revisions of the largest tsunamis occurred in the examined areas have been also taken into account (Guidoboni and Tinti, 1988; Tinti and Guidoboni, 1988). The earthquake catalog used is the one known as PFG seismic catalog compiled in the framework of the Progetto Finalizzato Geodinamica promoted by the Italian National Council of Research. The catalog includes the Italian earthquakes from ancient times until the end of 1982. The regions considered are shown in Figures 1 and 2. Regional boundaries are determined by the fact that for the subsequent analysis both areas are conveniently partitioned into regular equal $20' \times 20'$ cells.

The analysis of seismicity consists in a sequence of steps that may be summarized as follows. Firstly, catalog completeness is examined: the analysis is areally global, since it regards the whole region (either Southern Adriatic or Calabria and Eastern Sicily), but it is performed distinctly for each magnitude class. The classes used in this study are 2.4–3.0,...,6.0–6.6 with the addition of the class of earthquakes with magnitude exceeding 6.6. The main result of the first step is that for each magnitude class the apparent seismicity rate is evaluated as a function of time and may be compared with the true seismicity rate of the class. In the second step this allows one to estimate seismicity maps where the normalized frequency of the earthquakes is evaluated cell by cell for each magnitude class and is corrected from the incompleteness distortions. The third step consists in applying the Gutenberg–Richter magnitude–frequency law in each cell. The computation of the coefficients a and b allows one to evaluate the expected number of earthquakes occurring in each cell in any given range of magnitude. This capability may be used for many applications. In case of tsunami potential evaluation one is generally concerned with the mean number of tsunamis (or large tsunamis) generated in one place or equivalently with their return period. All these quantities can be determined, once the minimum magnitude that is assumed to originate tsunamis (or large tsunamis) is given in every cell. Of course, only events of seismic origin can be accounted for in this way, which leads to an underestimation of tsunami potential in regions where other tsunamigenic sources, especially volcanoes, are active. This problem does not affect evaluations for Southern Adriatic, but does concern Calabria and Eastern Sicily.

SOUTHERN ADRIATIC

Southern Adriatic neotectonic setting has been object of several investigations, but it is still not perfectly understood. The long controversial point regarding the question whether Adriatic is a promontory of the African continent or a detached microplate is still unsolved even though the latter hypothesis is gaining more and more support by the recent studies (Morelli, 1984; Anderson and Jackson, 1987b; Mantovani et al., 1990). From a geological point of view, the region shown in Figure 1 is the Gargano-Apulia

foreland of the southern part of the Adriatic platform that has a typical continental 30 km thick crust (see Nicolich, 1981 and 1987), while the western border is formed by the sedimentary structures of the Bradanic foretrough. The foreland–forethrough system has its natural westward continuation in the southern section of the Apennine front and main belt, that at this latitude runs almost along the central axis of the peninsula, at equal distance from the Adriatic and Tyrrhenian seas (see Ciaranfi et al., 1983). Southern Puglia is relatively stable from a seismic point of view. The largest earthquakes in this region occurred either along its western border in the margin of the Apennine chain or in the Gargano promontory. This latter area is of special interest since it is geologically a part of the foreland, but possesses distinctive features: it seems a horst system, characterized by large positive gravimetric and magnetic anomalies supporting the view that the crust is about 5-10 km thinner than in the surrounding platform (see Berti et al., 1988). Quaternary uplifting involves the whole region and may be interpreted as a result of the flexure of the Adriatic microplate in response to the compression exerted by the colliding African continent (Royden, 1988, Albarello et al., 1990). In Gargano a tensional regime of stresses is the predominant feature (Cristofolini et al., 1985; Gasparini et al., 1985) with active surface and deep normal faults that are located inshore and offshore and are mainly paralleling the coast in the northern part of the promontory (Ciaranfi et al., 1983; Patacca and Scandone, 1987). Southern Gargano is crossed by a long right–lateral strike-slip fault, known as the Carbonara fault, chiefly running West–East that was identified even on the basis of instrumental microseismicity. Tsunamis in the area are exclusively due to seismic sources, which makes our method fully applicable here. The major events invested the northern Gargano coasts. The most important tsunami in the region occurred in 1627 and was recently reviewed on the basis of all available historical coeaval sources (Guidoboni and Tinti, 1988). One relevant observation of that study was that the 1627 tsunami affected a coastline strip that was completely inhabitaded in those days, but that is rather densely populated today and is site of many touristic facilities, which would increase the consequences of the wave impact on the coast.

Following the method outlined in the previous section, first the seismic potential has been evaluated in the cells of the grid shown in Figure 1 and then the tsunami potential has been subsequently calculated. The smallest magnitude capable of producing a tsunami, say the threshold magnitude M_t, has been assumed to vary from cell to cell in accordance with the principle that the efficiency of the tsunami generation process is larger for earthquakes with epicenter in the sea and progressively diminishes landward (see Tinti, 1990): for fully marine cells a value of $M_t = 6.0$ has been taken to be reasonably suitable, while larger threshold values up to $M_t = 7.5$ have been chosen for cells on land. Figure 3 shows the mean number of tsunamis expected to be produced in each cell. According to the selected set of M_t, the shown tsunami potential globally includes tsunamis of any size, that is small as well as large events. It is quite evident that the area with the highest tsunami potential in the entire region is that that embraces the Gargano promontory. However, owing to the modest seismic activity elsewhere and especially in the rather stable southern foreland (the Murgie and Salentino areas), the global tsunami potential for the whole region is quite modest. Figure 4 shows the probability that at least one tsunami be generated in the region

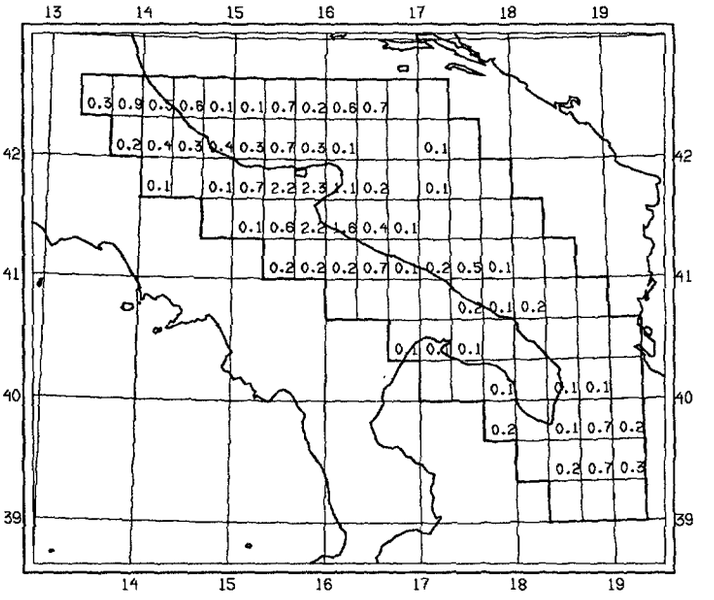

Figure 3. Tsunami potential for the Southern Adriatic region expressed in terms of the expected mean number of tsunamis generated in each cell over 1000 yr. White cells are practically nontsunamigenic. Tsunami potential is generally modest in the area. A well pronounced high of the expected activity may be found in the Gargano promontory.

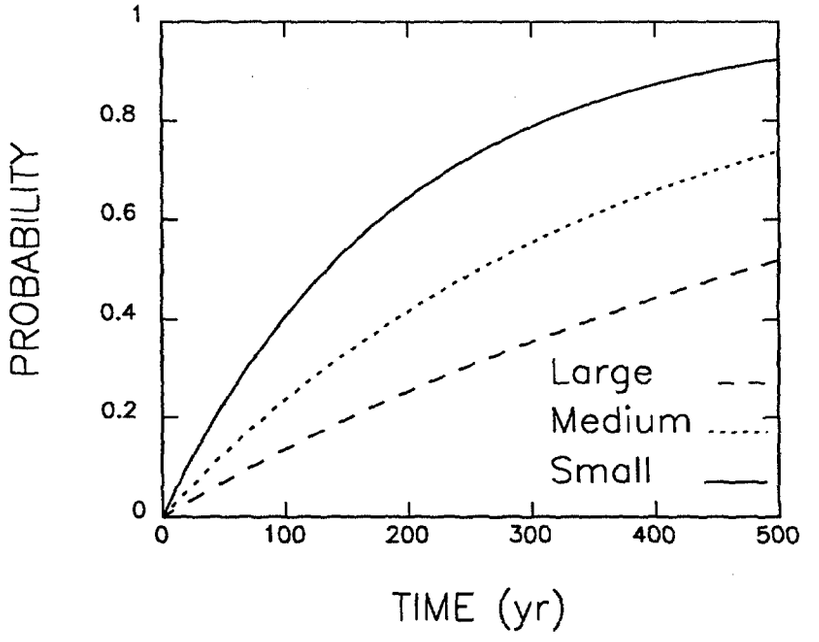

Figure 4. Probability of generation of at least one tsunami in Southern Adriatic within a time period starting from the present vs. the period length. The three curves refer to different sets of threshold magnitudes and distinctly display cumulative probabilities for large events, for intermediate–size events as well as for events of any size.

within a next time period as a function of the period duration. The computations are carried out on the basis of the Poisson statistics, the fundamental assumption being that the tsunami occurrence in each cell is a stationary stochastic point process (see Cox and Lewis, 1966) uncorrelated with the analogous processes going on in the neighboring cells. Three probability curves referring to different sets of threshold magnitudes M_t are displayed. The magnitudes M_t have been taken in such a way that the curves represent the generation probability for tsunamis of different sizes: namely i) large events, ii) medium or large events, and iii) events of any size, including very small tsunamis. We see that all evaluated probabilities for time period as long as 200 yr are modest and that even for a 300 yr period the probability for a large event occurrence does not exceed 40%. We remark, however, that probability estimates for stationary point processes are totally independent from the past history of the process and in particular from the time of the last tsunami occurrence: these processes are also said to have no memory of the past. Performing calculations by assuming stochastic processes with memory may lead to larger probabilities, especially in consideration of the fact that the last large tsunami occurred in 1627, that is a long time ago.

CALABRIA AND EASTERN SICILY

This region is one of the most studied in Central Mediterranean, since it is a common view that the correct interpretation of its neotectonic evolution is crucial for the understanding of the dynamical processes in the whole Mediterranean basin. Geophysical and geological investigations concerning this area are very numerous and to focus the attention only on the most recent contributions, we may recall seismic prospecting interpretations (Finetti and Del Ben, 1986), focal mechanism computations (Gasparini et al., 1985; Anderson and Jackson, 1987a), Moho depth mapping (Geiss, 1987), geostructural and neotectonic studies (Ghisetti and Vezzani, 1982; Ciaranfi, 1983), evolutionary models describing processes since the late miocene to the present (Malinverno and Ryan, 1986; Lavecchia, 1988; Mantovani et al., 1990). Figure 2 shows the epicenter distribution of shallow–focus medium to large earthquakes occurred in the region. Normal faulting is the predominant feature especially along the Calabrian section of the Apennines chain and in the Messina Straits, while reverse faults, thrusts and folds may be found in south-eastern Sicily, tectonically belonging to the African platform. Evidence of considerable uplifting has been found in Calabria and one possible, though still disputed interpretation is that it is the effect of a tensional regime of stresses associated with the plate flexure resulting from the collision of Africa against Europe (Mantovani et al., 1990). A remarkable cluster of seismic events of volcanic origin may be observed in the Etnean area. The major earthquakes in the region occurred in 1905 and in 1908 with epicenters in the Gulf of S.Eufemia and in the Messina Straits respectively. Estimates performed on the instrumental traces recorded in European observatories give magnitude values around 7.0 for both events. Other largely destructive earthquakes (with epicentral intensity XI in MCS scale according to the Italian seismic catalog) occurred in 1169, 1693 as well as on 5 and 7 Feb 1783. All these earthquakes set in motion at least sizable tsunamis, some of which were the object

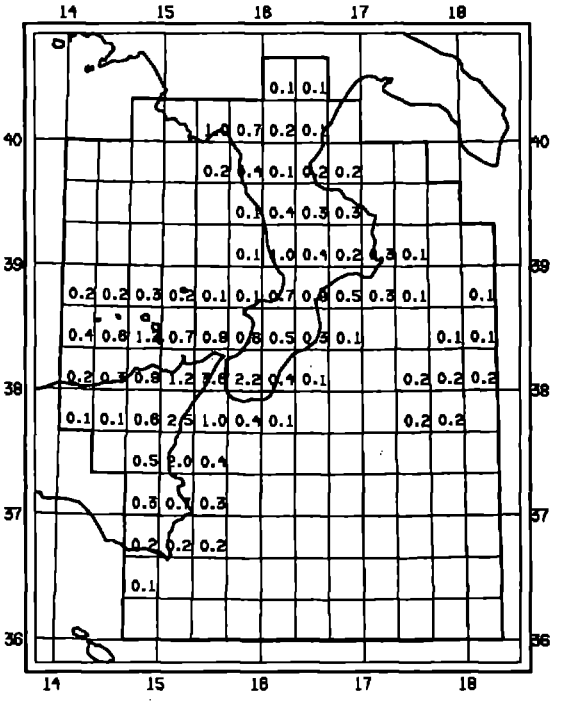

Figure 5. Tsunami potential for large tsunamis in the Calabria–Eastern Sicily region expressed in terms of the expected mean number of tsunamis generated in each cell over 1000 yr. The major expected activity is clustered in cells covering the Messina Straits and the northern part of the Eastern Sicily coasts.

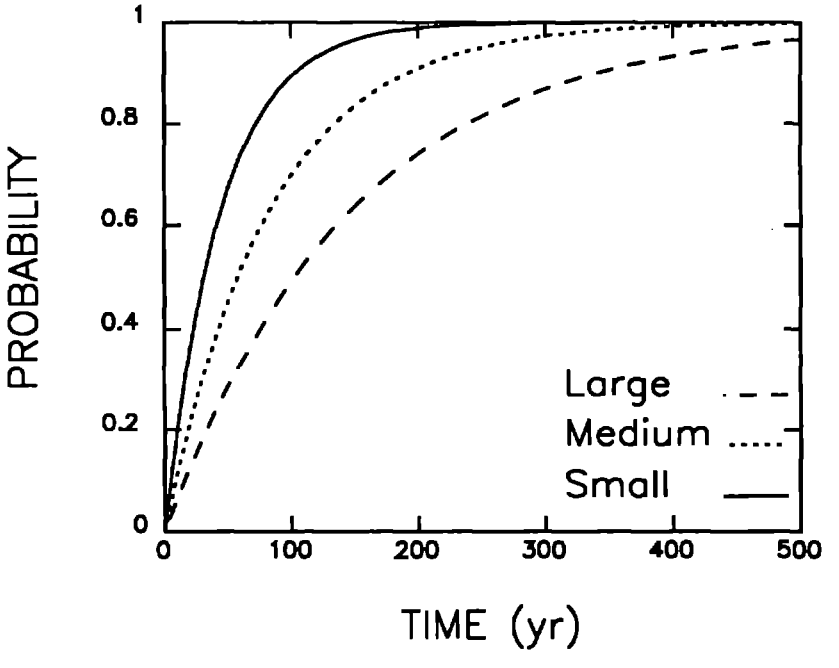

Figure 6. Probability of generation of at least one tsunami in Calabria–Eastern Sicily within a time period starting from the present vs. the period length. Calculations for large, medium–size and small events are displayed separately.

of recent careful reexaminations (see Tinti and Giuliani, 1983; Tinti and Guidoboni, 1988).

Figure 5 displays the tsunami potential distribution for large tsunamis. The minimum magnitude to produce such events is assumed to be $M_t = 6.6$ for marine cells and somewhat higher for cells on land. The Messina Straits is the area where the evaluated potential is abundantly higher than in any other places. But it is important to stress that the entire strip covering the north–eastern Sicily from Messina to Siracusa exhibits a remarkable potential for tsunami generation, which is a confirmation of our previous investigations (Tinti, 1990). Probability curves are plotted in Figure 6. As for the Southern Adriatic region, the probability of at least one tsunami generation is given vs time for tsunamis of various sizes. Computations are likewisely based on the stationary point process assumption. As may be seen, probability curves grow rather steeply in the range of short time periods, tending thereafter to a slowly sloping plateau. According to the curves, within a time interval of 200 yr the local production of a small tsunami is almost 100% certain, the generation of a medium–size event is about 90% probable, whereas the probability of originating a large event exceeds 70%. We observe that the stationary point process hypothesis is known to often lead to underevaluation of occurrence probabilites because the implied stochastic model cannot take into account the time elapsed since the last occurrence to the present. More elaborated assumptions are therefore expected to give rise to different, very likely higher probability curves. The tsunami potential of this region is by far larger than that estimated in Southern Adriatic and is the highest found in the whole Italian Seas. This consideration justifies to continue and intensify the investigations in order to refine the statistical evaluations so far performed. One possible improvement of the method adopted here could be its extension to include tsunami generated by sources other than earthquakes in the tsunami potential calculations. It is however worthwhile pointing out that the present evaluations do not exclude totally tsunami generation associated with volcanic activity. In fact volcanic eruptions are frequently accompanied by an increased level of seismicity that according to the present method corresponds to an increased capability of producing tsunamis. This consideration explains the local maxima in the computed tsunami potential that may be observed in the Aeolian Island and on Etna volcano (see Figure 5). Therefore the desirable generalization of our method is expected to lead to slight corrections of the tsunami potential estimates, probably only in the order of a few percent, even in the Calabria–Eastern Sicily region where volcanic activity is more substantial than in other Italian provinces.

REFERENCES

ALBARELLO D., MUCCIARELLI M. and MANTOVANI E., 1990. Adriatic flexure and seismotectonics in southern Italy, Tectonophysics, 179, 103–111.

ANDERSON H. and JACKSON J., 1987a. The deep seismicity of the Tyrrhenian Sea, Geophys. J.R.Astr. Soc., 91, 613–637.

ANDERSON H. and JACKSON J., 1987b. Active tectonics of the Adriatic Region, Geophys. J.R.Astr. Soc., 91, 937–983.

ANTONOPOULOS J., Data for investigating tsunami activity in the Mediterranean Sea, Science of Tsunami Hazards, 8, 39–52.

BEDOSTI B. and CAPUTO M., 1986. Primo aggiornamento del catalogo dei maremoti delle coste italiane (in Italian), Atti Accademia Nazionale dei Lincei, Rendiconti, Classe Scienze Fisiche, Matematiche, Naturali, Serie VIII, Vol. LXXX, 570–584.

BERTI G., DELLA VEDOVA B., MARSON I., PELLIS G. and PINNA E., 1988. Evidenze della crosta inferiore nell'area Adriatica da dati geofisici (in Italian), Atti del VII Convegno G.N.G.T.S., CNR, Roma, 1990, 1199–1213.

CAPUTO M. and FAITA G., 1984. Primo catalogo dei maremoti delle coste italiane (in Italian), Atti Accademia Nazionale dei Lincei, Memorie, Classe Scienze Fisiche, Matematiche, Naturali, Serie VIII, Vol. XVII, 213–356.

CRISTOFOLINI R., GHISETTI F., SCARPA R. and VEZZANI L., 1985. Character of the stress field in the Calabrian Arc and Southern Apennines (Italy) as deduced by geological and volcanological information, Tectonophysics, 117, 39–58.

CIARANFI N., GHISETTI F., GUIDA M., IACCARINO G., LAMBIASE S., PIERI P., RAPISARDI L., RICCHETTI G., TORRE M., TORTORICI L. and VEZZANI L., 1983. Carta neotettonica dell'Italia Meridionale (in Italian), Pubbl. 515 del P.F. Geodinamica, Bari, pp. 62.

COX D.R. and LEWIS P.A.W., 1966. The statistical analysis of series of events, Chapman and Hall, London, pp.285.

EL ALAMI S.O. and TINTI S., 1990. A preliminary evaluation of the tsunami hazards in the Moroccan coasts, Science of Tsunami Hazards, this issue.

FINETTI I. and DEL BEN A., 1986. Geophysical study of the Tyrrhenian Opening, Boll. Geofis. Teor. Appl., 28, 75–155.

GASPARINI C., IANNACCONE G. and SCARPA R., 1985. Fault-plane solutions and seismicity of the Italian peninsula, Tectonophysics, 117, 59–78.

GEISS E., 1987. A new compilation of crustal thickness data for the Mediterranean area, Ann. Geophys., 5B, 623–630.

GHISETTI F. and VEZZANI L., 1982. The recent deformation mechanism of the Calabrian Arc, in MANTOVANI E. and SARTORI R. (Eds), Structure, Evolution and Present Dynamics of the Calabrian Arc, Earth Evol. Sci., 3, 197–206.

GUIDOBONI E. and TINTI S., 1988. A review of the historical 1627 tsunami in the Southern Adriatic, Science of Tsunami Hazards, 6, 11-16.

LAVECCHIA G., 1988. The Tyrrhenian–Apennines system: structural setting and tectonogenesis, Tectonophysics, 147, 263–296.

MALINVERNO A. and RYAN W.B.F., 1986. Extension in the Tyrrhenian sea and shortening in the Apennines as result of arc migration driven by sinking of the lithosphere, Tectonics, 5, 227–245.

MANTOVANI E., BABBUCCI D., ALBARELLO D. and MUCCIARELLI M., 1990. Deformation pattern in the central Mediterranean and behavior of the African/Adriatic promontory, Tectonophysics, 179, 63–79.

MORELLI C., 1984. Promontorio Africano o microplacca Adriatica (in Italian), Boll. Ocean. Teor. Appl., 2, 151–168.

NICOLICH R., 1981. Crustal structures in the Italian peninsula and surrounding seas: a review of DDS data, in WEZEL F.C. (Ed.), Sedimentary Basins of Mediterranean Margins, Tecnoprint, Bologna, 3–17.

NICOLICH R., 1987. Crustal structures from seismic studies in the frame of the European Geotraverse (southern segment) and crop projects, in BORIANI A., BONAFEDE M., PICCARDO G.B. and VAI G.B. (Eds), The Lithosphere in Italy, Advances in Earth Science Research, Accademia Nazionale dei Lincei, Roma, 41–61.

PATACCA E. and SCANDONE P., 1987. Post-Tortonian mountain building in the Apennines. The role of the passive sinking of a relic lithospheric slab, in BORIANI A., BONAFEDE M., PICCARDO G.B. and VAI G.B. (Eds), The Lithosphere in Italy, Advances in Earth Science Research, Accademia Nazionale dei Lincei, Roma, 157–176.

ROYDEN L., 1988. Flexural Behavior of the Continental Lithosphere in Italy: Constraints imposed by Gravity and Deflection Data, J. Geophys. Res., 93, 7747–7766.

SOLOVIEV S.L., 1990. Tsunamigenic zones in the Mediterranean Sea, Natural Hazards, 3, 183–202.

TINTI S., 1990. Assessment of tsunami hazard in the Italian Seas, Natural Hazards, (in press).

TINTI S. and GIULIANI D., 1983. The Messina Straits tsunami of the 28th of December 1908: a critical review of experimental data and observations, Il Nuovo Cimento, 6C, 424–442.

TINTI S., VITTORI T. and MULARGIA F., 1987. On the macroseismic magnitudes of the largest Italian earthquakes, Tectonophysics, 138, 159–178.

TINTI S. and GUIDOBONI E., 1988. Revision of the tsunamis occurred in 1783 in Calabria and Sicily (Italy), Science of Tsunami Hazards, 6, 17–22.

NUMERICAL SIMULATION OF SLIDE GENERATED WATER WAVES

CARL HARBITZ

Department of Mathematics, University of Oslo,
P.O. Box 1053, Blindern, 0316 Oslo 3, Norway.

ABSTRACT

A mathematical model based on the hydrodynamic shallow water equations is developed for numerical simulation of slide generated waves in fjords. The equations are solved numerically by a finite difference technique. Special algorithms are developed to handle the effect of depth changes due to the slide. To examine the performance of the numerical model we have simulated the slide catastrophe in Tafjord, western Norway, 1934. Results from this investigation is presented, with focus on modelling of wave reflection, wave energy trapping and wave run-up.

1 Introduction

There are several historic records of the occurrence of large destructive water waves associated with rock slides and avalanches into fjords and lakes. Wave formation and propagation due to slides is a complex phenomena which may be divided in three parts: Energy transfer from slide motion to water motion, wave propagation in open water and wave run-up along the shores. From a modelling point of view the second part may be the easiest part where the model equations can be deduced directly from the hydrodynamic equations. The physical processes taking part in the first part is much more complex and no common model equations are available which can describe the motion of different slide materials as rock, clay, mud, ice and snow and the energy transfer mechanism between the slide and the fluid. The run-up part has received relatively little attention in modelling slide generated waves but these problems were discussed by Pedersen and Gjevik [5, 6].

2 The linearized shallow water equations

Waves generated by slides can often be classified as long waves. In other words most of the energy that is transferred from the slide to water motion is distributed on waves with typical wave-length, ℓ, which is much larger than the characteristic water depth, h_0. From the assumption $h_0/\ell \ll 1$ it may be deduced that the pressure is approximately hydrostatic and that the vertical variations of the horizontal velocity are small. We will also assume that the characteristic amplitude of the waves, a, is much less than h_0. On basis of these assumptions we may derive the linearized shallow water equations (see [7, 8]).

The equations are formulated in a Cartesian coordinate system with horizontal axes, Ox and Oy in the undisturbed water level and the vertical axis, Oz, pointing upwards. The fluid is confined to $-h < z < \eta$ where h is the depth referred to the datum $z = 0$, η the water surface displacement and we denote the total water depth by $H = h + \eta$. Since the slide introduces bathymetric changes h will be a function of time (t). Mass conservation in a vertical fluid column leads to a continuity equation of the form:

$$\frac{\partial H}{\partial t} \equiv \frac{\partial \eta}{\partial t} + \frac{\partial h}{\partial t} = -\nabla \cdot \vec{Q} \tag{1}$$

where $\vec{Q}$ is the vertically integrated volume flux density and ∇ is the horizontal component of the gradient operator. In terms of the averaged horizontal velocity, $\vec{u} = u\vec{i} + v\vec{j}$, the volume flux density can be approximated by:

$$\vec{Q} = h\vec{u} \tag{2}$$

and by substitution in eq.(1)

$$\frac{\partial H}{\partial t} = -\nabla \cdot (h\vec{u}) \tag{3}$$

We note that while eq.(1) is an exact form of the continuity equation, the use of eq.(2) introduces relative errors of order a/h_0 in eq.(3). Provided the pressure is hydrostatic and the nonlinear terms and the bottom shear stress can be neglected the momentum equation becomes:

$$\frac{\partial \vec{u}}{\partial t} = -g\nabla\eta \tag{4}$$

where g is the acceleration of gravity and ρ is the density of the fluid. Eq.(4) inherits relative errors of order a/h_0 as well as order $(h_0/\ell)^2$.

3 Numerical solution of the linearized shallow water equations

The numerical approximation to a parameter f at a grid-point with coordinates $(\beta\Delta x, \gamma\Delta y, \kappa\Delta t)$ where Δx, Δy and Δt are the grid increments, is denoted by $f^{(\kappa)}_{\beta,\gamma}$. In order to make the difference equations more readable we introduce the symmetric difference operator, δ_x, and the midpoint average operator, $^{-x}$, by:

$$\delta_x f^{(\kappa)}_{\beta,\gamma} = \frac{1}{\Delta x}(f^{(\kappa)}_{\beta+\frac{1}{2},\gamma} - f^{(\kappa)}_{\beta-\frac{1}{2},\gamma}) \qquad (\overline{f}^{x})^{(\kappa)}_{\beta,\gamma} = \frac{1}{2}(f^{(\kappa)}_{\beta-\frac{1}{2},\gamma} + f^{(\kappa)}_{\beta+\frac{1}{2},\gamma}) \tag{5}$$

Difference and average operators with respect to the other coordinates y and t are defined correspondingly. We note that all combinations of these operators are commutative. To abbreviate the expressions further we also group terms of identical indices inside square brackets, leaving the super- and subscripts outside the bracket.

The equations (3) and (4) are discretized on a grid that is staggered both in time and space. The spatial distribution of the nodes is often referred to as the Arakawa C grid [4]. Velocities and surface elevations are evaluated at different values for t. The discrete quantities are denoted by:

$$\eta_{i,j}^{(n)} \ , \ u_{i+\frac{1}{2},j}^{(n+\frac{1}{2})} \ , \ v_{i,j+\frac{1}{2}}^{(n+\frac{1}{2})} \ , \ h_{i,j}^{(n)} \tag{6}$$

A finite difference version of (3) reads:

$$[\delta_t \eta = -\delta_t h - \delta_x(\overline{h}^x u) - \delta_y(\overline{h}^y v)]_{i,j}^{(n+\frac{1}{2})} \tag{7}$$

Equation (7) assures exact volume conservation.

Discretization of the components of the momentum equation (4) gives:

$$[\delta_t u = -g\delta_x \eta]_{i+\frac{1}{2},j}^{(n)} \qquad [\delta_t v = -g\delta_y \eta]_{i,j+\frac{1}{2}}^{(n)} \tag{8}$$

Equation (7) through (8) defines an explicit finite difference method of second order accuracy for which $\vec{u}$ and η are evaluated at subsequent half time steps.

A rigid impermeable wall is represented by a sequence of line segments parallel to the axes. Each segment passes through nodes for the corresponding normal velocity component which is set to zero. A slide penetrating the water surface at a shore gives a non-zero normal flux at the boundary. Additional complications will arise from the fact that the shore-line under such circumstances must be regarded as time dependent.

A grid cell is defined as the volume element circumvented by straight lines normal to the velocity directions in four velocity points around one point of surface elevation. When the motion of the slide causes the depth in a grid cell to become negative, the shore line is moved to the seaside of this cell. The last calculated fluid volume in the cell, defined by

$$V_{i,j}^{(n)} = \Delta x \Delta y(\eta + h)_{i,j}^{(n)} \tag{9}$$

is spread equally over cells which have boundaries in common with the one drained, and still have a positive depth. Thus the total fluid volume is kept constant.

The time increment Δt is adjusted from the velocity of the slide in such a way that the slide can not move further than one grid distance per time step.

4 The slide catastrophe in Tafjord, April 7th 1934

The slide catastrophe in Tafjord in 1934 has been chosen for a complete analysis of a real event, mainly because a relatively large number of measured run-up heights is available, fig.1.

Tafjorden is a branch of Storfjorden, western Norway. The depth is about $200 - 220$ m. Approximately 3 mill. m^3 of rock and scree fell into the sea at the position indicated in fig.1. According to the eye witnesses the slide produced at least three separated huge waves, with 3-4 minutes in between. The sea was very rough for more than half an hour, and did not become calm until 7-8 hours later. The measured run-up heights revealed large local variations. Forty people living in the villages Fjøra and Tafjord were killed and there were severe damages along the shore-line.

The values used for the parameters governing the volume, the shape and the movement of the slide are based mainly on the information given in [2, 3]. The wave pattern estimated by the model will develop as shown in fig.2-fig.4. The first figure shows the wave pattern just outside the slide area at $t = 10.0$ s. The maximum wave height is here 45.0 m. Fig.3 shows how the primary wave at $t = 30.0$ s impacts the opposite side of the fjord with a height of about 25 m, while fig.4 shows one wave with amplitude about 2 m approaching the bend in the fjord branch while another wave with amplitude about 4 m is approaching the innermost part of the branch at $t = 75.0$ s.

5 Reflection of wave energy in the fjord bend

The numerical results indicate that maximum wave height near the shore line in the eastern part of the fjord occured later than the time of arrival of the primary wave. Together with the persistence of the observed wave motion, this suggests that the energy was somehow trapped. Considering the geometry of the fjord, fig.1, it is reasonable to link the energy trapping to the bend near Fjøra. The reflection and

transmission in the bend is examined by estimating the energy contents at both sides at $t = 150.0\ s$. At this time the primary wave has passed the actual area.

The coefficient of reflection is defined as $R = (\frac{1}{2}E_0 - E_w)/\frac{1}{2}E_0$, where E_0 is the potential energy in the initial wave and E_w is the energy in the western part of the fjord. By choosing symmetric initial conditions, we may assume that approximately one half of the initial wave energy is propagating towards the bend. R represents the fraction of this energy that is left in the eastern part of the fjord, i.e. inside the bend, after reflection.

An initial surface displacement outside the slide area as shown in fig.5a gives $R = 33.4\%$, while the displacement shown in fig.5b gives $R = 84.0\%$. The more the extension of the initial wave is reduced, i.e. the closer we come to a slide generated wave, the higher is the value of R. This verifies that most of the energy in slide generated waves is reflected in the bend: $R = 98.6\%$. The high percentage of reflection explains the observations of at least three separated huge waves, and why there was rough sea for more than half an hour.

In view of the repeated reflections we may also expect the waves to interfere. In addition to varying run-up conditions along the shore line, this explains the large local variations observed.

6 Standing waves, time series analysis

The occurence of trains of huge waves may also be explained as standing waves. In order to document this, we analysed time series from different points in the fjord, shown in fig.6. As an example, fig.7 shows the time series from point 9 indicated in the previous figure. Fig.8 gives the matching amplitude spectrum. The basic wave component with one nodal point on the mid-line of the fjord comes out with a large coefficient. This indicates that we have crosswise standing waves. As opposed to the observations, the time series indicate more than three huge waves. This is most likely because energy loss due to wave breaking and imperfect reflection along the shore line is neglected in the model. These effects would probably also smooth the time series by first damping the shorter waves. Besides one should keep in mind that only the run-up height of the highest waves have been recorded. Furthermore the eye witness discriptions differ, and might be called into question. The amplitude spectra also confirm that the condition of long waves has been fulfilled.

7 Discussion of run-up heights

Fig.9 shows a comparison between measured and estimated run-up heights. The jagged appearance is partly due to the decomposition of the grid, and partly due to local effects. On the north side there is good agreement in Sylte, Fjøra and Muldal, in addition to large values around the slide area as expected. On the south side the curve has got the right tendency, but the wave heights are clearly underestimated at gentle beach slopes. This is because run-up effects are not properly represented in the basic model which assumes perfect reflection along the shore line. The implementation of more realistic run-up calculations along the line of [5, 6] is in progress.

8 Conclusions

Methods are developed to handle the complete process of a slide rushing into water and the possible blocking of grid cells along the shore line, energy transfer from slide motion to water motion, wave propagation in open water regions by the shallow water equations and estimation of run-up heights in exposed areas by results from previous numerical and experimental studies.

Time series analysis and energy considerations confirm that we may have energy trapping and standing waves in certain fjord geometries, as for instance in Tafjord.

In view of the complexity of the problem there is a surprisingly good agreement between model predictions and observations. The model can therefore be used for prediction of slide generated water waves.

The author wish to thank Drs. B. Gjevik and G. Pedersen for the benefit of many helpful discussions.

References

[1] Jørstad,F. 1968: Waves Generated by Landslides in Norwegian Fjords and Lakes. *Norwegian Geotechnical Institute* Publ. **79**, pp.13-31.

[2] Kaldhol,H. 1936: Bølgehøgdene ved Tafjordskredet. *Sunnmøre historiske lag* Tidsskrift b. **22/23**, pp. 37-45.

[3] Kaldhol,H. and Kolderup,N.-H. 1937: Skredet i Tafjord 7.april 1934. (Bergen). *Bergens museums Årbok 1936* Naturvidenskapelig rekke **11**, 15pp.

[4] Mesinger,F. and Arakawa,A. 1976: Numerical methods used in atmospheric models. *GARP, Publ. Ser. WMO* **17**, 64 pp.

[5] Pedersen,G. and Gjevik,B. 1982: Numerical Simulation of Run-Up of Long Water Waves. *Preprint, International Symposium on Refined Modelling of Flows, Paris, sep. 1982.*

[6] Pedersen,G. and Gjevik,B. 1983: Run-Up of Solitary Waves. *J. Fluid Mech* Vol.**135**, pp. 283-299.

[7] Pedersen, G. 1989: On the Numerical Solution of the Boussinesq equations. *Preprint Series, Dep. of Mathematics, University of Oslo* No.**1**.

[8] Wu,T.Y. 1981: Long Waves in Ocean and Coastal Waters. *Proc. ASCE, J. Eng. Mech. Div.* **107**, EM3, pp.501-522.

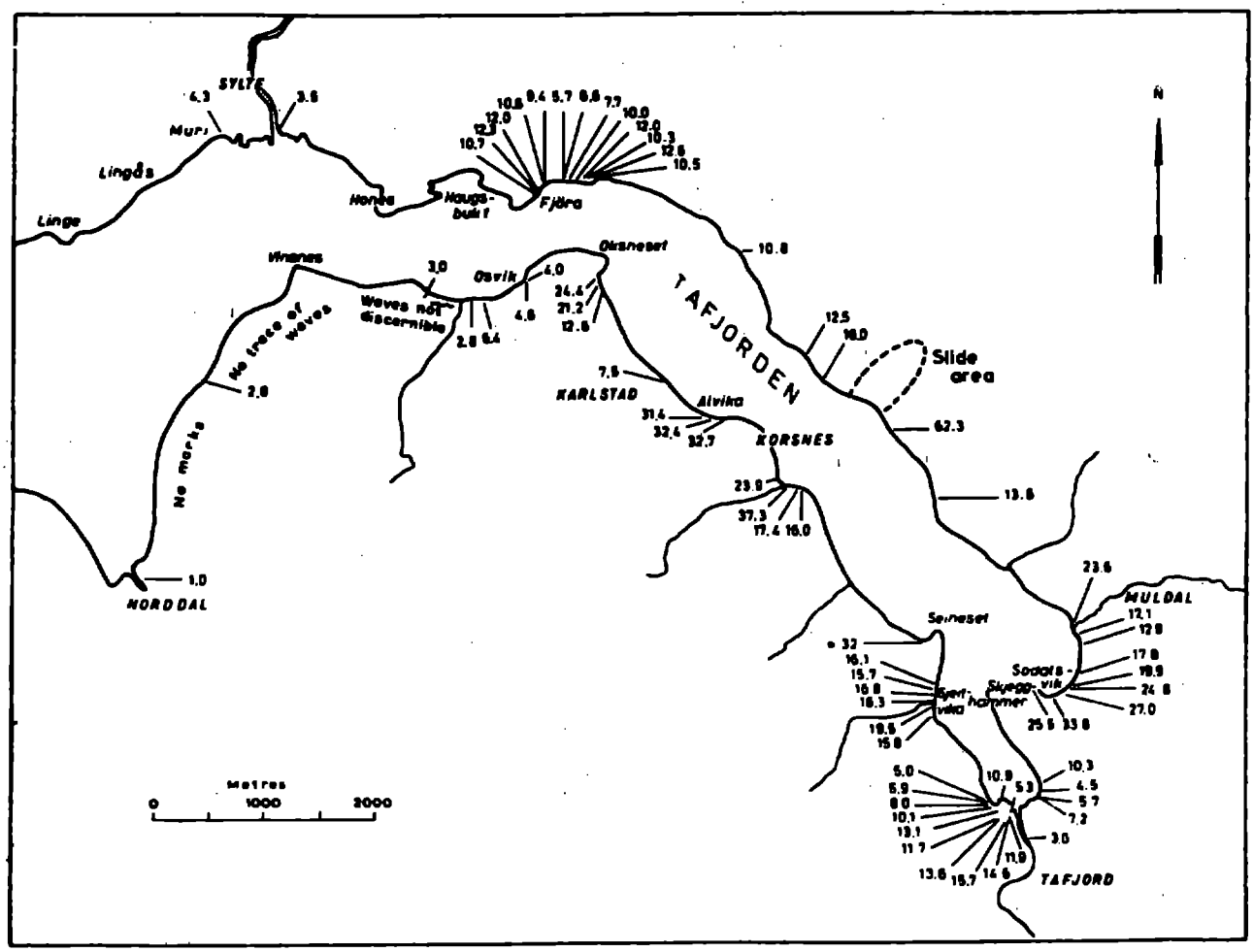

Figure 1: Map of Tafjorden. Wave heights in metres after rock slide April 7th 1934 (from [1, 2, 3]).

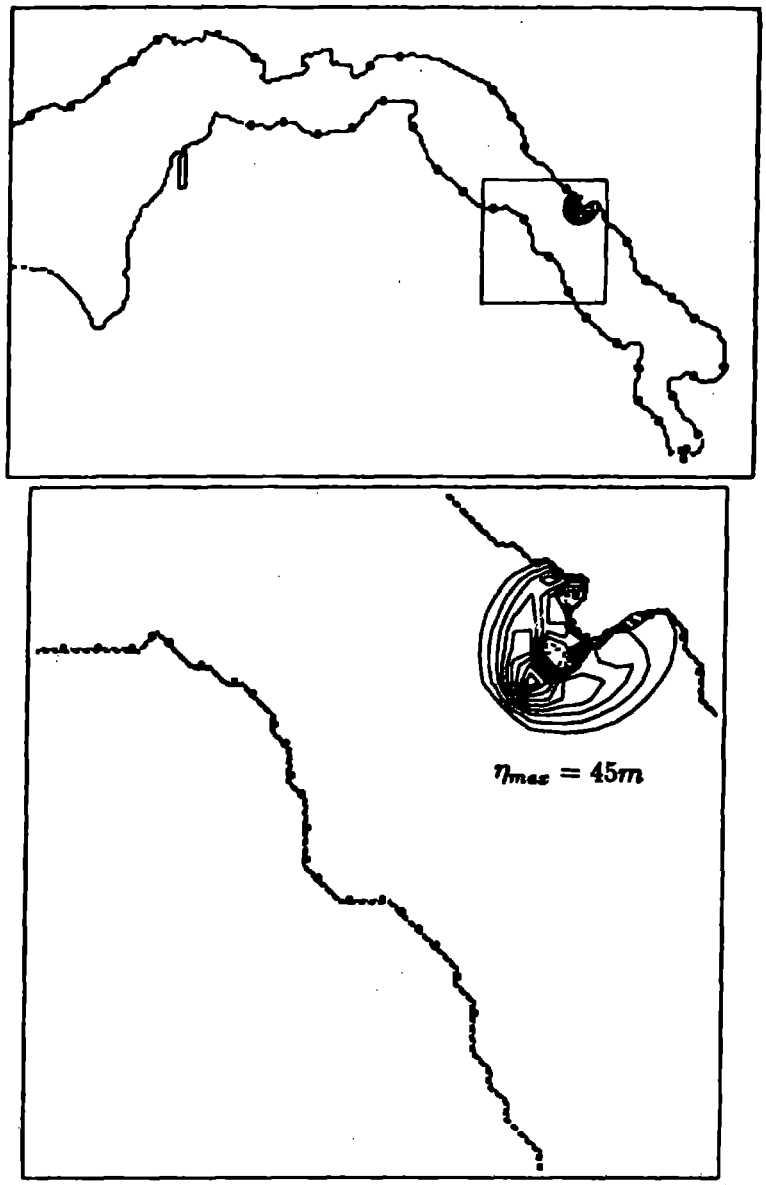

Figure 2: Estimated wave pattern at $t = 10.0$ s. Contour line interval: 5.0 m. Dotted lines indicate negative values. Inner frame magnified in the lower figure.

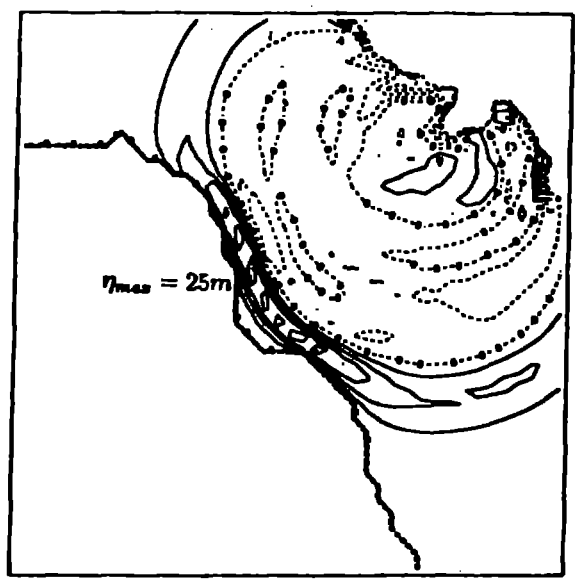

Figure 3: Estimated wave pattern at $t = 30.0$ s. Contour line interval: 5.0 m.

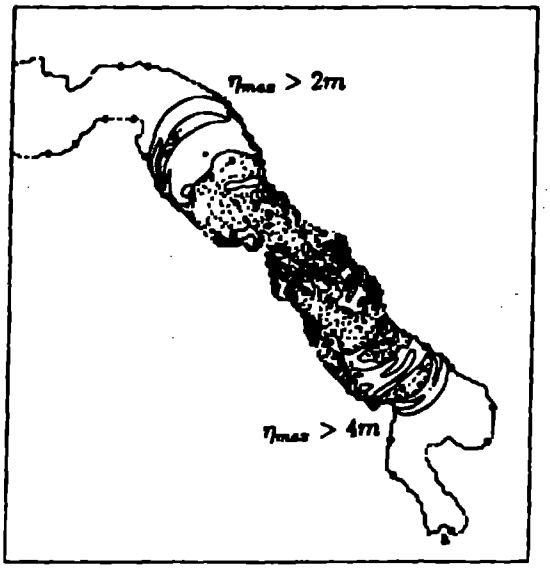

Figure 4: Estimated wave pattern at $t = 75.0\ s$. Contour line interval: 2.0 m.

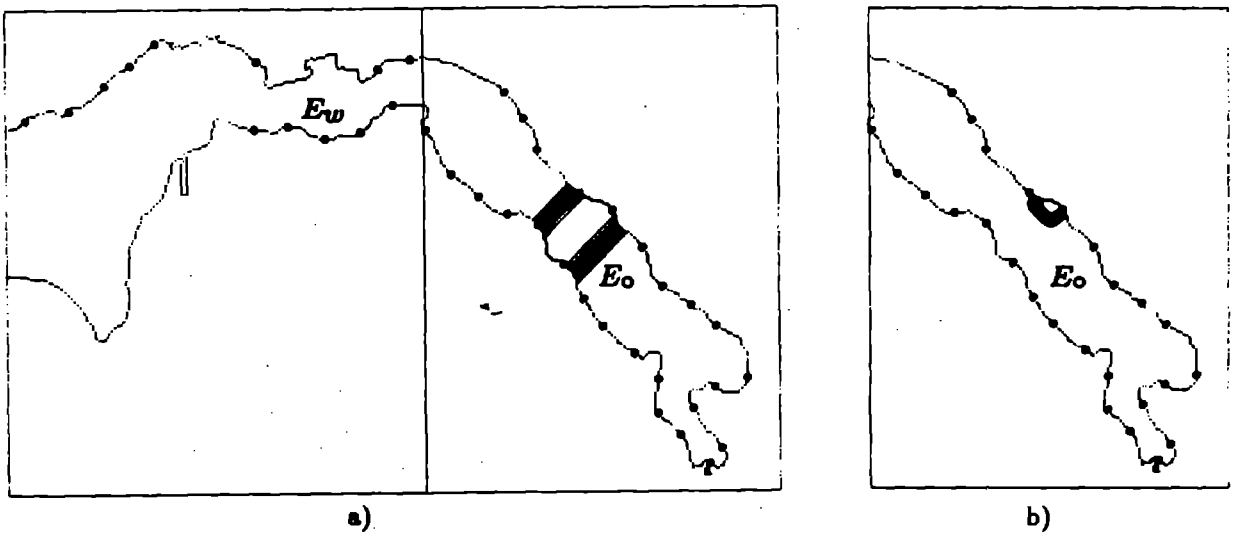

Figure 5: Initial surface displacements.

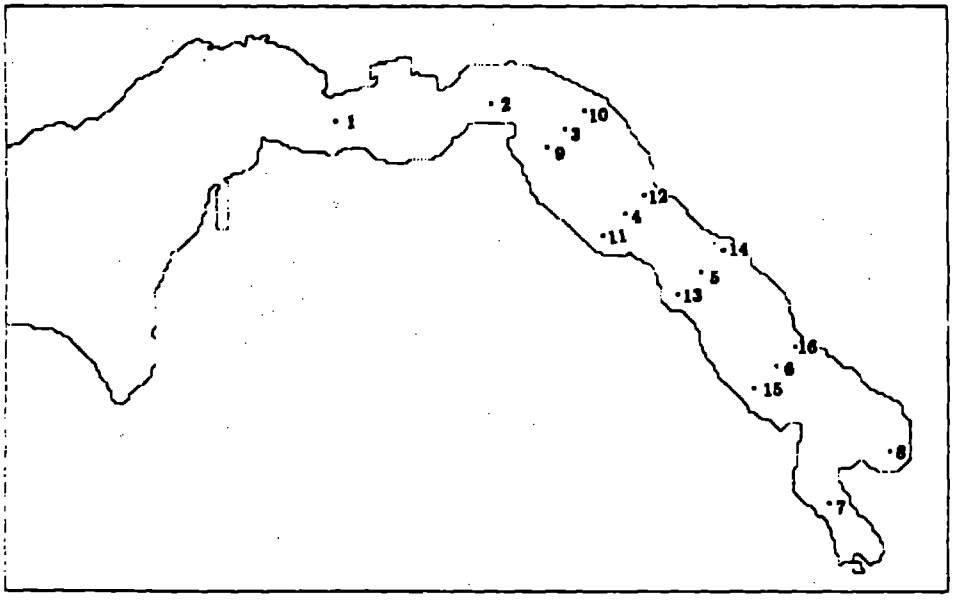

Figure 6: Positions of the points were time series are studied.

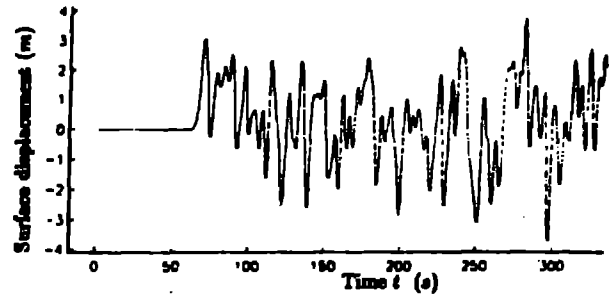

Figure 7: Time series, point 9.

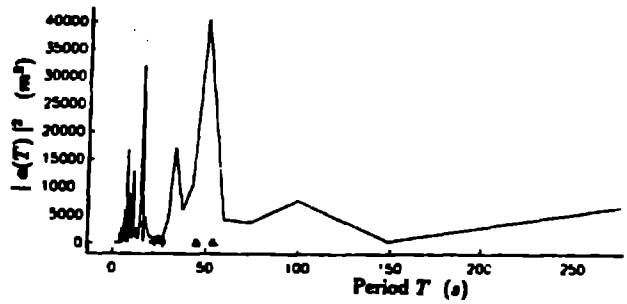

Figure 8: Amplitude spectrum, point 9.

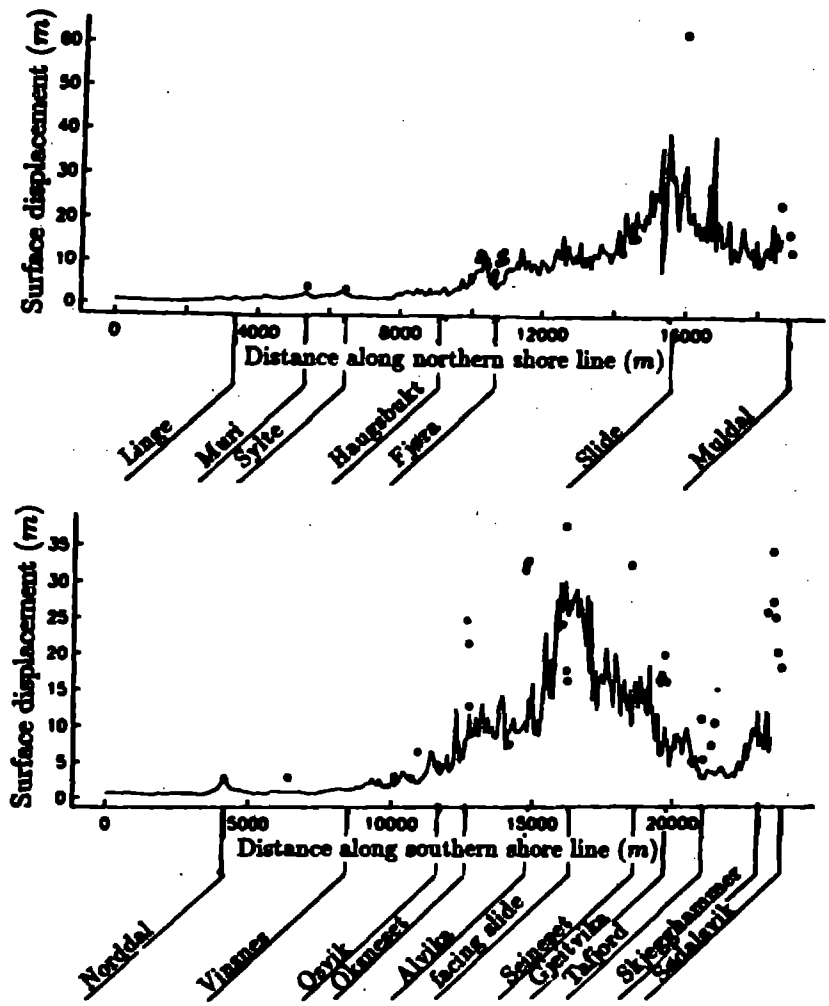

Figure 9: * Measured run-up heights along shore line. — Estimated wave heights at a minimum depth of 10.0 m along shore line. $t_{max} = 360.0$ s

MODELLING OF TSUNAMI GENERATION AND RUN-UP

H.I. BUNDGAARD[1], I.R. WARREN[1]
and
A. BARNETT[2]

(1) Danish Hydraulic Institute,
Agern Allé 5, DK–2970 Hørsholm, Denmark.

(2) Barnett Consultants Limited, P.O. Box 9463,
Hamilton, New Zealand.

ABSTRACT

A new method has been found whereby the generation of tsunamis can be included easily and simply in a standard modelling system for vertically integrated 2–D flows. To simulate the run–up of the tsunami wave at the coastline, a new technique – based on the introduction of narrow slots in the bed in each model grid – has been developed.

1. INTRODUCTION

A tsunami event can be divided into three phases, each with its own physical characteristics, namely generation at the sub-sea earthquake site, propagation to the coast and run-up at the shore line.

Many authors have shown that the propagation phase can be well simulated in mathematical models solving the depth-integrated shallow water wave equations (see e.g. Warren and Bundgaard, 1987). However, the generation and run-up phases present more difficult physical problems.

When a tsunamigenic earthquake occurs close to land the transitory earth and water movements can be important factors in determining the shape and height of the wave and the subsequent run-up at the coastline. In modelling such situations it is necessary to include the effects of the vertical and horizontal acceleration of the earth on the water movements. A method will be presented whereby these accelerations can be easily and simply included, in the 2-D depth-integrated shallow water wave equations, as mass and impulse source terms.

At the coastline, an accurate simulation of the run-up is necessary and this implies a progressive flooding of dry land which is known to give rise to many difficulties in numerical modelling. Successful techniques have been developed for inter-tidal flats, but tsunamis present a far more dynamic case to be simulated. A technique based on the introduction of narrow slots in the bed in each model grid point will be presented.

These new facilities have been built into a 2-D depth-integrated shallow water model, System 21, which has been developed by the Danish Hydraulic Institute.

As a test case for the above approach, the model has been used in a project: "Prediction of seiching and tsunamis in Wellington Harbour", prepared for the Museum of New Zealand Te Papa Tongarewa. Selected results from this report will be presented.

2. THE DEPTH-INTEGRATED MODEL

The two-dimensional model (System 21), used as basis for the introduction of tsunami generation and slots, is based on the vertically integrated equations for mass and momentum conservation (the Saint Venant equations). The model is used for simulations of unsteady free surface flows in homogeneous fluids. The model consists of the following equations:

$$\text{Continuity} : \frac{\partial \zeta}{\partial t} + \nabla \vec{Q} = 0 \tag{2.1}$$

$$\text{Momentum} : \frac{D\vec{Q}}{Dt} + 2\,\Omega \times \vec{Q} + gh\nabla\zeta - \nu\nabla^2 \vec{Q} + \frac{g\vec{Q}|\vec{Q}|}{C^2 h^2} = \vec{F}_{ext} \tag{2.2}$$

where ζ = water surface level; $\vec{Q} = (p,q)^T$, p and q being the fluxes in the x- and y-directions, respectively; Ω = Coriolis tensor; g = acceleration due to gravity; h = water depth; ν = eddy viscosity; C = de Chezy resistance No.; $\vec{F}_{ext}$ = external forcing; t = time.

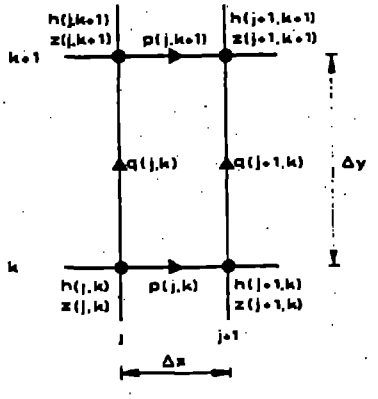

FIGURE 1 Computational grid adopted in System 21.

The equations are solved by an implicit finite difference technique with variables defined on a space-staggered rectangular grid as shown in Fig. 1. The ADI (Alternating directions implicit) algorithm wiht a special 'side-feeding' technique is used to advance the solution non-iteratively in time (Abbott et al., 1979).

The model, System 21, has been described in detail by Abbott et al., 1981.

3. TSUNAMI GENERATION

The transitory movement of the sea bed during a tsunamigenic earthquake can be divided into 3 separated movements, namely one vertical movement along the z-axis and two horizontal movements along the x- and y-axes. These movements will result in an acceleration of the earth and thereby also the waterbody. In the two following chapters it will be shown how the effect of these vertical and horizontal accelerations can be included in the 2-D depth-integrated model.

3.1 Vertical Movement of Sea Bed

The vertical movement of the sea bed can be modelled by an upthrust or downset of the bathymetry grid points, see Fig. 2. The direct follow of this movement is a vertical acceleration of the waterbody which can be included in the continuity equation as a mass source term, see Eq. (3.1).

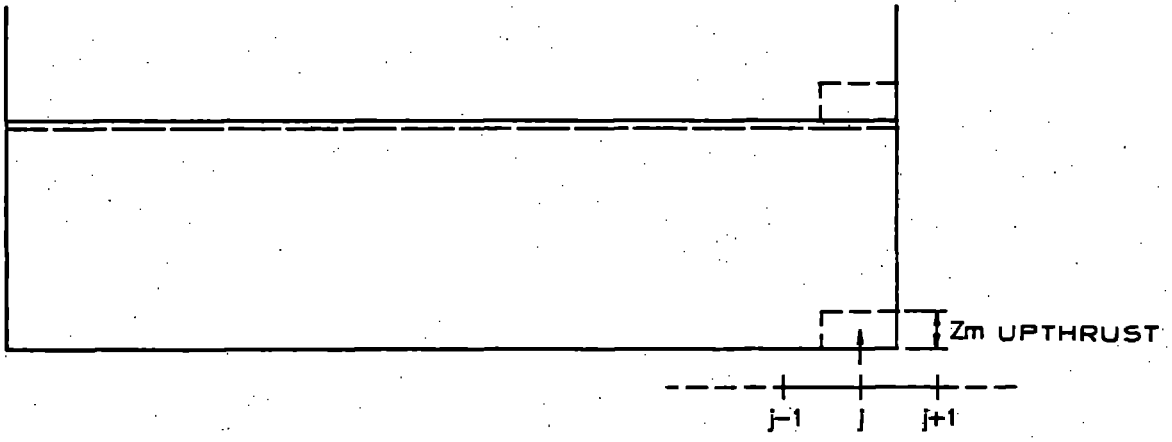

FIGURE 2 Upthrust of Sea Bed

Continuity:

$$\frac{\partial \zeta}{\partial t} + \frac{\partial p}{\partial x} + \frac{\partial q}{\partial y} = \frac{\partial z}{\partial t} \tag{3.1}$$

The discretization of this new mass source term can be seen below in Eq. (3.2).

$$\frac{\partial z}{\partial t} = \frac{Z_j^{n+\frac{1}{2}} - Z_j^n}{\Delta t/2} \tag{3.2}$$

3.2 Horizontal Movement of Sea Bed

The horizontal movement of the sea bed can be modelled by giving the water body an acceleration in the opposite direction of the horizontal earth movement, see Fig. 3.

This horizontal acceleration of the water body can be included in the momentum equation as an impulse source term. It is shown below how it is included in the x-direction, see Eq. (3.3).

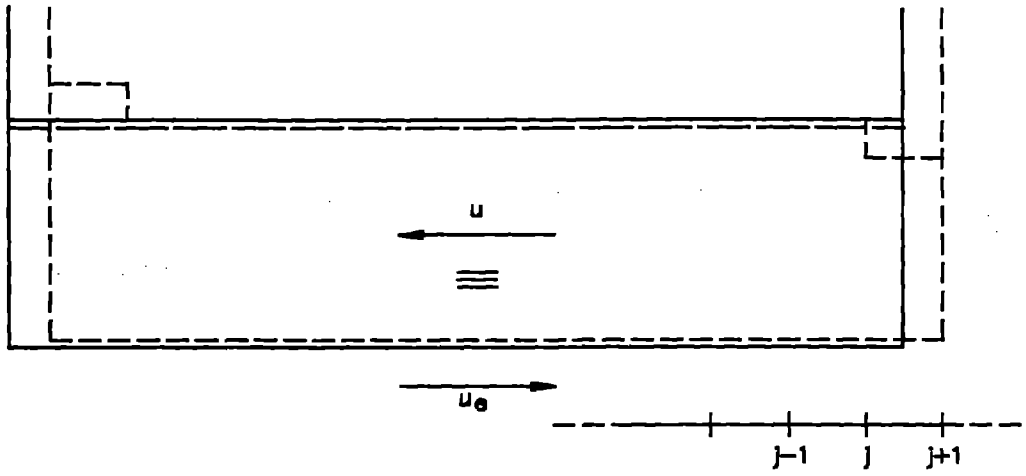

FIGURE 3 Horizontal Movement of Sea Bed with Velocity u_e

X-Momentum

$$\frac{\partial p}{\partial t} + \frac{\partial}{\partial x}\left(\frac{p^2}{h}\right) + \frac{\partial}{\partial y}\left(\frac{pq}{h}\right) + gh\frac{\partial \zeta}{\partial x} + \frac{\frac{p}{gh}\sqrt{p^2 + q^2}}{C^2} = -D\frac{\partial\left(u_e\right)}{\partial t} \qquad (3.3)$$

where D = still water depth.

The discretization of this new impulse source term can be seen in Eq. (3.4)

$$-D\frac{\partial\left(u_e\right)}{\partial t} = -D^*\frac{u_{ej}^{n+1} - u_{ej}^{n}}{\Delta t} \qquad (3.4)$$

where

$$D^* = \frac{1}{2}\left(D_j^n + D_{j+1}^n\right) \qquad (3.5)$$

4. RUN-UP AT SHORELINE

To simulate the run-up of the tsunamigenic waves at the shoreline a special approach, including 'slots', will be applied. This approach was presented by Warren et al. (1985) for the run-up of a solitary wave on a beach under the angle of 45 degrees.

A 'slot' is a very narrow canal which is introduced in each grid point in the model, see Fig. 4. That means that every grid point in the model will be a 'water point' at any time during a simulation.

This introduction of a 'slot' at every grid point influences the mass-equation and the water depth h in the 2-D depth integrated model, System 21. The mass equation will now look like Eq. (3.6).

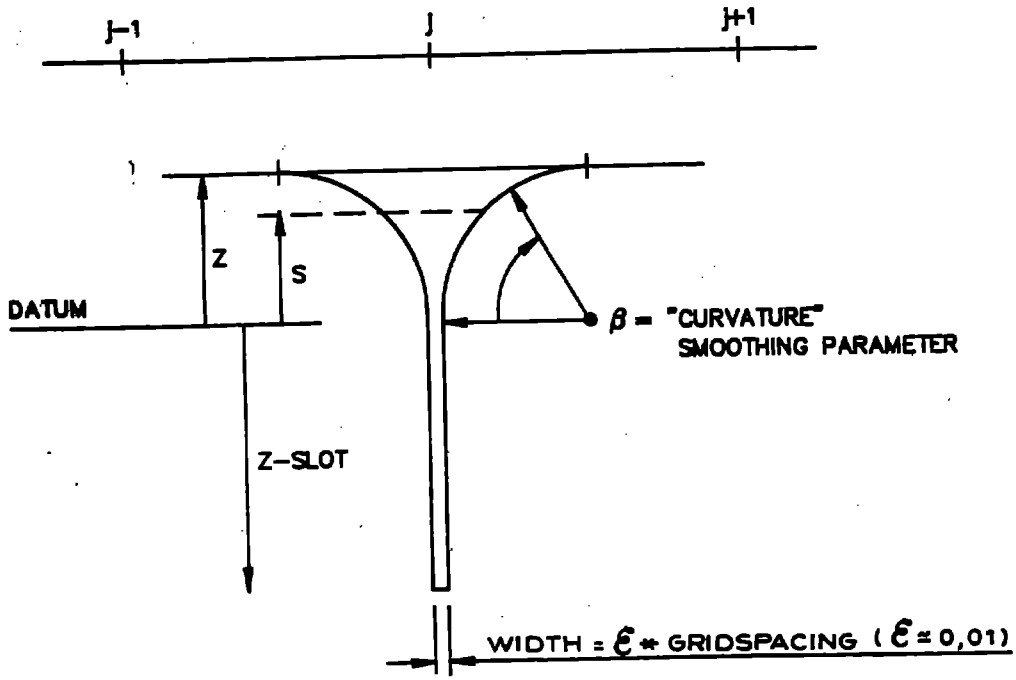

FIGURE 4 Description of a 'Slot'

$$F(\Lambda)\, S_t + \frac{1}{2}\left[(2-F(\Lambda))\, P_x^n + F(\Lambda)\, P_x^{n-1}\right]$$

$$+ \frac{1}{2}\left[(2-F(\Lambda))\, Q_y^{n-\frac{1}{2}} + F(\Lambda)\, Q_y^{n-3/2}\right] = 0 \qquad (3.6)$$

where

$$\Lambda = (S-Z) \;/\; (Z\_SLOT-Z) \qquad (3.7)$$

$$F(\Lambda) = \begin{cases} 1 & S>Z \\ \epsilon+(1-\epsilon)\, e^{-\beta\Lambda} & S<Z \end{cases} \qquad (3.8)$$

Instead of the water depth h, a new variable A(Λ) will be used in the equations to take the 'slot area' into account, see Eq. (3.9).

$$A(\Lambda) = \begin{cases} (Z-Z\_SLOT)\left\{ \epsilon(1-\Lambda) + \dfrac{(1-\epsilon)}{\beta}\left[e^{-\beta\Lambda} - e^{-\beta}\right] \right\} & \text{for } S<Z \\ (S-Z) + (Z-Z\_SLOT)\left\{ \epsilon + \dfrac{(1-\epsilon)}{\beta}\,(1-e^{-\beta}) \right\} & \text{for } S>Z \end{cases} \qquad (3.9)$$

5. CASE STUDY

A study; 'Prediction of seiching and tsunamis in Wellington harbour, New Zealand' was carried out in 1989, using the above presented model.

The study was undertaken by Barnett Consultants Ltd. with a substantial contribution from the Danish Hydraulic Institute (DHI) who had previous experience with seismic wave modelling, including a major study of tsunami effects in Morocco.

The region of Wellington harbour is subject to permanent ground displacements associated with large earthquakes. A number of fault movement scenarios have been identified in a New Zealand Geological Survey (NZGS) report.

This study investigates the harbour waves generated by seismic disturbance as discussed in the above report, with main emphasis on the likelihood of such waves overtopping the existing quay level at a proposed museum site.

Based on the estimates given by the NZGS it was decided to simulate the 1855 earthquake translation of 4.9m horizontally with a duration of movement of between one and three seconds. The immediate wave formed by the translation of steeply sloping beds such as the breastwork surrounding the Museum site was of most interest, as all the local major earthquake scenarios feature substantial horizontal movement. Since this wave is caused by the collapse of the mound of water thrust up by the sudden lateral movement of the breastwork, the wave impact on the Museum site is highly dependent on the wave dissipation characteristics of the site perimeter. If no dissipation measures are taken the wave will impact on building walls somewhat like a beach wave striking a sea wall, with a brief surge in wave height as the wave reflects from the wall.

The selected results from this study is presented in Fig. 5 and Fig. 6. As it can be seen from these figures the duration of the horizontal translation is of great importance to the wave run-up against the Museum building.

The 'slots' in the above simulation is introduced in the quay to simulate the run-up at the initial dry quay.

6. CONCLUSIONS

The results obtained in the above case study show that models generated by System 21 are capable of simulating the generation and run-up of tsunami waves.

The model has also been verified against simple test cases and shown a very good agreement with analytical results.

7. ACKNOWLEDGEMENT

Results from the report "Prediction of Seiching and Tsunamis in Wellington Harbour, New Zealand" is presented by courtsey of the Museum of New Zealand Project Development Board.

REFERENCES

Warren, I.R. and Bundgaard, H.I. (1987). A comparison between physical and numerical models of tsunamis. IAHR XXII Congress in Lausanne, 1987.

Abbott, M.B. (1979). Computational Hydraulics: Elements of the Theory of Free-Surface Flows, Pitman, London.

Abbott, M.B., McCowan, A. and Warren, I.R. (1981). Numerical Modelling of Free-Surface Flows that are Two-Dimensional in Plan, Transport Models for Inland and Coastal Waters, Academic Press, pp. 222-283.

Warren, I.R., Larsen, J. and Madsen, P.A. (1985). Application of short wave numerical models to harbour design and future development of the model. Int. Conference on Numerical and Hydraulic Modelling of Ports and Harbours. Birmingham, England, BHRA, pp. 303-308.

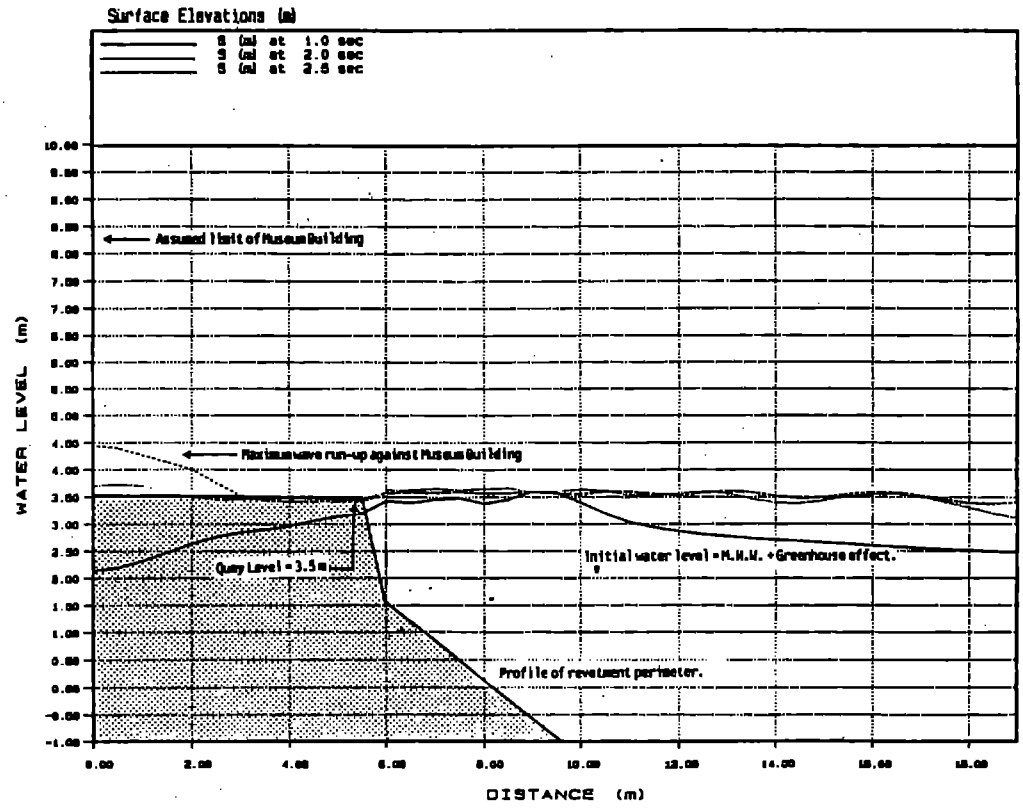

FIGURE 5 Cross-section through Museum site of water surface elevations at 1.0, 2.0 and 2.5 seconds. dx=0.5m, dt=0.1 seconds, 'x' translation=4.9m, duration=3.0 sec.

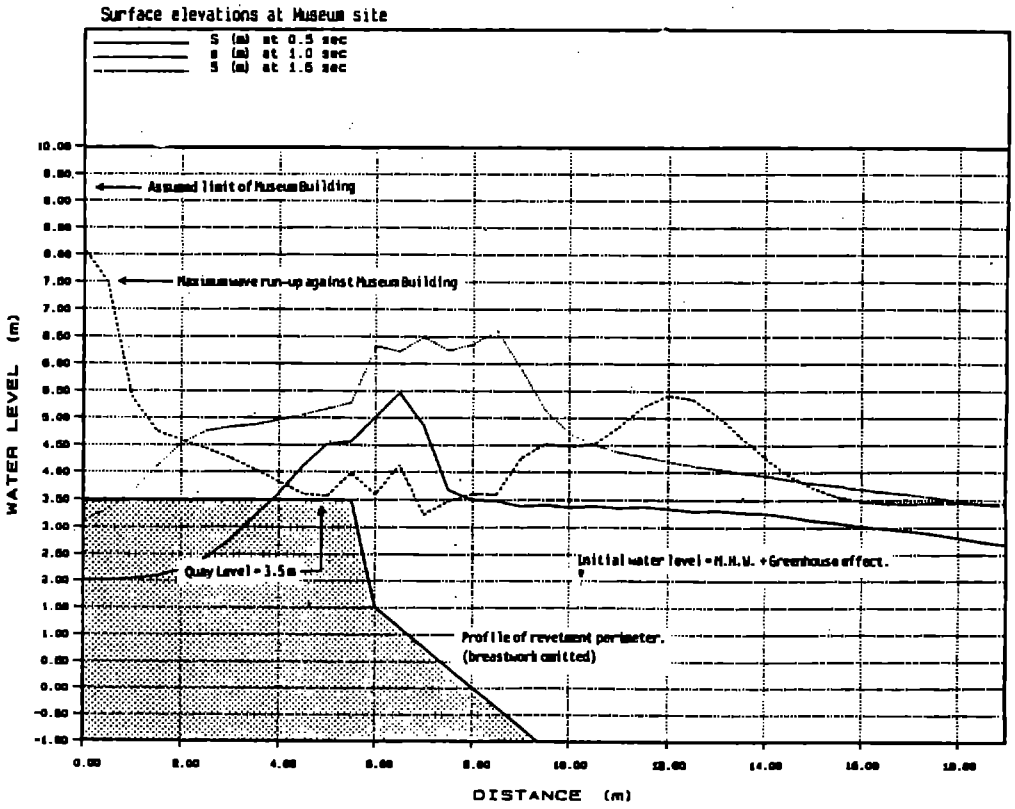

FIGURE 6 Cross-section through Museum site of water surface elevations at 0.5, 1.0 and 1.5 seconds. dx=0.5m, dt=0.1 seconds, 'x'translation=4.9m, duration=1.0 sec.

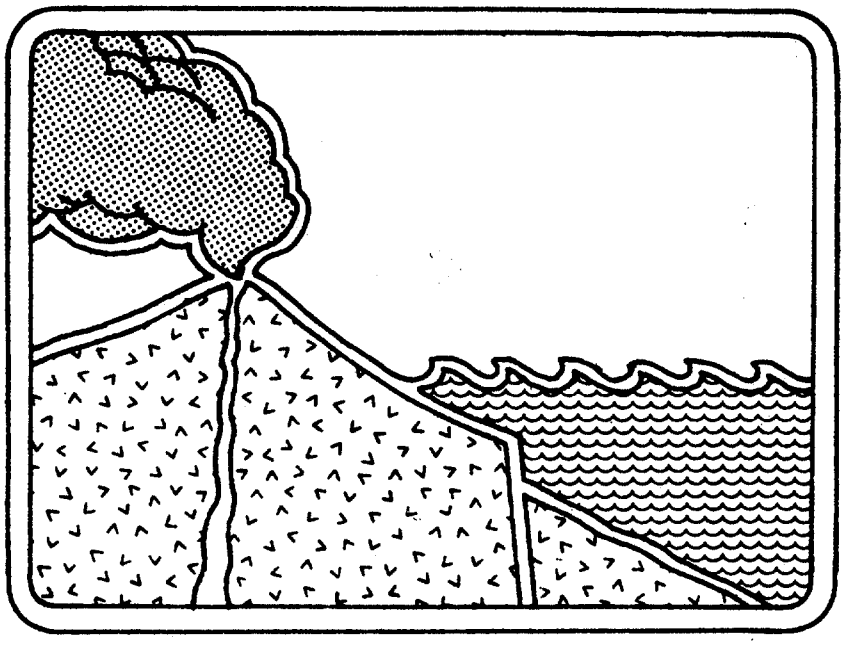

A PRELIMINARY EVALUATION OF THE TSUNAMI HAZARDS IN THE MOROCCAN COASTS

S.O.El Alami[1] and S.Tinti[2]

(1) Université Mohammed V, Institute Scientifique,
Département de Physique du Globe,
Av.Ibn Battouta, B.P. 703, Agdal–Rabat, Morocco.

(2) Università di Bologna, Dipartimento di Fisica,
Settore di Geofisica, V.le Berti Pichat, 8
40127 Bologna, Italy.

ABSTRACT

Morocco is probably the African country most affected by water waves generated by submarine earthquakes. Moroccan coasts on the Atlantic Ocean are more exposed to tsunami threat than the coasts to the East of the Straits of Gibraltar. The most remarkable known example of tsunami hitting Morocco is the 1 Nov 1755 event: the generating earthquake caused large damage in Lisbon as well as in very many towns and villages of the Iberian Peninsula, while the ensuing water waves inundated violently Southern Portugal, Atlantic Spain and Morocco. The most recent tsunami recorded along the Moroccan coasts is due to the 28 Feb 1969 M=7.3 earthquake occurred in the region west-southwestwards of cape St.Vincent, that was the source of the 1755 seismic shock. Reports on tsunamis in Morocco are rare and scarcity of data makes the application of traditional statistical methods to the sole tsunami dataset useless in order to make hazard evaluations. In the present investigation tsunami data are therefore complemented by the set of the available earthquake data, namely the 1901–1986 seismic catalog of Morocco and surrounding areas assembled by the Institute Scientifique, Rabat. Analysis of seismicity is used as an important tool to estimate the potential for tsunamigenic earthquakes in the region and the ensuing hazards for the Moroccan coasts.

INTRODUCTION

Morocco is probably the country most affected by tsunami in the whole African continent. All the known tsunamis were generated by either submarine or coastal earthquakes. Morocco has a very long coastline watered by the Atlantic Ocean to the West and by the Mediterranean Sea to the East. The coasts on the Atlantic Ocean are the most subject to tsunami attacks. The largest known tsunami investing Morocco occurred on 1 Nov 1755: the generating earthquake (M=8.5–9.0) caused severe damage in many towns and villages of the Iberian Peninsula and especially in Lisbon. The produced water waves inundated Southern Portugal and the Atlantic coasts of Spain and Morocco with extraordinary violence. The tsunami was studied by several investigators who posed special attention to the descriptions regarding Portugal and Spain (see for example Campos, 1989). In Tanger the maximum amplitude of the first wave was estimated to be 17 meters (Debrach, 1946); sizeable waves were also observed in Salé, Rabat, Casablanca, Essaouira and Safi. The most recent tsunami recorded along the Moroccan coasts is due to the 28 Feb 1969 M=7.3 earthquake occurred in the same region that was the source of the 1755 earthquake, that is some 200 km west–southwestwards of cape St.Vincent. The catalog of tsunamis in Morocco includes only few events, since tsunamis are rather unfrequent and since in the past a positive scientific attention to these natural phenomena was scarse or even absent in Morocco as in many other countries. Paucity of data discourages the application of traditional statistical methods to the sole tsunami data, since the resulting hazards evaluation would be unreliable. In this study in order to integrate the scarce information content of the tsunami data, recourse is made to the earthquake data: therefore the main dataset analyzed in this investigation consists of a seismic catalog spanning the period 1901–1986 and covering Morocco and the surrounding area. Analysis of seismicity is used as an essential means to estimate the potential for tsunamigenic earthquakes in the region and the consequent hazards for the Atlantic and Mediterranean Moroccan coasts.

METHODOLOGY

If one takes into account the global neotectonic setting, the geodynamic processes as well as the seismicity of the considered region (see e.g. Udias et al., 1976; Hatzfeld et al., 1977; Ben Sari, 1978), it seems that three important seismic zones can be identified as being seismically homogeneous at least for the purposes of the present investigation. The first zone embraces the Atlas chain and the interior of Morocco. Seismic sources are here too distant from the sea to cause any perceivable perturbations in the sea waters This region will be therefore ignored in the subsequent tsunami hazards evaluation. The second zone embodies the Alboran Sea together with the encircling coasts of northern Morocco, of north–eastern Algeria and southern Spain. The third region concerns the Atlantic Ocean and the related coasts of eastern Morocco, of south–eastern Spain and of Portugal. The boundaries of the last two regions are depicted in Figure 1, superimposed to a map of the epicenters of the recorded earthquakes. The seismic catalog used contains 4605 events. It consists of two separate subcatalogs:

one covers the interval 1901–1984 (Cherkaoui, 1988), the other spans the two–year period 1985–1986 and is derived from the seismological annual bulletins of Morocco. All events are included in a space window between 20°N to 38°N and 0°W to 20°W.

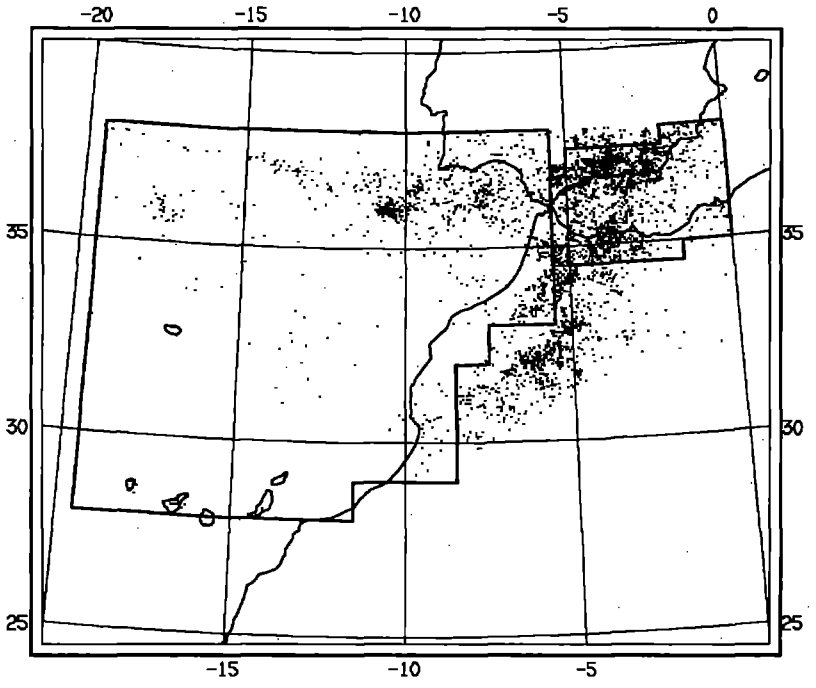

Figure 1. Map of the epicenters reported in the 1901–1984 catalog used in this research. Thick lines delineate the boundaries of the two regions (Alboran Sea and Atlantic Ocean) that will be individually analyzed in order to perform tsunami potential evaluations.

The study carried out consists essentially in the application of a method of analysis that has been developed by one of the authors particularly to overcome the difficulties arising from shortage of tsunami data. It was already employed in studying tsunami hazard in the Italian seas with satisfactory results (Tinti, 1990a and 1990b). The idea is that tsunami activity rate may be inferred from estimates of seismic potential in coastal and marine regions; for the purpose these are partitioned into regular cells, inside each of which the probability of occurrence of a tsunamigenic earthquake is evaluated.

The preliminary analysis of the used earthquake catalog of Morocco reveals that an appreciable portion of catalog events is useless for our purposes, having no magnitude nor intensity determinations. Only the events with either magnitude or intensity specifications are considered. In order to produce a seismic data set suitable for the subsequent analysis, intensities are converted into magnitudes by means of appropriate transformation laws. These are separately determined for the three regions mentioned above, i.e. Atlas, Alboran Sea and Atlantic Ocean, though the partition boundaries are slightly modified for convenience. Standard statistical routines are applied to evaluate polynomial regression of intensities vs. magnitudes on the basis of the 745 earthquakes with both intensity and magnitude specified. Only earthquakes with focal depth less than a given threshold are selected, deeper earthquakes being jugded irrelevant for tsunami generation. The threshold is estimated to be 100 km to account for the significant focal–depth uncertainties: one of the earthquakes known to have produced a

tsunami observed on all atlantic Moroccan coasts is the 25 Nov 1941 M=8.3 earthquake with a hypocenter determination of 81 km, that is an apparently overestimated value. The total number of events retained after the above preparatory preselection phase is 4091 that is about 15% less than the original number of 4605.

The analysis of seismicity performed on the catalog so obtained involves a number of steps applied distinctly in each region. First each regional catalog is examined as regards completeness. It is known that the seismicity rate apparent from seismic catalogs departs from the true rate as a result of incompleteness affecting chiefly the eldest historical portions. In order to study the completeness of a seismic series a method can be used that is applicable on sequences of main shocks and on magnitude classes (see Tinti and Mulargia, 1985). For each magnitude class the method allows to evaluate the completeness period, to value the incompleteness level of any portion of the catalog, to estimate both the mean true seismic rate of the region as well as its spacial distribution (magnitude–class true–seismicity maps). It essentially consists of two phases. In the first phase the main shocks are detected, while aftershocks and swarms are removed by using a suitable window depending on time, on space and on magnitude. It follows a second phase in which each magnitude class is repeatedly tested against poissonianity through a Kolmogorov–Smirnov one–sample test. In the present case the classes used are 2.4–3.0,...,6.0–6.6, integrated by the $M > 6.6$ class. Once completeness analysis is finished, each region is partitioned into regular cells. The aforementioned seismicity maps allow the computation of the coefficients a and b of the Gutenberg–Richter magnitude–frequency law, that may be estimated by using suitable maximum likelyhood techniques (see e.g. Tinti, 1989).

At this stage of the analysis, one is able to evaluate the true seismicity rate for the desired range of magnitudes and for the desired cell in the region. The subsequent step regards the evaluation of the tsunami potential of a cell, involving some assumptions on the capability of an earthquake occurring in that cell to set in motion a tsunami. The earthquake features that most influence tsunami generation are fault geometry, size, and slip, focal mechanism, focal depth and location. Magnitude is frequently used to represent the main characteristics of the earthquake source and hence is a reasonable candidate to describe earthquake capacity of tsunami excitation. In the present study a magnitude threshold (M_t) has been established for each cell: M_t is assumed to be the minimum magnitude for a tsunamigenic earthquake in that cell and at the same time the hypothesis is made that all earthquakes with larger magnitudes do engender visible tsunamis.

RESULTS AND CONCLUSIONS

The analysis shortly described in the previous section has been applied to the two regions shown in Figure 1, where it is known from tsunami literature that there are sources active in producing tsunamis in the past (see e.g. Campos, 1990). The Alboran Sea (region 1), that is the extreme western part of the Mediterranean Sea terminating at the Gibraltar Strait, is a small region which is site of moderate seismicity. Earthquake sources are diffuse and cannot be delineated neatly; but most of the recorded epicenters

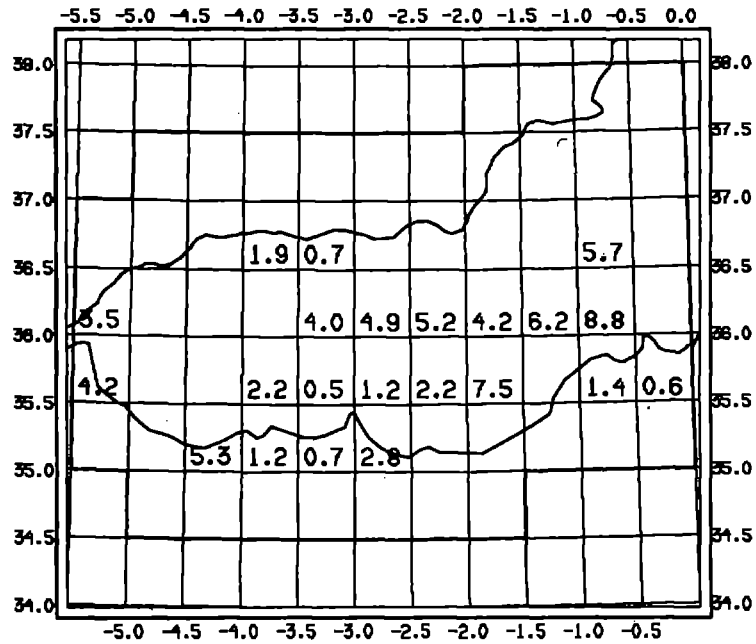

Figure 2. Tsunami return periods in 1000–year units estimated for all cells included in the region delimited by the thick boundaries, namely the Alboran Sea and the surrounding coastal areas. Smaller values of M_t have been used in the computations (see text). In the blank cells the assessed return times exceed 10000 years. The return period for the whole region is 71 years.

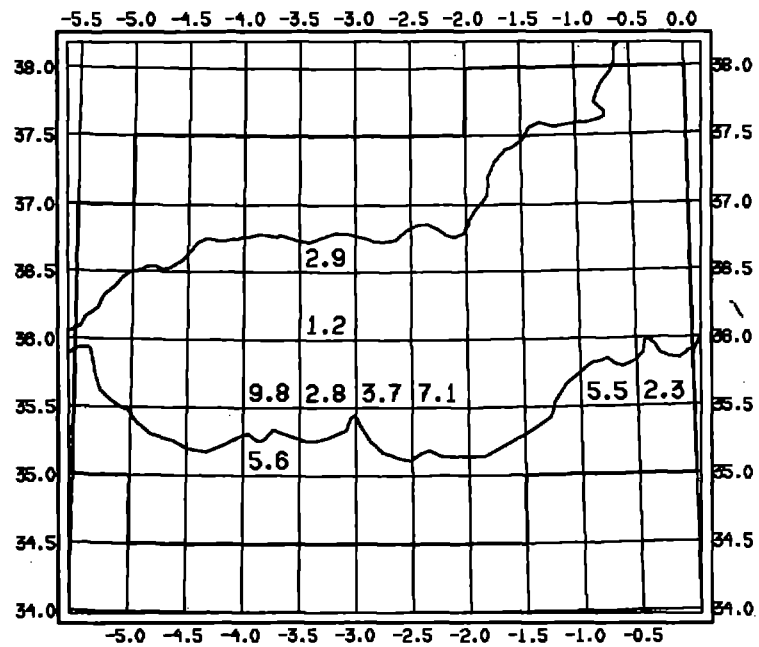

Figure 3. Tsunami return periods in 1000–year units estimated for the same cells as in Figure 2. The set of the higher values of M_t has been assumed in the calculations, producing more conservative estimates. Blank cells correspond to return times larger than 10000 years and therefore may be omitted from the tsunamigenic sources. The evaluated mean return time for the entire area is 269 years.

are clustered in the Sierra Nevada chain between the coastal towns of Malaga and Almeria in Spain and in the zone lying on the opposite Moroccan coasts between Al-Hoceima and Melilla. The Atlantic Ocean region considered here (region 2) is comparatively much larger. The earthquake epicenters reported in the catalog are not very numerous. They tend to concentrate in a rather narrow zone between 36°N and 38°N, probably marking the margin between the African and the Eurasian plates. The westernmost part of this zone, about a thousand kilometers far from the nearest coastline, is characterized by an observed seismic rate that is not substantial, but large earthquakes are not unfrequent here where events exceeding magnitude 8 have been recorded. Observed epicenters tend to cluster in the easternmost part of the seismic belt, where national seismic networks provide a better coverage. Submarine sources are here within a distance of a few hundreds of kilometers from the Iberian and the Moroccan coasts. A smaller group of epicenters may be noted in the Azores Islands.

Region 1 has been partitioned in $30' \times 30'$ cells. In each cell the mean rate of tsunamigenic earthquake has been evaluated in two experiments based on different assumptions regarding the value of M_t. This has been supposed to increase with the distance of the cell from the sea. For simplicity the functional dependence of M_t from the sea distance has been specified by means of 4 discrete classes: class 1 includes all cells fully or partially in the sea; classes 2, 3 and 4 include cells that are fully on land and whose center distance from the nearest coastline is within the respective range of 0–30, 30–50, 50–75 (km). In the first experiment the set of M_t values attributed to the four classes is 6.0, 6.5, 7.0 and 7.5, whereas in the second experiment the values are slightly increased, being 6.6, 7.0, 7.4, 7.9 from classes 1 to 4 respectively. Figures 2 and 3 show the results of our computations for both M_t assumptions, in terms of the expected return period of tsunamis produced locally in each cell. By properly combining the contribution of all cells according to probability theory, the mean return period of the whole region may be evaluated. It is 71 years for first set of M_t values and 269 years for the second more conservative set. Though in our present study we are not able to ascertain unequivocally which of the two sets is more suitable for the region under consideration, it is however worth observing that the magnitude threshold for an earthquake to be tsunamigenic seems to be less in the Mediterranean Sea than in most other areas of the world (see Soloviev, 1990); which may favour the first choice against the second. The cells with the highest tsunami potential are in the narrow seismic strip between 3°W and 3.5°W stretching from the moroccan gulf to East of Melilla to the opposite coast of Spain and including the ispanish Island of Alboran. A second relevant source is found in the algerian coast between Oran and Mostaganem.

Region 2 has been subdivided into $1^\circ \times 1^\circ$ cells, for each of which the same two experiments have been performed that have been carried out for region 1. The return times estimated for the whole area are respectively 9.5 years and 25 years. The results are given in Figures 4 and 5. Both experiments attest that tsunami potential here is substantially larger than in the contiguous region 1. Contrarily to that region, there is no clear preponderance of considerations favouring one set of M_t values over the other and illumination on the subject may derive from future investigations. What is patently and consistently inferrable from both figures, however, is the identification of the tsunami sources. Two are the most important tsunamigenic areas: one covers the northwestern

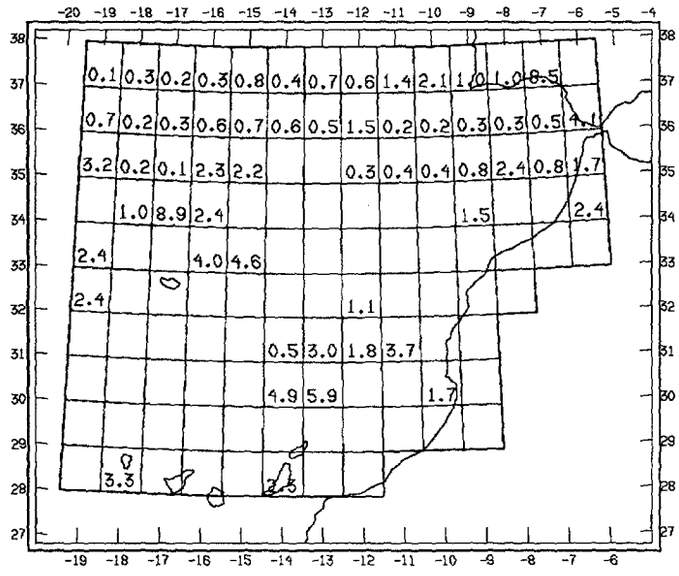

Figure 4. Tsunami return periods in 1000–year units estimated for cells inside the thick boundaries, i.e. the Atlantic region and the neighbouring coasts of SW Iberian peninsula and E Morocco. The lower–value set of M_t (6.0, 6.5, 7.0, 7.5) has been adopted (see text). Blank cells are practically non-tsunamigenic areas, with assessed return times exceeding 10000 years. The return period for the global region is 9.5 years.

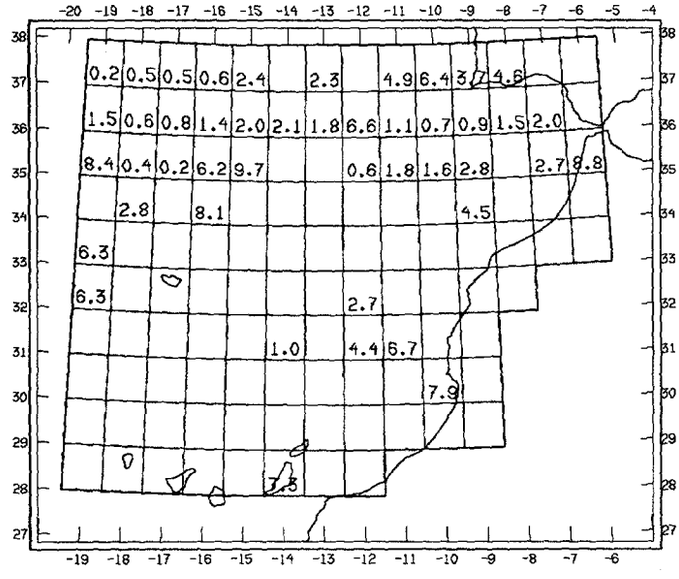

Figure 5. Tsunami return periods in 1000–year units estimated for the same region shown in Figure 4. Results pertain to the experiment with the set of the higher values of M_t, yielding as expected longer return–time evaluations. Blank cells correspond to times larger than 10000 years. The evaluated mean return time for the total region is 25 years.

corner of the region, the other extends south-southwest of Cape St.Vincent. In Figure 4 they are almost the same strength, whereas in Figure 5 the former slightly predominates, in virtue of the characteristic large–earthquake seismicity. The two zones are connected by a narrow strip of cells with appreciable tsunami potential, which is consistent with the epicenter clustering along the interplate oceanic margin. It is interesting to observe that for both experiments that cell where the famous 1 Nov 1755 occurred is in the number of the cells displaying the shortest tsunami return period and consequently the highest tsunami activity.

As a conclusive remark, it may be stressed that, in spite of the scarsity of data found in the existing tsunami lists, by means of the present preliminary analysis the most active tsunamigenic sources affecting Moroccan coasts have been identified, to the East as well to the West of the Strait of Gibraltar. Future analysis will be useful to refine seismicity computations and will be especially helpful in guiding the assumptions on the complex dependence of M_t on the earthquake parameters.

REFERENCES

BEN SARI D., 1978. Connaissance géophysique du Maroc (in french), Thése d' état, Univ. Grenoble, France.

CAMPOS L., 1989. Sismicidad de la costa sudoccidental de España. Analisis y valoracion geografica de los posibles riesgos como consequencia de los tsunamis en la zona (in spanish), Doctoral Tesis, Univ. Complutense de Madrid, pp.734.

CAMPOS L., 1990. Tsunami hazard on the Spanish coasts of the Iberian peninsula, Science of Tsunami Hazards, (this issue).

CHERKAOUI T.E., 1988. Fichier des séismes du Maroc et des régions limitrophes 1901–1984 (in french), Trav.Inst.Sci., Série Géol.Géog.Phys., 17, Rabat, Maroc, pp.158.

HATZFELD D., FROGNEUX M. and GIRARDIN N., 1977. Etude de la sismicité dans la région de l'arc de Gibraltar et l' Algérie du Nord, B.S.F.G., 19, 741–747.

DEBRACH J., 1946. Raz de marée d'origine sismique enrigistré sur le littoral atlantique du Maroc (in french), Service de Physique du Globe et de Météorologie, Annales, Maroc.

SOLOVIEV S.L., Tsunamigenic zones in the Mediterranean Sea, Natural Hazards, 3, 183–202.

TINTI S., 1989. Bayesian interval estimation of the parameter *b* for grouped magnitudes, Tectonophysics, 168, 319–326.

TINTI S., 1990a. Assessment of tsunami hazard in the Italian Seas, Natural Hazards, (in press).

TINTI S., 1990b. Tsunami potential in Southern Italy, Science of Tsunami Hazards, (this issue).

TINTI S. and MULARGIA F., 1985. Completeness analysis of a seimic catalog, Annales Geophysicae, 407–414.

UDIAS A., LOPEZ ARROYO A. and MEZCUA J., 1976. Seismotectonics of the Azores–Alboran region, Tectonophysics, 31, 259–289.

A PROPOSAL FOR A NEW CATALOG ON TSUNAMIS IN THE MEDITERRANEAN AREA

A. Maramai - C. Gasparini

Istituto Nazionale di Geofisica - Roma- Italy

ABSTRACT

Several catalogs on tsunamis concerning single regions of the Mediterranean area (as Greece, Italy, Portugal, Spain etc.) have already been published on literature. Unfortunately, none of them is so complete to include all the events of the whole Mediterranean region. The aim of this study is to create an analytical catalog in order to unify and digitize all the available data sets, as is already in existence for the Pacific area. The catalog, in preparation, consists of six interacting sections articulated that is a main part called the Main Catalog and five more sections or subcatalogs, i.e. the Localities Subcatalog, the Graphic Data Set, the "Digital" Subcatalog, the Revision Subcatalog and the Bibilographic Subcatalog. All section will be detailed in the paper even by means of appropriate illustrative examples.

The Main Catalog

The Main Catalog (MC) represents the "body" of the catalog and contains all the relevant data on tsunamis and their sources (earthquakes, volcanic eruptions, submarine landslides). The devised basic record format is suited for the creation of a data bank easy to manage and to use (consider expansion, deletion, insertion, information retrieval,etc.). An example of a typical MC string is given in Figure 1 where data pertinent to the tsunami following the Messina earthquake (Sicily-December 28, 1908) have been inserted. The explanation of all the items included in the record will be given in the following with the aid of the Figure 1.

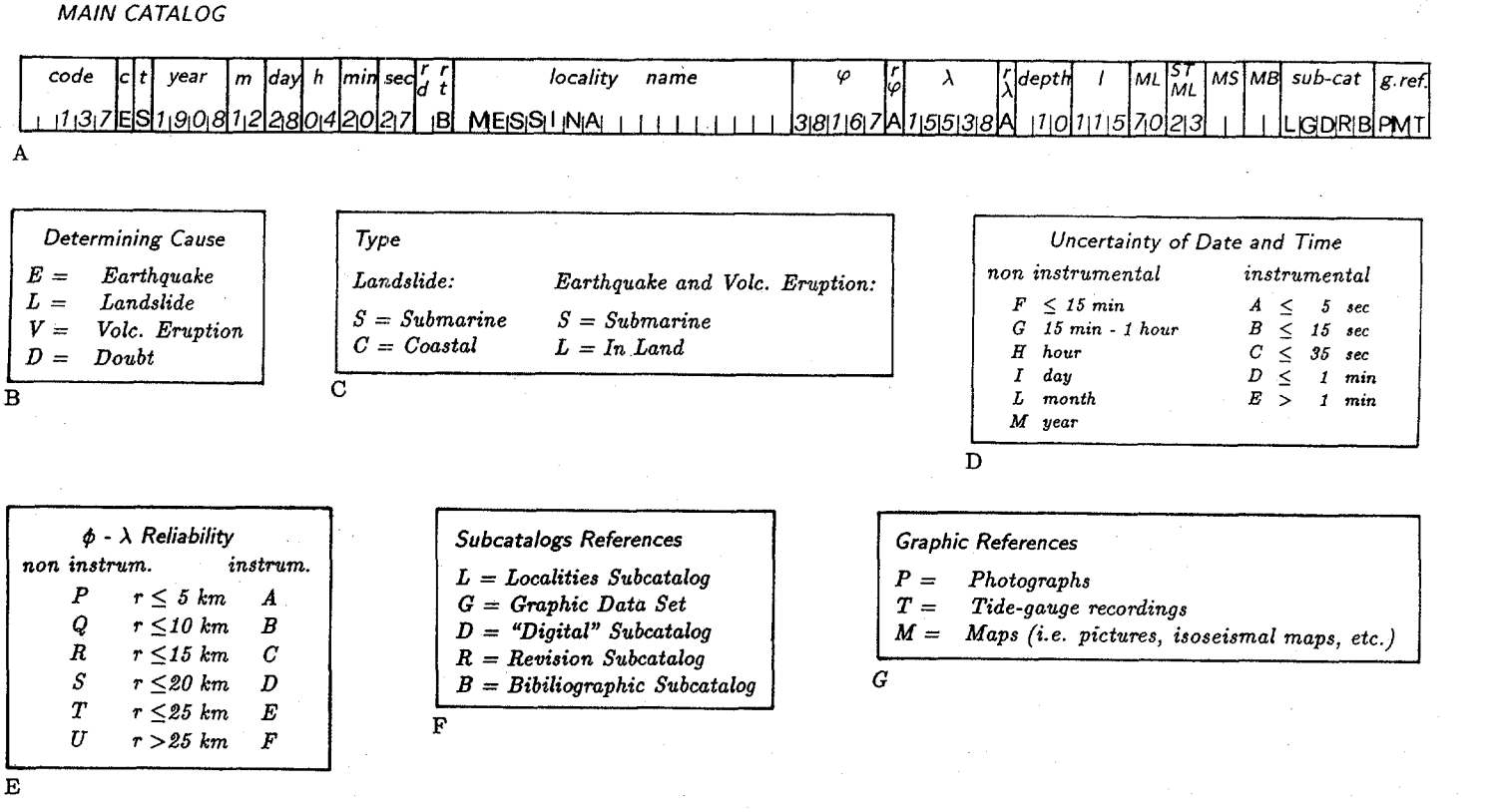

Figure 1: Example of the Main Catalog record (A) filled with data of the Messina tsunami (1908). In parts B to G the explanations of the items reported in the record itself are shown.

1.0- *Event Code*: the first item is a numeric code unambiguously identifying the event. It should be pointed out that the code may be used as a key to obtain all further information on the tsunami, contained in the subcatalogs.

2.0- *Determining Cause*: is a single character indicating the main cause of the tsunami. As explained in Figure 1- Part B, if the cause is an earthquake it is marked with the letter E, while V will be used for a volcanic eruption and L for a landslide. When the cause is unknown or uncertain, as often occurs for ancient events, the letter D (doubt) is used.

Detailed information on the determining cause is given in the items immediately following the first two, here after described in points 3.0 to 9.0. Generally, the largest number of information is available when the cause is an earthquake, while in the case of both a landslide and a volcanic eruption the non-empty items will be restricted to date and time, coordinates, name of the locality where the event took place and type of landslide or eruption.

3.0- *Type*: by means of a literal code is possible to know if the determining cause is submarine (S) or coastal (C) in case of lansdslides, submarine (S) or in land (L) in case of earthquakes and eruptions (see Figure 1- Part C).

4.0- *Date and Reliability Index*: the complete date of the cause includes year, month, day and hour in which the event took place. The related uncertainties are specified by means of a reliability index that is the item of the MC record denoted as "rd". The code, shown also in Figure 1- Part D, is: M = uncertainty in the year; L = uncertainty in the month; I = uncertainty in the day; H = uncertainty in the hour; G = uncertainty in the range 15 minutes - 1 hour; F = uncertainty $\leq$ 15 min. The non instrumental data generally refer to ancient events for which the uncertainty on the information is rather high.

5.0- *Time and Reliability Index*: complete information on time includes minutes and seconds of the onset of the tsunamigenic event. Typically this item, denoted as "rt" in the MC record shown in Figure 1, will be filled in only for causative events for which instrumental records are available. A letter code is again used as a relibility index (see Figure 1- Part D).

6.0- *Locality Name*: it is the geographical name of the place or of the region where the tsunamigenic event occurred (in the case of an earthquake it refers to the epicenter).

6.1- *Locality Coordinates and Reliability Indexes*: geographical latitude and longitude, both expressed in degrees and thousandths of degrees. In the example in Figure 1 the epicentral coordinates are reported, taken from the Italian seismic catalog (Console et al.,1979). Uncertainties in coordinates (reliability indexes) are expressed by a literal code based on a kilometric scale, displayed in Figure 1- Part E. In the MC record these indexes are indicated as "rϕ" and "rλ". In the case of an earthquake the "non instrumental" data come from macroseismical observations.

7.0- *Focal depth*: if the tsunami was caused by an earthquake three spaces in the MC record are reserved for the focal depth, expressed in kilometres. As regards Italy, this is taken from the Italian seismic catalog.

8.0- *Intensity*: always in the case of an earthquake, the next item is the epicentral intensity, here defined as the maximum value of the intensity felt in land, based on the Mercalli -Cancani-Sieberg (MCS) scale.

9.0- *Magnitude*: information about the tsunamigenic earthquake include magnitude value as well. As may be seen in Figure 1, we have a local magnitude (ML) and the number of stations used for its determination (ST-ML); then the surface-wave magnitude (MS) and the body-wave magnitude (MB) are reported. Also these data are taken from the seismic catalog.

As already mentioned, the largest number of information is obtained when the determining factor of the tsunami is an earthquake. Therefore, in the case of both landslides or eruptions (less frequent than earthquakes), the part of the MC record reserved for seismic data will remain empty.

10.0- *Subcatalogs References*: emphasis is here placed on the need for five subcatalogs (or collections), that integrate the main catalog, and that can be used separately for specific purposes. The first subsection (L) is the Localities Subcatalog and contains all the localities known to be affected by the tsunami; the second collection (G = the Graphic Data Set) reports all graphic information available for the event; the third one (D= the "Digital" Subcatalog) contains digitized mareograms (when available), the fourth subcatalog (R= the Revision Subcatalog) reports all updatings and revisions on the tsunami. Finally there is a fifth subcatalog (B= Bibliographic Subcatalog) for the bibliography used for the compilation

of the whole catalog. The detailed description of all above subsections will be given in the following. The item "sub-cat" in the MC record id used to specify the subcatalog or subcatalogs in which further information on the tsunami may be found. In this way, an overall picture is straightforwardly available of the kind of information archived for the tsunami of interest (see Figure 1- Part F).

11.0- *Graphic References*: the last part of the MC record gives some further information about the graphic data set; in fact this part allows to know immediately what kind of graphic data are contained in the graphic subcatalog. The explanation of this part is shown in section G of Figure 1.

The Localities Subcatalog

A tsunami, depending on its size, usually involves several localities along the coast, in different times and with different effects. It is therefore necessary to create a data bank containing information on all localities affected by the event. To this purpose, a localities subcatalog has been devised where all the places involved in the same tsunami are listed in correspondence with the same code number used to identify the event in the Main Catalog. Figure 2 shows an example of three records of this subcatalog all referring, for convenience, to the Messina tsunami already described in Figure 1. To analyse all information reported in the record of the Localities Subcatalog (LS), see Figure 2.

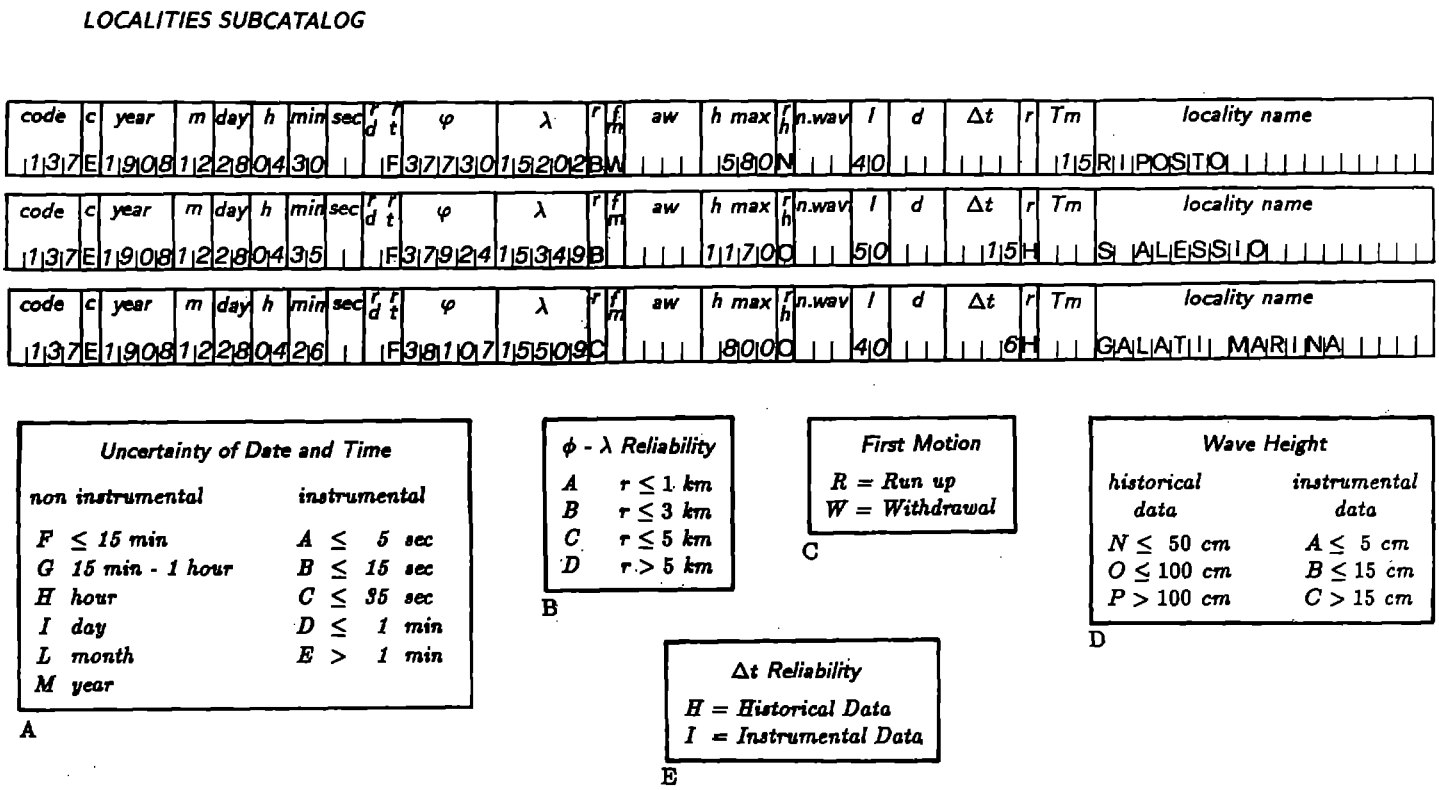

Figure 2: Example of three records of the Localities Subcatalog referred to the Messina tsunami. In parts A to E the explanations of the items reported in the records are shown.

1.0- *Event Code*: as in the MC record, also in this record the first item is the code of the event which plays a fundamental role in identifying the number of localities affected by the same tsunami.

2.0- *Determining Cause*: by means of the same letters used in the MC record, the main cause of the tsunami is reported.

3.0- *Date and Reliability Index*: in the LS record the date in which the tsunami took place at a specific locality is reported. The complete date includes year, month, day and hour: for these data a reliability index (the item "rd" in the LS record) is used to specify the uncertainties. This index is expressed by means of different letters for instrumental and non-instrumental data, as shown in Figure 2 - Part A.

3.1- *Time and Reliability Index*: if tide-gauge are available, complete information on time includes also minutes and seconds in which the tsunami affected the locality of interest.(Of course it's usual to find different times for different localities involved in the same tsunami, according to the distance of the locality from the source). A letter code is again used as a reliability index ("rt" in the LS record), as in Figure 2 - Part A.

4.0- *Locality Coordinates and Reliability Index*: for each locality affected by the tsunami geographical coordinates, expressed in degrees and thousandths of degrees, are reported. Any uncertainties that may arise based on the extent of the locality itself along the coast are expressed by a literal code (item of the LS record denoted as "r"). This reliability index is based on a kilometric scale and shown in Figure 2 - Part B.

5.0- *First Motion*: next item in the LS record is the first motion of the sea, denoted as "fm". It allows to know the behaviour of the sea at the beginning of the phenomenon at each locality; i.e. if the sea recedes from the coast or runs up suddenly flooding the coast itself also for many metres. This datum is expressed by means of two letters: R = run up, W = withdrawal (see Figure 2 - Part C).

6.0- *Amount of Withdrawal*: if the first motion is a withdrawal, the item of the LS record denoted as "aw" is the amount of the withdrawal itself, expressed in metres.

7.0- *Wave Height*: it is the maximum height reached at each locality, in centimetres. It is necessary to distinguish instrumental data from historical ones; to this purpose different letters are used in the part of the LS record denoted as "rh" (see Figure 2 - Part D).

8.0- *Number of Waves*: for a full description is very interesting to know some peculiar information as, for instance, the number of waves observed at a specific locality during the event. This datum is reported in the LS record in the space called "n.wav.".

9.0- *Intensity*: on the basis of the effects produced by the waves on the coast in a specific locality, it's possible to evaluate the tsunami's intensity at that locality, referred to the modified Sieberg scale (Ambraseys, 1962). In the LS record this information is denoted as "I".

10.0- *Perturbation Lenght*: the item of the LS record indicated as "d" reports the duration of the perturbation observed at each locality, expressed in hours. Generally this datum is very questionable in term of precision, unless instrumental data are available.

11.0- *Travel-Time and Reliability Index*: in the LS record the three spaces marked with "Δt" contain information about the travel-time. It is the time, in minutes, taken by a wave to reach the locality of observation from the source. In the case of non-instrumental data (historical data) this parameter is quite uncertain because it is related to the origin time of the tsunamigenic event and its reliability index. If instrumental data are available, this parameter can give important information about the source of the tsunami. Therefore a reliability index is introduced, by means of a literal code, in order to distinguish if we have a historical datum (H) or an instrumental one (I) (see Figure 2 - Part E)

12.0- *Wave Period*: if instrumental data are available, in the LS record the mean period of the waves is reported ("Tm"). It is obtained by the mean of the first three waves reached at the locality of

observation.

13.0- *Locality Name*: the last item in the LS record is the name of the locality involved by the tsunami.

Graphic Data Set

This subcatalog is a collection containing the graphic material - photographs, maps, tide-gauge recordings, drawings, etc.- related to a specific tsunami. All the material referring to the same tsunami is gathered under the same code number used to identify the event in the Main Catalog and in the subcatalogs. Figure 3 shows an example of some photographs and tide-gauge recordings for the Messina tsunami hold in this data set.

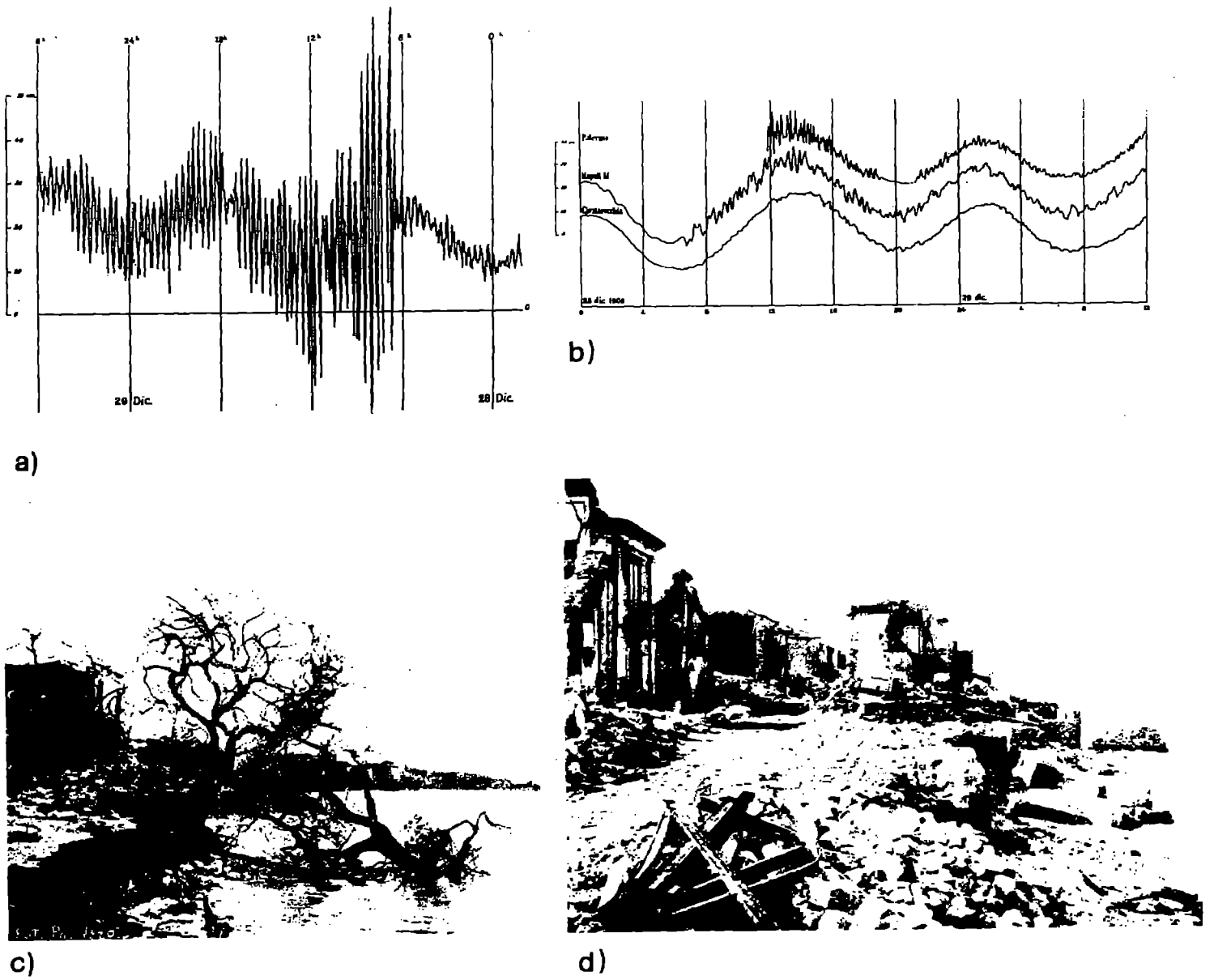

Figure 3: Tide-gauge recordings of Malta (a) and Palermo, Neaples and Civitavecchia (b) for the Messina tsunami. The two photographs show the damages produced by the tsunami respectively in Archi (c) and Pellaro (d). (after Platania,1909)

"Digital" Subcatalog

This subcatalog collects all the digitized waveforms of the tide-gauge recordings, when they are available.

Revision Subcatalog

The data stored in the Main Catalog and in all the subcatalogs are often subject to changes and updatings following further researches. The Revision Subcatalog (RS) consists of a file containing one or more record for each event that underwent changes (i.e. in the date or time of the event, intensity, height of the waves, etc.). In each RS record the old data are retained, supplied with the date of the variation. Moreover, if an event is considered false during the study, it is removed from the Main Catalog but it is conserved in the Revision Subcatalog.

Bibliographic Subcatalog

This subsection consists in a file containing all the sources utilized to describe a specific tsunami, collected under the same code number. Therefore, if it is necessary to see which references were used to study a tsunami, it is sufficient to enter into the file recalling the code number of the pertinent event. In Figure 4 an example of a part of the file containing the sources for the Messina tsunami is shown.

137

ALFANO G. B. - "Gli epicentri sismici dell'Italia con particolare riguardo a quelli rovinosi, disastrosi e disastrosissimi", Bollettino Società Naturalisti in Napoli , vol XLVI, Atti, Napoli 1934.

BARATTA M. (1936)- I terremoti d'Italia. "R. Acc. Naz. Lincei", pubblic. della Comm. ital. per lo studio delle grandi calamità, vol. VI. Le Monnier, Firenze 1936.

CAVASINO A. (1935)- I terremoti d'Italia nel trentacinquennio 1899-1933. App. al vol. IV, sez III delle memorie R. Uff. Centr. Meteorologia e Geofisica. Istituto Poligrafico dello Stato, Roma 1935.

CAROZZO M.T., DE VISINTINI G., GIORGETTI F., IACCARINO E. (1973)- General Catalogue of Italian earthquakes. Comitato Nazionale Energia Nucleare (CNEN) RT/prot. (73) 12, Roma 1973.

HECK N. H. (1947)- List of seismic sea vawes. "Bull. of Seism. Soc. of america", 37, October, 1947, n.4.

PLATANIA G. (1909)- Il maremoto dello Stretto di Messina del 28 Dicembre 1908. "Boll. Soc. Sism. Ital.", vol. XIII, 1908-1909.

Figure 4: Example of a part of the file of the Bibilographic Subcatalog referred to the Messina tsunami. All texts are collected under the code number (137).

REFERENCES

Ambraseys N.N.,1962. Data for the investigation of the seismic sea-waves in the eastern Mediterranean. *Bull.Seism.Soc.Am.*, vol.52, n.4, pp.895-913.

Console R.,De Simoni B.,Gasparini C.,Marcelli L.,Spadea M.C.,Vecchi M., 1979. Preambolo al Catalogo Sismico Nazionale (Forward to the National Seismic Catalogue). *Annali di Geofisica*, vol.XXXII, pp.37-77.

Platania G.,1909. Il maremoto dello Stretto di Messina del 28 dicembre 1908. *Boll.Soc.Sism.Ital.*,vol XIII, f. 7-8, pp. 369-464.

COASTAL ALGERIAN EARTHQUAKES: A POTENTIAL RISK OF TSUNAMIS IN WESTERN MEDITERRANEAN ? PRELIMINARY INVESTIGATION

A. YELLES CHAOUCHE

Centre de Recherche en Astronomie, Astrophysique et Geophysique (C.R.A.A.G.), B.P. 63, Bouzareah, Algiers, Algeria.

ABSTRACT

A careful analysis of the algerian seismic catalogs and other reports has revealed several examples of tsunamis that have occurred along the Algerian coast (Algiers, 1365; Djidjelli, 1856...). Results of this first investigation indicate that the shallow coastal seismicity of the northern part of Algeria, as well as the associated submarine slides of unconsolidated sediments in the Algerian continental slope, may be responsible of these tsunamis. Their occurrence, with a severity however much less important than that of the major tsunamis in other regions, requires intensive investigations for a reliable determination of the tsunami hazard along the Algerian coast.

1. INTRODUCTION

Historically, the Western Mediterranean basin in comparison with other regions (the Pacific and Atlantic Oceans, the Eastern Mediterranean) has been less affected by important tsunamis. However, careful analysis of historical documents and recent obsevations have shown that coastal earthquakes and submarine slide-generated turbidity currents taking place in this area might be responsible for tsunamis of various size. Indeed, several examples could be mentioned: in the region around Nice in 1887 (Capponi et al., 1980) and 1979 (Genesseaux et al., 1980); on the eastern coast of Sicily (Guidoboni and Tinti, 1990); on the spanish coast (Campos, 1990); and all these examples point out the actual risk of tsunamis in the Western Mediterranean sea.

In Algeria, little is known about sea level oscillations affecting the Algerian coast. The first reason of this is because of the relatively rare occurrence of these phenomena. The second reason is the scarcity of historical reports and a further reason is the lack of adequate equipment. At the Algerian Geophysics Center (C.R.A.A.G.), these investigations have been just started with the main purpose of evaluating and quantifying the risk of tsunamis generated by local and remote sources, particularly of those events determined by the Algerian coastal seismicity that could appear as one of the major causes of tsunamis in the Western Mediterranean sea. In this paper, some characteristics of the Algerian seismicity are presented, in consideration of their importance in the tsunami generation. In the second part of the paper several examples of tsunamis observed along the Algerian coast will be illustrated.

2. ALGERIAN SEISMICITY

Algerian seismicity is known from the fourteenth century when the first earthquake was described and reported on documents (As Suyuti, 1505; Delphin 1922). It occurred on January 2nd, 1365 in Algiers and destroyed almost all the town. In order to synthesize all Turkish and French archives containing reports on historical earthquakes, various seismic catalogs were been compiled during the last decades (Rothé, 1950; Grandjean, 1954; Benhallou and Roussel, 1971; Benhallou, 1980). Their analysis reveals that the algerian seismicity is essentially concentrated in the northern part of the country. Taking into account the varied geological setting of this area forming the southern branch of the Alpine chain, the seismic activity can be mainly divided into three zones: the Tellian Atlas, the High Plateaus and the Saharian Atlas (see Fig. 1). On considering the location and the occurrence frequency of Algerian earthquakes, one can conclude that the Tellian Atlas and its coastal front are the most important seismic zones. These zones, directly exposed to the collision between the African and the European plates, are more deformed than the others, which induces a more intense seismic activity. Recently these areas were subjected to several large events that provided valuable information about the tectonics of North Algeria. Among these events we can mention the El-Asnam earthquakes (1954 M=6.7 and 1980 M=7.3), the Constantine earthquake (1985 M=6.0) and the Tipaza - Mt Chenoua earthquake (1989 M=6.1). A summary of the most important results obtained from studying these events can be outlined as follows.

The El Asnam (west central Algeria) earthquake of October 10th, 1980, the most important event recorded in northern Algeria, was of magnitude M_S=7.3. It was due to a thrust fault, visible at the Earth surface for a distance of about 40 km in length, dipping 52° to the NW and associated with a fold oriented N70 (Meghraoui, 1988). The focal mechanism, in a remarkable concordance with surface tectonics and aftershock distribution, displayed a left lateral thrusting movement (Ouyed et al., 1981). The results of different studies carried out after this event, have pointed the importance of compressional phenomena that actually affect the Tellian Atlas, confirming at the same time the NNW-SSE shortening direction between the European and African plates (Mc Kenzie, 1972).

The Constantine (eastern Algeria) earthquake occurred five years later on October 27th, 1985 and was of magnitude M_S=6.0. Results of field observations and station recordings indicated pure sinistral shearing along a N45 nearly vertical fault plane (Bounif et al., 1987).

More recently, on October 29th, 1989, the northern part of the Tellian Atlas (Tipaza region, central Algeria) was once again shaken by an earthquake of magnitude M_L=6.1 causing 29 victims. In the seismic sequence that followed, several important aftershocks, most of them located offshore, were recorded. The macroseismic epicenter of the main shock was located at Sidi Amar, a small village 80 km west of Algiers (Fig. 2). Field investigations in the epicentral area showed discontinuous surface ruptures over 5 km with an average displacement of 7 cm and corresponding to flexure slip on folded terrains (Meghraoui, in press). The focal mechanism solution, calculated from first motion polarities observed on long and short period seismograms of global networks (WWSSN, GDSN) yielded to a reverse faulting mechanism associated with a fault plane striking N45 and dipping 60° to the northwest (Bezzeghoud et al., in prep.). One interesting aspect of this event is the distribution of the seismicity between the continent and the offshore side involving an offshore extent of 20 km of the inland faulting. Hence, this event reveals that many coastal earthquakes recorded previuosly could have been mislocated as the offshore seismicity has been very often dubious.

From a global review of all results obtained from the study of coastal events, several relevant points can be emphasized. First of all, it is now well established that this seismic activity is the consequence of the convergence between the European and African plates inducing in some cases large events that cause severe damage to human environment (buildings, dams...). On land, landslides as well as fault escarpment and liquefaction phenomena can be sometimes observed.

In the three previous examples, we could note that the seismicity is differently expressed from east to west. Meghraoui (1988) indicates that, in fact, two domains can be distinguished. He explained that, in the east, recent tectonics is manifested in the meridional Tell by an E-W major dextral strike-slip fault and by NE-SW sinistral dip-slip and strike-slip faults. In south Bejaia (200 km east of Algiers) and towards the Hodna basin, the strike-slip faults are associated with folds and could present a reverse mechanism. In the west, the deformation showing a NNW-SSE compression is expressed in the northern Tell inside Plio-Quaternary basins such as the Mitidja and the Cheliff basins. Thrust faults are the main active structures occurring in these regions.

Offshore, the seismicity is lower and is distributed all over the margin. Some authors (Auzende, 1975) suppose that this seismicity may result from a subduction process between the African and the European plates, but no evidence of a Benioff zone has been yet demonstrated. On the other hand, the coastal distribution of these earthquakes indicate that these events could be generated by structures that correspond to the extent of those seen inland as it was observed in the last Tipaza - Mt Chenoua earthquake. Hence, the offshore deformation pattern could be, for some events, similar to that observed for events occurring on the continent.

From the study of the El-Asnam earthquakes it has been proven that these strong coastal earthquakes destabilized the unconsolidated sediments of the continental slope inducing turbidity currents (El Robrini et al., 1985). Furthermore, one of the characteristics of the algerian earthquakes is their shallowness. A statistical study carried out by Roussel and Benhallou (1971) points out that the most frequent depth of algerian earthquakes is around 8 km and that no earthquakes over a depth of 20 km have been recorded so far. Finally, our investigation has revealed that several coastal earthquakes have induced tsunamis of various size.

In the following part, we will present the different cases where tsunamis have been observed along the algerian coastline. In concluding this section, it is important to stress that the occurrence of these tsunamis leads to the evidence that the particular characteristics of the coastal earthquakes presented above plays an important role in their generation.

3. ALGERIAN TSUNAMIS

Because of the inexistence of archives concerning tsunamis in the algerian administration or in other public officies (libraries...), identification of different algerian tsunamis was carried out from the various seismic catalogs or from previous works on algerian seismicity (Rothé, 1950; Ambraseys, 1982, 1988).

The first historical algerian tsunami corresponds to the first reported known algerian earthquake (January 2nd, 1365) in the catalogs. Ambraseys and Vogt (1988) who mention this event indicate that part of the city of Algiers was flooded at that time.

Rothé (1950) as well as Ambraseys and Vogt (1988) mention that the violent shock of November 8th, 1802 that occurred in the region of Kolea (20 km west of Algiers) was felt on board by several ships 30 miles offshore and that agitation of the sea in the Bay of Algiers was observed.

Continuing their description of the most important earthquakes that affected Algiers region and its surrounding, Ambraseys and Vogt (1988) report that the strong earthquake that shook the region of Gouraya (200 km west of Algiers) on January 15th, 1891 was followed by a tsunami: to a first withdrawing of the sea of about 30 m followed a return that flooded the shore. Six miles away from Cape Cherchell, a Norvegian ship called "Porro" reported three of four large waves travelling from south to north.

The Tsunami of Djidjelli, August 21st, 1856

Because of the severity of the phenomenon, the Djidjelli tsunami of August 1856 has been extensively described. Thus, compilation of all reports and documents allowed Rothé (1950) and Ambraseys (1982) to provide a lot of information relative to this event. The authors report that on August 21st, 1856, Djidjelli, a small town located 300 km east of Algiers, was hit by a strong earthquake felt over a large area (i.e. from Algiers in the west to La Calle in the east and from Batna in the south to Nice in the north) in a radius of about 700 km. The shock was strongly felt by the aviso "Tartar", 15 miles N 7E of Djidjelli on which the crew were almost thrown on deck. Ambraseys mentions that, following the shock, the sea retired for some distance and suddenly returned flooding the low lying part of the coast. On the following day, a second important shock of intensity VIII almost destroyed the town (Fig.3). A water wave 2 to 3 m high, triggered by the shock, flooded the coast a number of times and during three days the sea remained turbulent. At Bougie, the sea withdrew about 35 m and then returning, flooded the shore three times. As to the other localities, the authors mention that at Mahon (Minorca) flooding of the harbour led to the brake of the boats moorings. All the information obtained from this seismic crisis supports the evidence that the epicentral region could have been located few kilometers north of Djidjelli and that the tsunami would have been generated by a turbidity current similar to that triggered by the Orleansville earthquake of September 9th, 1954.

More recently, Campos (1990), in her study of the tsunami hazards on the Spanish coasts, assumes that the two earthquakes of El-Asnam region (1954, 1980) produced tsunamis that were recorded by Spanish stations. Thus, the author reveals that the tsunami generated by the first earthquake took 180 min to reach Malaga and 50 min to reach Alicante where a rising of tide level of 34 cm was noticed. The second event produced oscillations on tide levels in Alicante, Malaga, Ceuta and Algesiras.

Following the last earthquake that occurred in the Tipaza region (October 29th, 1990), interviews of inhabitants of the coastal villages have been carried out by a C.R.A.A.G. team. Among the persons who were at that time in the port of these villages some of them remarked an unusual agitation of the ships and a small rising of the sea. Some fishermen explained that the shock was strongly felt on board of their boats which were moved up by an anomalous seawave. However, analysis of the recently installed tidegauge in the Algiers harbour shows no special signal neither for the main shock of the October 29th nor for the strong aftershock of April 12th, 1990 (M_L = 5.2) (see Fig.3).

4. CONCLUSIONS

Our first investigation has revealed that several tsunamis have been observed along the Algerian coast. Although these tsunamis have, in general, locally affected the Algerian coast, the previous examples have revealed that in some cases their effects were felt in the surrounding areas.

Among the various sources which could be involved in the generation of these tsunamis are the large coastal earthquakes. At present, nothing is known about their

own capacity to trigger tsunamis. We only know that a part of these coastal earthquakes have generated sea wave oscillations and we suppose that the characteristics presented above, such as shallowness for example, play a role in the triggering of these tsunamis. On the other hand, recent studies have proven that the sediment cover in the continental slope could be destabilized by these large earthquakes and consequently the generated submarine slides could produce tsunamis.

Compared to other regions, the tsunami hazards in Algeria seems to be rather low. Nevertheless, the analysis of historical documents reveals that there is a clear risk that is important to evaluate.

AKNOWLEDEMENTS

I would like to thank my colleagues M.Meghraoui and M.Bezzeghoud for helpful discussions.

REFERENCES

As Suyuti, J.E.D., 1973. Kashf al salsala an wasf al zalzala, 1505; translated in french by Said Nejjar, chaiers du Center Universitaire de la Recherche Scientifique, Rabat.

Auzende, J.M., Bonin, J. and Olivet, J.L., 1975. La marge Nord-Africaine considéree comme marge active, Bull. Soc. Geol. France, XVII, 486–495.

Ambraseys, N.N., 1982. The seismicity of North Africa. The earthquake of 1856 at Jijelli, Algeria, Boll. Geofis. Teor. Appl., 24, 93, 31–37.

Ambraseys, N.N. and Vogt, J., 1988. Material for the investigation of the seismicity of the region of Algiers, European Earthquake Engineering, 3.

Benhallou, H., 1985. Le catastrophes seismiques de la region d'Ech-Cheliff dans le contexte de la sismicité historique de l'Algerie, Tesis Doctorat, USTHB, Algiers.

Benhallou, H. and Roussel, J., 1971. Sur le seismes et la sismicité de l'Algerie de 1951 à 1970, Note IMPGA, 4.

Bounif, A.H., Haessler, H. and Meghraoui, M., 1987. The Constantine (northeast Algeria) earthquake of October 27, 1985, surface ruptures and aftershock study, EPSL, 85, 451–460.

Bezzeghoud, M., Bonin, A. and Boughacha, M., Preliminary seismological study of the Mt Chenoua - Tipaza earthquake (in preparation).

Capponi, G., Eva, C. and Merlanti, F., 1980. Il terremoto del 23 febbraio 1887 in Liguria occidentale, Atti dell'Accademia Ligure di Scienze e Lettere, 37.

Campos, L., Tsunami hazard on the Spanish coast of the Iberian peninsula (this issue).

Delphin, G., 1922. Histoire des Pachas d'Alger, Journ. Asiatique.

El Robrini, M., Genesseaux, M. and Mauffret, A., 1985. Consequences of the El-Asnam earthquakes: turbidity currents and slumps on the Algerian margin (western Mediterranean), Geo. Mar. Lett., 5, 171–176.

Genesseaux, M., Mauffret, A. and Pautot, G., 1980. Les glissements sous marins de la pente continentale et la rupture des cables en mer ligure (Mediterranée occidentale) CRAS, Paris, 290, 959–962.

Guidoboni, E. and Tinti, S., 1990. The 4 February 1169 tsunami in eastern Sicily, Italy, Ann. Geophys., p.333.

Meghraoui, M., 1988. Geologie des zones seismiques du nord de l'Algerie, Tesis Doctorat, University of Paris Sud.

Meghraoui, M., Blind reverse faulting system associated with the Mont-Chenoua-Tipaza earthquake of October 1989 (submitted).

Mc Kenzie, D.P., 1972. Active tectonics of the Mediterranean region, Geophys. J.R. Astr. Soc., 30, 109–185.

Ouyed, M., Meghraoui, M., Cisternas, A., Deschamps, A., Dorel, J., Frechet, J., Gaulon, R., Hatzfeld, D., and Philip, H., 1981. Seismotectonics of the El Asnam earthquake, Nature, 292 (5818), 26–31.

Rothé, J.P., 1950. Les seismes de Kherrata et la sismicité de l'Algerie, Publ. Sev. Carte Geol. de l'Algerie, 24, pp 40.

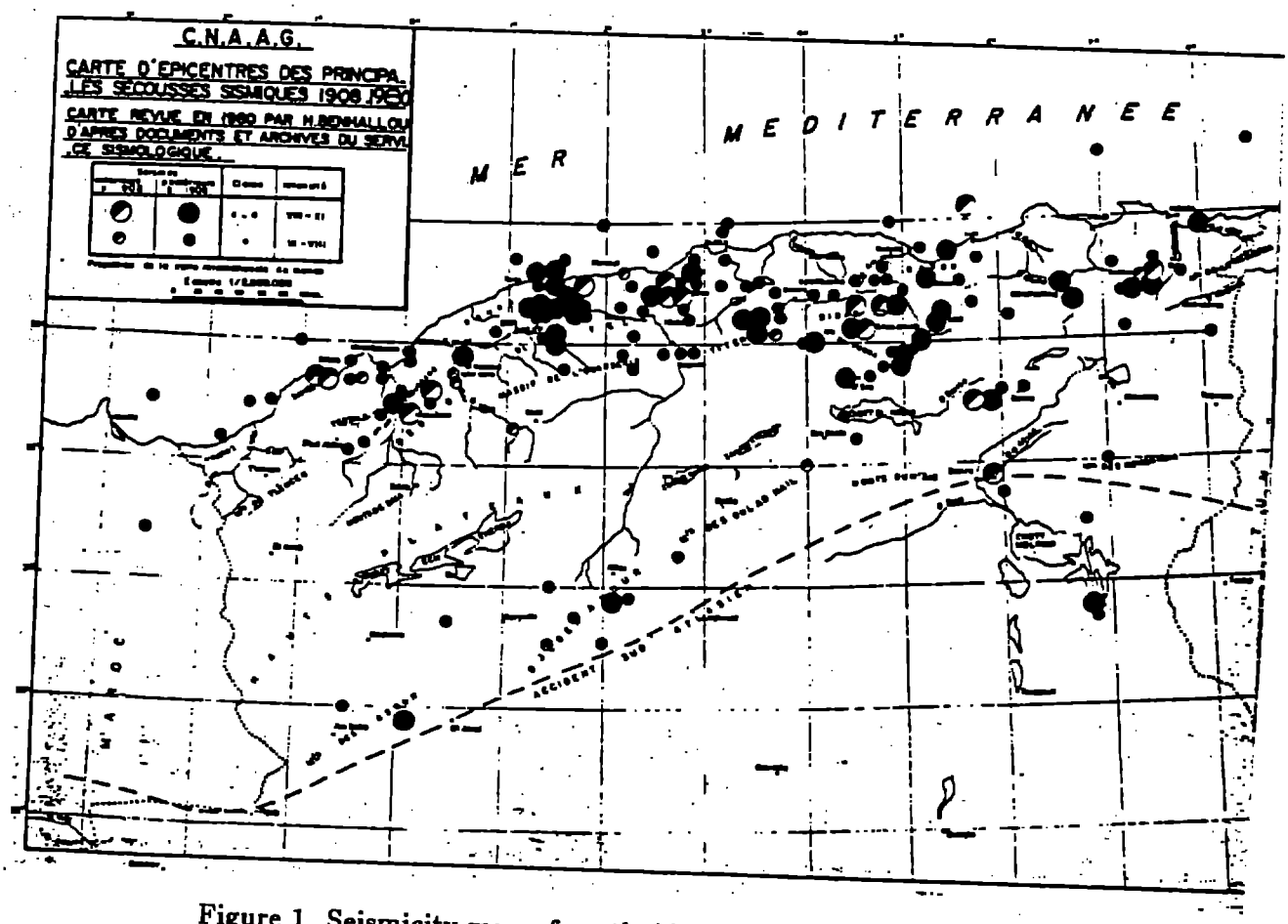

Figure 1. Seismicity map of north Algeria (from Benhallou, 1985).

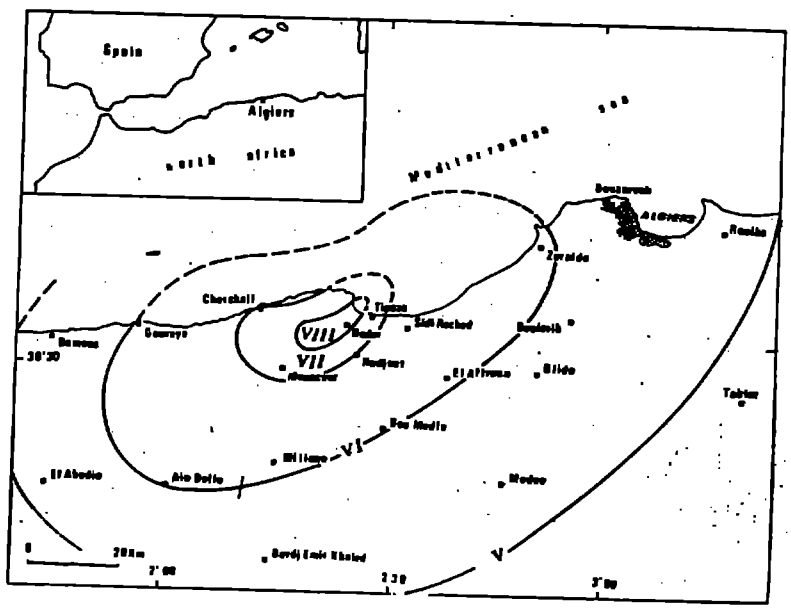

Figure 2. Isoseismal map of the Mt Chenoua - Tipaza earthquake of October 27th, 1989.

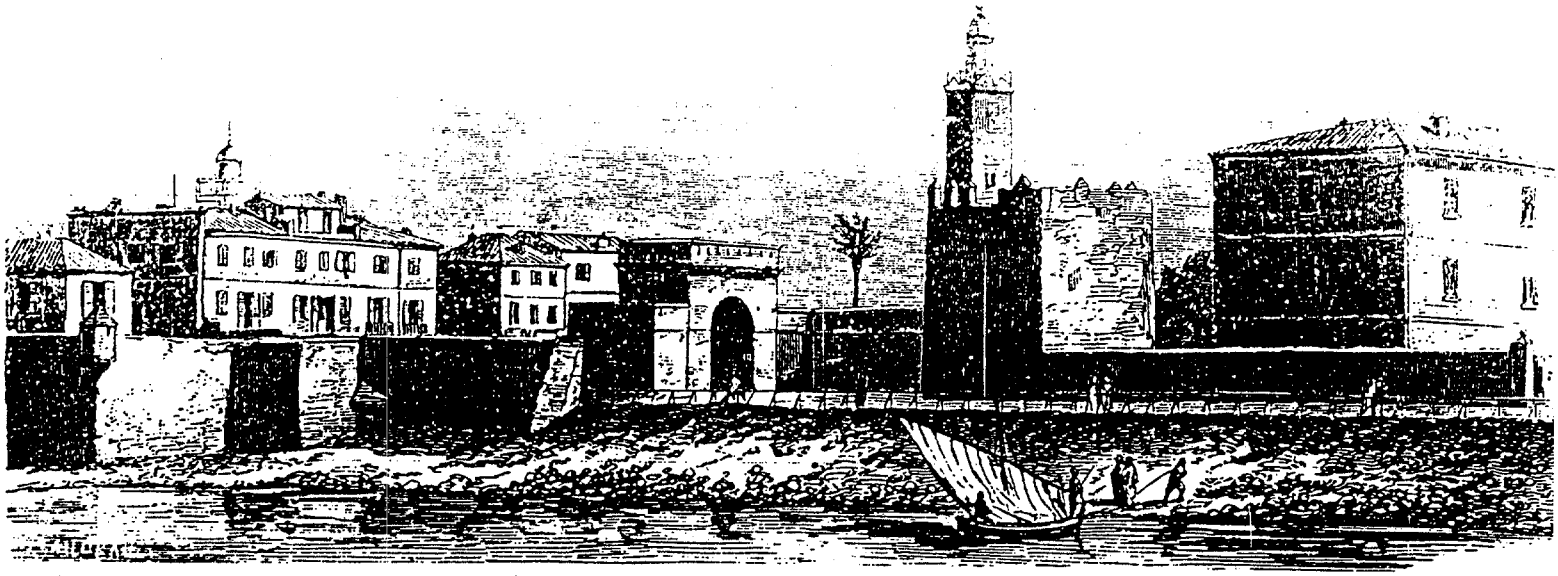

Côté ouest de la ville de Djijelly,l'avant le tremblement de terre du 22 août 1856.

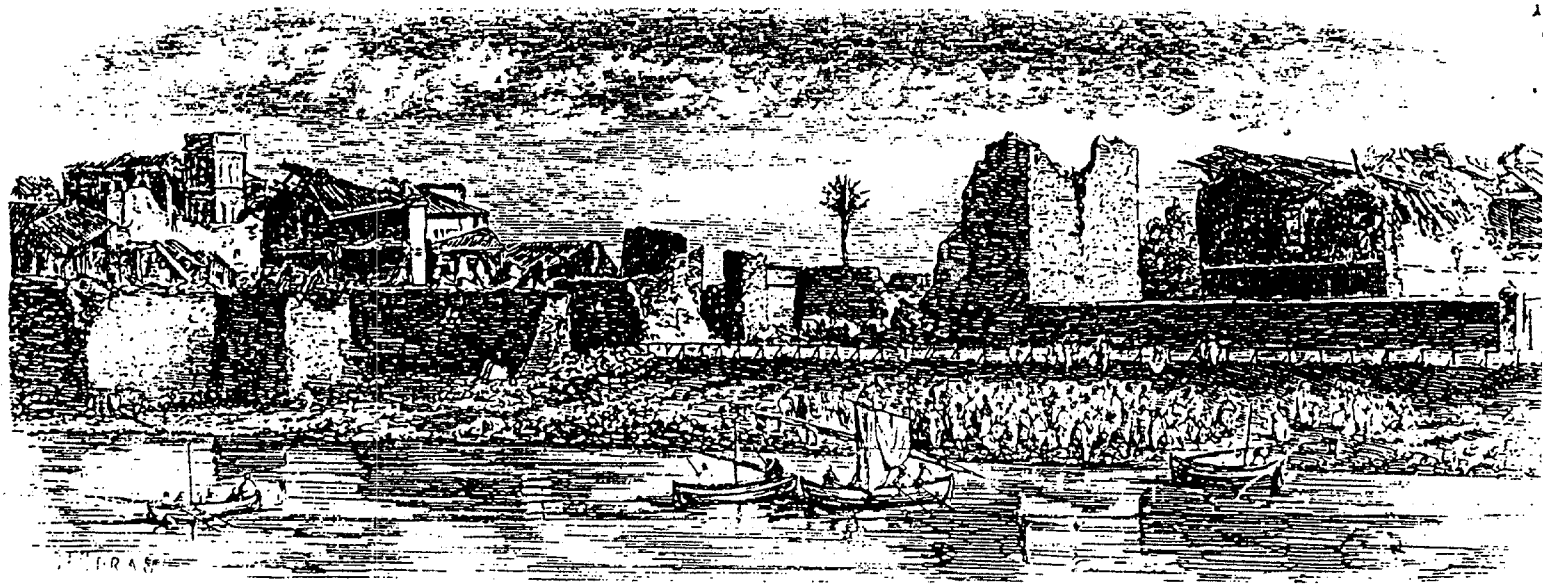

Aspect du même côté de la ville après le désastre.

Figure 3. Pictures from lower part of Djijelli before and after the earthquake of August 22nd, 1856 (from Ambraseys, 1982).

THEORETICAL AND EXPERIMENTAL TSUNAMIGENIC MODELS TO STUDY INLAND ACTIVE GEOSTRUCTURES

G. FINZI-CONTINI

Dipartimento di Ingegneria Civile, Università di Firenze,
Via di Santa Marta, 3, 50139 Firenze, Italy.

ABSTRACT

This specific work has been done in the frame of researches envisaged to propose interpretations of certain local shallow earthquakes (that is those earthquakes that have a hypocenter at 5–40 km depth and that, with reference to the Adriatic foredeep, are located along the eastern side of the Italian peninsula) and extended to investigate local tsunami generation (Finzi-Contini, 1977, 1981a, 1981b, 1982a, 1982b, 1986, 1988, 1989a and 1989b).

In order to clarify some kinematical features of the proposed tsunamigenic mechanism, very simple experimental models are described. Their response is compared with that of suitably devised mathematical models.

1. Introduction

According to a number of geodynamical and geophysical evidences (Giese and Morelli, 1975; Mongelli et al., 1975), a very schematic uni–dimensional visco–elastic model was suggested by the author (Finzi–Contini, 1977) in order to explain certain features characterizing the eastern side of the Apennine ridge, running along the Italian peninsula: namely the horizontal deformations and the qualitative distribution of seismic events. Subsequent developments of this visco–elastic approach (Finzi–Contini, 1982a and 1982b) – supported by further pieces of information (Corrado and Rapolla, 1977; Scandone, 1979) – have provided a more adequate representation for a mechanism able to justify particular families of seismic events having a hypocenter in the 5–40 km depth range.

2. Recent visco–elastic models and possible tsunami generation

It has to be emphasized that one advantage of the visco–elastic approach is that it takes into account even very small stresses that are able to induce continuous deformations within the considered geo-structures, no equilibrium configuration being reached, whereas the opposite case holds for elastic systems. In particular, this scheme represents geophysical responses of sub-regional situations (Finzi-Contini, 1982a, 1982b and 1986), repeatedly occurring along the Apennine ridge (see for example Salati, 1971 for the Modenese Apennine): from SE to NW, that is from Irpinia to Romagna, one can see sub-regional gravimetric highs along an evident gravimetric trough parallel to the ridge itself (Adriatic foredeep), those highs being related to topographical highs and groups of seismic events (see also Mantovani and Boschi, 1982). In addition to this, relation with geothermal features has been shown (Panichi et al., 1982; Finzi-Contini, 1988). All these aspects are illustrated in Figures 1 to 3.

Effects produced by sudden perturbations for elementary examples have been already described by using Laplace transform procedures in connection with both hazard and energetic considerations (Finzi-Contini, 1989a and 1989b). Summarizing, the used visco-elastic approach accounts for quite a large group of mechanical phenomena, ranging from very short time scale events to extremely slow surface evolutions, such as landslides possibly caused by geo-structures acting from below (Finzi-Contini, 1986; see also Almagià, 1931; Cavasino, 1931; Oddone, 1931; Crescenti, 1982; Crescenti et al., 1983). More recent studies in the area of the finite-element theory are developing this line of research. (Finzi-Contini and Majorana 1989a and 1989b; Finzi-Contini et al., 1989a and 1989b).

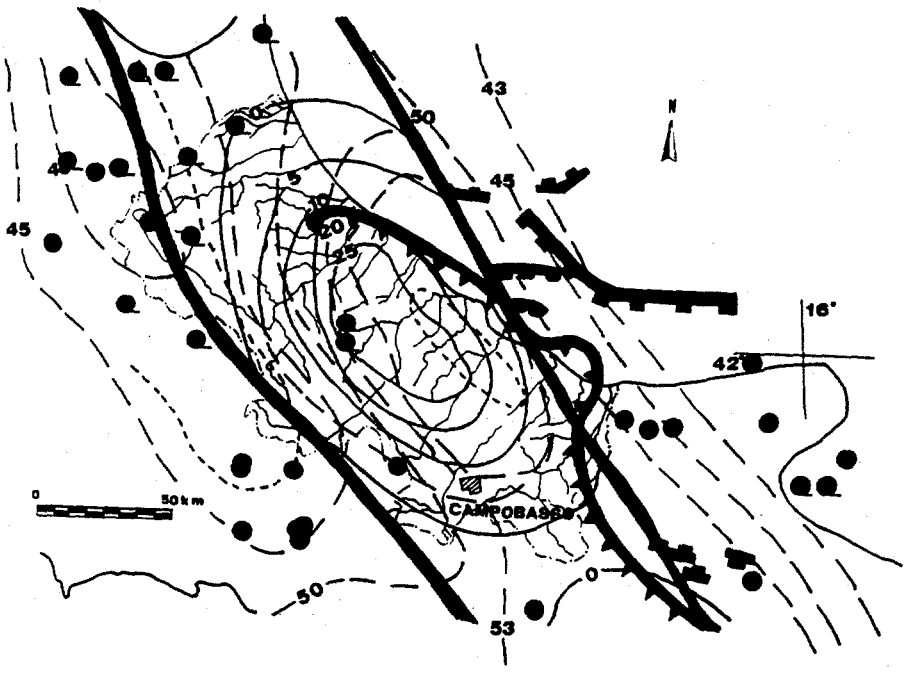

Figure 3. A more detailed picture of the Maiella topographic high area (Finzi-Contini, 1988). Dots represent epicenters: simple dots (M larger than 3), dots with bar (M larger than 4). Continuous heavy lines mark the zero-borders of the gravimetric negative trough, running parallel to the Apennine ridge.

3. The proposed inland tsunamigenic mechanism

According to a suggestion by Soloviev (Soloviev, 1989; Finzi-Contini, 1989b), particular attention has been devoted in selecting those situations suitable to admit tsunami generation associated with inland collapse mechanisms.

3.1 A simple tsunamigenic mechanism.

At this stage of the present research, only elementary geo-structures are considered in order to discuss a simple tsunamigenic mechanism. The tsunamigenic geo-structures consists indeed of a model-land, a model-sea and a model-perturbation as may be seen in Figure 4.

This geo-structure is pseudo-twodimensional, in the sense that the generated model-tsunami can be described by a unidimensional independent coordinate, say x, at the instant of the sudden perturbation imposed to the model-land. At this instant, a new approximate profile (y coordinate) for the model-sea can be drawn. The model-land deformation may be studied by means of the Laplace transform techniques, as mentioned earlier on. The motion of the sea-model after the time of the sudden perturbation is not considered in detail by this work, since the attention is mainly focused on the generation phase.

3.2 Laboratory experiments.

At this propaedeutic level, it has been considered useful to arrange a tentative experimental model, in order to inspect certain qualitative features of the

seismogenetic model concerning tsunami generation. At present, the experimental model is proposed in a one-dimensional version, since it is much simpler to build up. The suggested model scheme is shown in Figure 5, while the experimental results are presented in Figure 6.

Actually, in the laboratory experiments that are presently being carried out, the model-land is simulated by a mainly elastic rubber plate, about 1 cm thick, 30 cm wide and 120 cm long. This rubber plate is suddenly stressed according to the scheme shown in Figure 5, which is the model-perturbation phase. The model-sea is simulated by a commercial fluid soap. At this stage of the work, the model-sealine movements can be easily appreciated by careful visual inspections on a reference ruler.

4. Preliminary conclusions

A number of positive conclusions can be already suggested at this level of the present research programme, even in spite of the very limited financial support.

Firstly, the suggestion by Soloviev appears quite consistent with the basic shallow earthquake seismogenetic model already discussed elsewhere.

On the other hand, the possibility of building up an experimental laboratory model to study the transient aspects of the considered phenomena seems very profitable, also in view of three-dimensional extensions.

In addition to this, the possibility of using different viscous fluids to obtain model responses enlarges the model reliability, also with regard to qualitative simulations of actual case histories.

Acknowledgements

I am personally indebted to Dr. Soloviev, who suggested to me to extend my visco-elastic seismogenetic model research towards the exciting sphere of tsunamigenic models.

In addition to this, I express my gratitude to both the Ministero della Pubblica Istruzione and the Ministero della Ricerca Scientifica, Rome, Italy, for the financial helps supporting this research line during recent years.

Essential References

Almagià, R., 1931. Note ad un abbozzo della distribuzione delle frane nella Penisola Italiana, in "R.Acc. Lincei, Mem.Scient. Tecn., Pubbl. Comm. It., Studio Grandi Calamità", Vol. II, Roma, 1–24.

Cavasino, A., 1931. Note sul catalogo dei terremoti distruttivi dal 1501 al 1929 nel Bacino del Mediterraneo, in "R.Acc. Lincei, Mem.Scient. Tecn., Pubbl. Comm. It., Studio Grandi Calamità", Vol. II, Roma, 29–60.

Corrado, G. and Rapolla, A., 1977. Structural model of Italy deduced by gravity data (MAPS), CNR, Geodynamic Project, Operative Unit 5-2-7, Map 3.

Crescenti, U., 1982. La grande frana di Ancona del 13 dicembre 1982, Studi Geologici Camerti, Dipartimento di Scienze della Terra, Special Issue.

Crescenti, U., Ciancetti, G.F., Coltorti, M., Dramis, F., Gentili, B., Melidoro, G., Nanni, T., Pambianchi, G., Rainone, M., Semenza, E., Sorriso-Valvo, M., Tazioli, G.S. and Vivalda, P., 1983. La grande frana di Ancona del 1982, XV Conv. Naz. Geot., Spoleto 1983, Comune di Ancona - Univ. di Ancona, Collana "Problemi del Territorio".

Finzi-Contini, G., 1977. An elementary mechanical model for the Apennine range areas, Riv. It. Geof. e Sc. Aff., IV, 5/6, 221–224.

Finzi-Contini, G., 1982a. Evoluzione spazio–temporale di geostrutture viscoelastiche/viscose e modellistiche geodinamiche, Atti Accademia Patavina Sc., Lett. e Arti, AA 1980/81, Vol. 93, 93–103.

Finzi-Contini, G., 1982b. Una modellistica viscosa per geostrutture profonde interessante la penisola italiana ed evidenze geofisiche e tettoniche, Atti I Conv. GNGTS, CNR, Roma, 563–579.

Finzi-Contini, G., 1986. Schemi di connessioni tra fenomeni sismici e franosi per modelli tridimensionali viscoelastici, Atti V Conv. GNGTS, 393–395.

Finzi-Contini, G., 1988. Indizi geodinamici nell'avanfossa Adriatica per un approccio interpretativo di anomalie di Bouguer mediante filtraggio, Lecture given on 15 Jan 1988 at the Dept. of Material Science, Univ. of Lecce, Italy, Thalassa (in press).

Finzi-Contini, G., 1989a. Geophysical/visco-elastic models of deep geo-structures to simulate long-term hazard situations along the Italian peninsula (Adriatic foredeep areas), XIV EGS Gen. Ass., 13-17 March 1989, Barcelona.

Finzi-Contini, G., 1989b. An inland model to interpret tsunami effects for certain Italian seas, 34th Int. Geophys. Symposium, 4-8 September 1989, Budapest.

Finzi-Contini, G. and Majorana, C., 1989a.. Comparing gravimetrical and geothermal interpretations of sub-regional anomalies along the Apennines, Southern Italy, 51st EAEG Meeting, 29 May - 2 June 1989, Berlin.

Finzi-Contini, G. and Majorana, C., 1989b. Interdisciplinary models to elaborate theoretical heatflows along NE side of the Apennines chain (Italy), 1989 Geothermal Workshop, Univ. of Auckland, 8-10 November 1989, Auckland (NZ).

Finzi-Contini, G., Losito, G. and Majorana, C., 1989a. Modellazioni numeriche di risposte geofisiche in aree regionali e rischio nel dominio termo–meccanico, Atti I Conv. Ingegneria del Territorio, Dip. Ing. Civ., Facoltà di Ingegneria, Univ. di Firenze, 1-3 June 1989, Firenze.

Finzi-Contini, G., Losito, G. and Majorana, C., 1989b. Modelli visco-elastici geo-strutturali (3D) agli elementi finiti finalizzati a ricerche di geotermia ed elettromagnetismo, VIII Conv. GNGTS, CNR, 7-9 november 1989, Rome.

Giese, P. and Morelli, C., 1975. Crustal structure in Italy, in "Structural Model of Italy", Ogniben, L., Parotto, M. and Praturlon, A. (eds), Quad. Ric. Scient., CNR, 90, 453–489.

Mantovani, E. and Boschi, E., 1982. Short period Rayleigh wave dispersion in the Calabrian Arc and surrounding regions, in "Structure, evolution and present dynamics of the Calabrian Arc", Mantovani, E. and Sartori, R. (eds), Earth Evol. Science, 3, 266–270.

Mongelli, F., Loddo, M. and Calcagnile, G., 1975. Some observations on the Apennines gravity field, Earth Pl. Sci. Letters, 24, 385–393.

Oddone, E., 1931. Sulla carta della frequenza dei terremoti disastrosi nel Bacino del Mediterraneo, in "R.Acc. Lincei, Mem.Scient. Tecn., Pubbl. Comm. It., Studio Grandi Calamità", Vol. II, Roma, 25–27.

Panichi, C., Funicello, R., Parotto, M. and Praturlon, A., 1982. Valutazione delle risorse geotermiche del territorio nazionale (SPEG), in Elias, G., "Progetto finalizzato Energetica 1976–1981", 2nd ed., CNR, Rome, 85–92.

Salati, A., 1971. Studio gravimetrico dell'Appennino Settentrionale, Grad. Thesis, Univ. of Modena.

Scandone, P., 1979. Origin of the Tyrrhenian Sea and Calabrian Arc, Mem Soc. Geol. It., 98, 27–34.

Soloviev, S.L., 1989. Personal communication, Barcelona, EGS General Assembly.

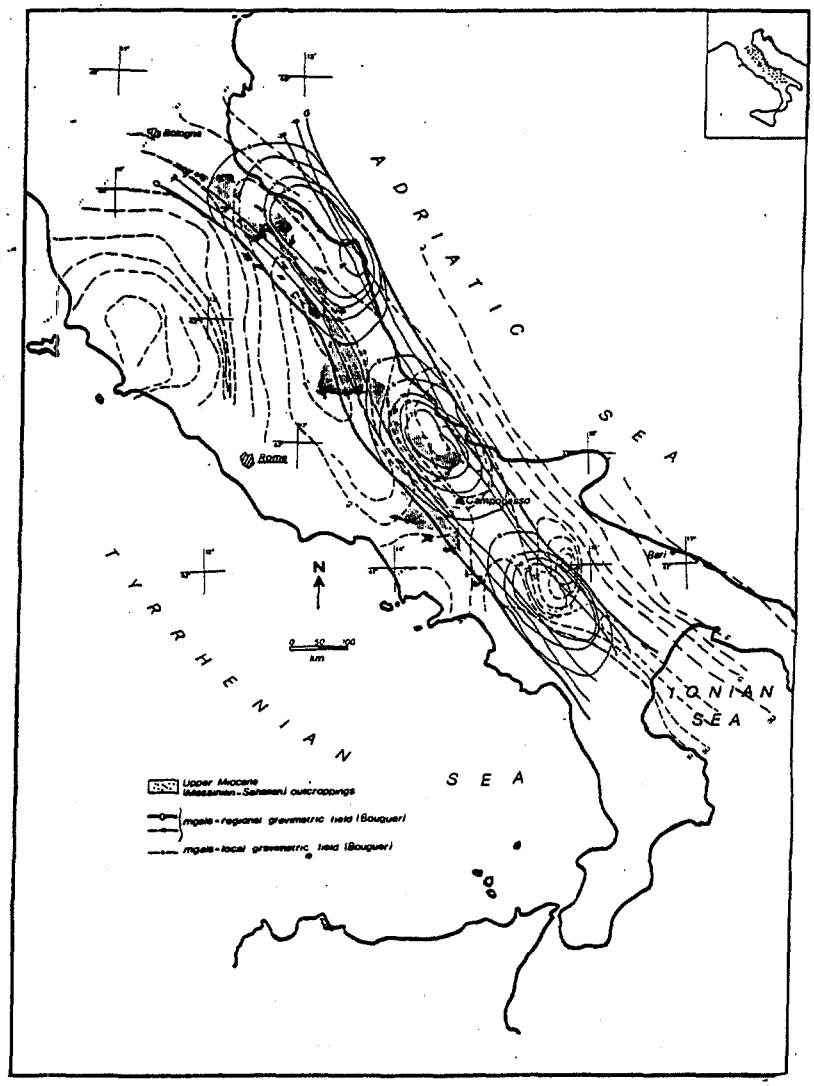

Figure 1. A sketch of the area considered for the seismogenetic model. Solid oval patterns represent three sub-regional positive Bouguer anomalies, mainly interesting from NW to SE Marche, Abruzzo-Molise and Campania-Basilicata regions along the regional gravimetric trough. Dashed lines refer to the geothermal field.

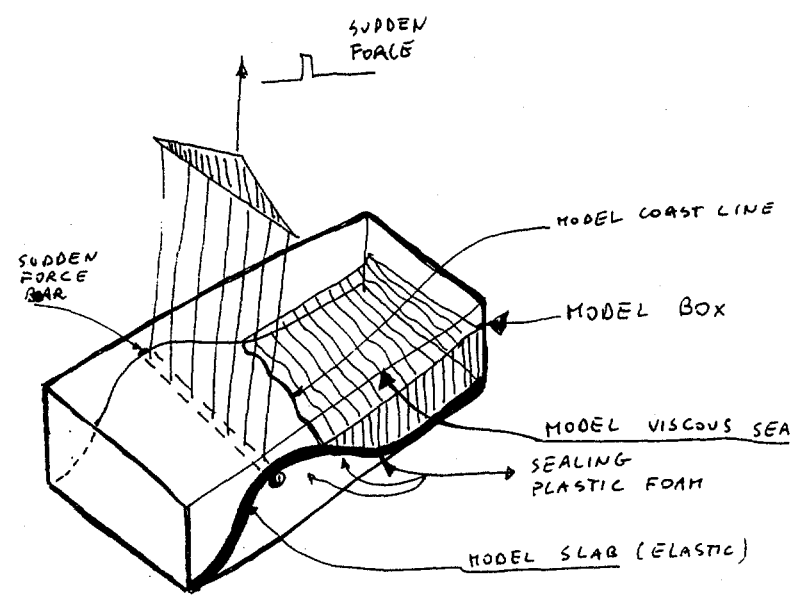

Figure 5. The experimental model scheme.

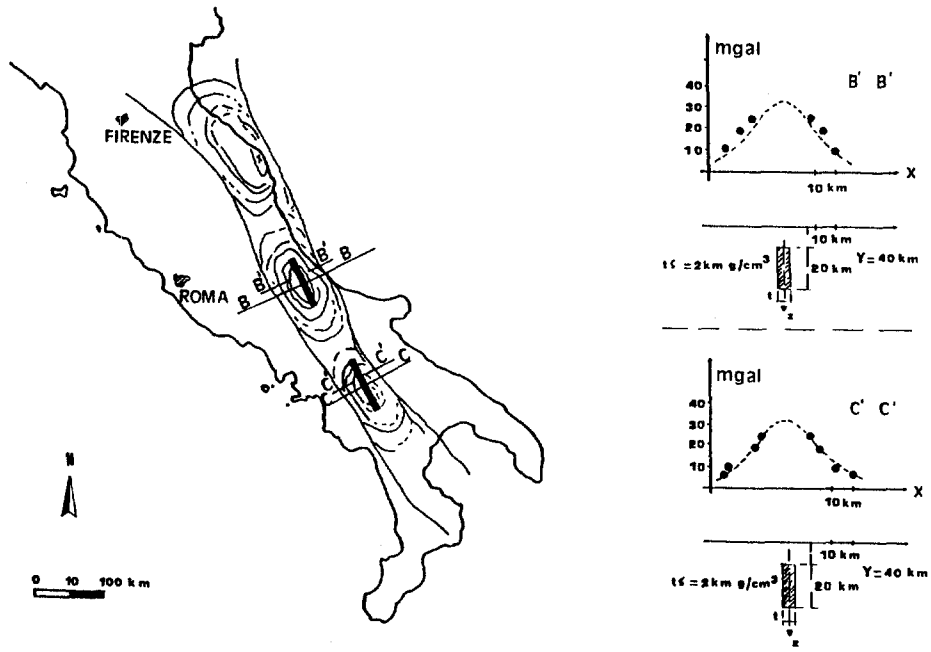

Figure 2. Gravimetric three-dimensional interpretation of two families of the sub-regional Bouguer anomalies (see also Figure 3, where an example is shown in greater detail). The interpretation of the sub-regional anomalies represented by the continuous oval patterns, is made by using thin vertical parallelepipeda, supposedly squeezed as a consequence of the anti-clockwise rotation of the Italian peninsula. They are uplifted according to this squeezing and are assumed to act as inland seismogenic geo-structures (in Figures 4 to 6 a possible consequent inland tsunamigenic mechanism is outlined)

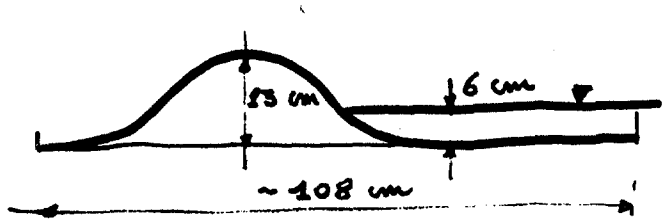

For the experimental layout shown above, the model gave:

SUDDEN TOP ELEV.	OFF-SHORE DISPLAC.	IN-SHORE REC.	DISPLAC. TIME
1 cm appr.	.5-.7 cm appr.	.1-.2 cm	1-1.5 sec
3 cm appr.	1.5-2 cm appr.	.2-.3 cm	2-2.5 sec
4 cm appr.	2.5 cm appr.	.4 cm	3 sec

The energy involved was comprised between 2 and 4 Joules, approxim.;
A tsunami effect on the model was in evident connection with the SUDDEN TOP ELEVATION; the fluid viscosity clearly made easier time evaluations.

Figure 6. First experimental results.

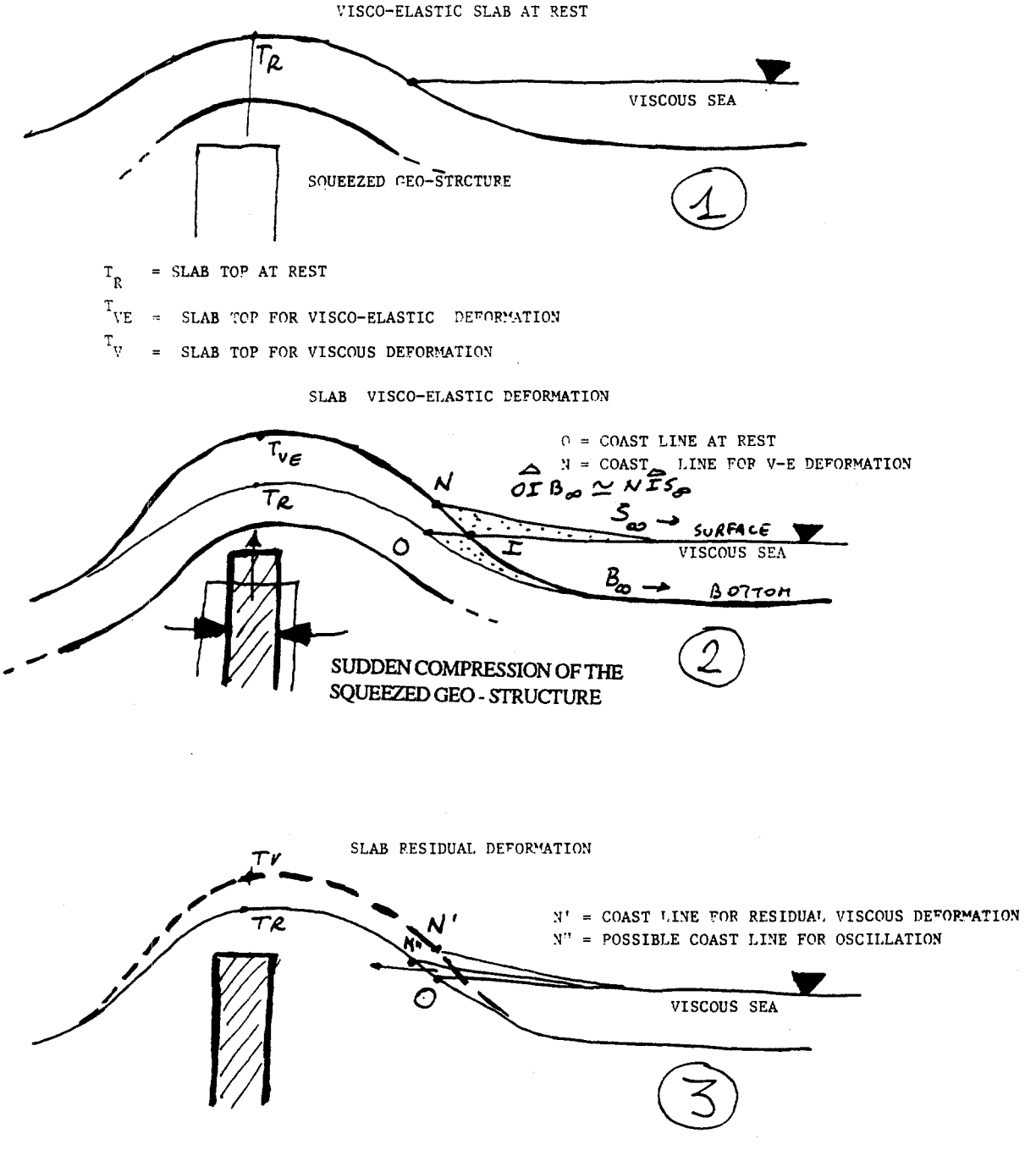

Figure 4. The adopted basic model scheme.

NUMERICAL MODEL ON TSUNAMI PROPAGATION

Th. V. Karambas , Y. Krestenitis and C. Koutitas

Division of Hydraulics and Environmental Eng.
Dept. of Civil Eng. Aristotle University of Thessaloniki
Thessaloniki 54006
GREECE

ABSTRACT

A numerical model , based on Boussinesq equations is developed in order to simulate tsunamis propagation across the ocean ,both deep and shallow.

The dispersion term of the above equations plays an important role in the propagation of a tsunami. From the other hand the truncation errors, which appear in the F.D. expansion of the significant terms, are also important and have to be included in the F.D. formulation, especially when depth and grid size are of the same order.

In order to keep small C.P.U. time an Alternative Direction Implicit scheme is used and the linear system of equations is solved using Thomas method.

Finally the model is applied on a tsunami reproduction in the Eastern Mediteranean sea.

1. INTRODUCTION

A number of Finite Difference models have been developed in order to simulate tsunami wave propagation. These models are based on the linear or non-linear long wave equation.

In the formal analysis of long-wave theory two important parameters are introduced.The first is the ratio of the wave heigt to the water depth, $\varepsilon = H/d$, and the second is the square of the ratio of the water depth to wave length , $\sigma^2 = (d/L)^2$. The ratio of these terms gives the well-known Ursell number , $Ur = \varepsilon/\sigma^2$.

The parameter ε accounts for the amplitude dispersion while σ^2 for the frequency dispersion (non hydrostatic pressure).

In shallow waters (d<50 m) ε becomes important ($Ur >> 1$) and Non Linear Long Wave Equation has to be used. In deeper waters σ^2 varies from very small values up to 1, for deep ocean, ($Ur << 1$) and the inclusion of terms of order $O(\sigma^2)$ is recommended.

Both regions covered by the models based on the Boussinesq type of equations which include terms of order up to $O(\varepsilon)$ and $O(\sigma^2)$. The numerical solution of the above equations can simulate non-linear waves so long as $\sigma = d/L$ remains small. The equations degenarate into the linear long wave equations, when $Ur << 1$, and the Shallow Waters Equations (SWE) when $Ur >> 1$.

The equations are (Peregrine, 1972)

$$\zeta_t + (u(d+\zeta))_x + (v(d+\zeta))_y = 0$$

$$u_t + uu_x + vu_y = - g\zeta_x + d/2\,((du)_{xxt} + (dv)_{xyt}) - d^2/6\,(u_{xxt} + v_{xyt}) - \tau_{bx}/\rho d + v_h\,(u_{xx} + u_{yy})$$

$$v_t + uv_x + vv_y = - g\zeta_y + d/2\,((du)_{xyt} + (dv)_{yyt}) - d^2/6\,(u_{xyt} + v_{yyt}) - \tau_{by}/\rho d + v_h\,(v_{xx} + v_{yy})$$

(1.1)

where u,v are the depth averaged horizontal velocities, ζ is the elevation, τ_b the bed shear stress components, and v_h the "eddy viscosity coefficient"

However for the propagation of a tsunami wave over a deep sea, the non linear terms seem not to be important and the linearized Boussinesq equations can be used. Taking as a practical boundary between deep and shallow sea the depth of 50 m, the linear Boussinesq equations can be applied in almost all regions.

2.EQUATIONS AND BOUNDARY CONDITIONS.

After simple mathematical munipulations the linearised form of equations 1.1 become:

$$\zeta_{tt} - (gd\zeta_x)_x - (gd\zeta_y)_y = d^2/3\ (\zeta_{ttxx}+\zeta_{ttyy}) - k\zeta_t \qquad (2.1)$$

where is a bed friction factor.

As the initial condition is taken the vertical displacement of the water surface the same as that of the sea bottom (Imamura and Shuto, 1989).

At the open sea boundary the free transmission condition is used, from the linear long wave theory:

$\zeta_t - c\ \zeta_n = 0$ with n is the inward normal to the boundary.

In the land boundary the full reflection is assumed :

$\zeta_n = 0$

It is more realistic to use in the last case the partial reflection condition:

$\zeta_t = 1/(1-r)\ c\ \zeta_n$ where r is a reflection coefficient

if r=0 we have free transmission

3.NUMERICAL SOLUTION

Equation 2.1 can be numerically solved using finite differences in the approximations of the partial derivatives. Therefore derivatives of the variable ζ both in space and time, centered in point $i\Delta x$ at time$n\Delta t$, are:

$$\zeta_{tt} = (\zeta_i^{n+1} - 2\zeta_i^n + \zeta_i^{n-1}) / \Delta x^2$$

$$\zeta_{xx} = (\zeta_{i+1}^n - 2\zeta_i^n + \zeta_{i+1}^n) / \Delta x^2$$

where Δx ,Δt are the space grid size and the time step respectively.

Truncations errors of the finite differences schemes (such as the above, as well as leap-frog, Crank-Nicolson) result in the damping of the wave height and an increasing oscillatory tail (Imamura and Goto,1988)

In order to overcome this numerical dispersion and dissipation, some correction terms has to be included in the F.D. integration. These terms are dedected by the Taylor series expansion of the significant terms.

The above derivatives can be expanded using Taylor series :

$$\zeta_{tt} = (\zeta_{tt})^{F.D.} - (\Delta t)^2/12\ \zeta_{tttt} = (\zeta_{tt})^{F.D.} - dg\ (\zeta_{xxtt}+\zeta_{yytt})$$

The above term as well, as the space derivative one ,have the same form with the dispersion term of eq. 2.1 and so are very easily indroduced in the numerical solution.

In order to reduce C.P.U. time an Alternative Direction Implicit scheme is used based on the split Peacmen-Rachford formula. Thus after the F.D. expansion of eq. 2.1 :

$$(1-A\delta_{xx})\ (1-A\delta_{yy})\zeta^{n+1} = B^{n,n-1}$$

where $A = (d^2/3 - \Delta x^2/12 + gd\ \Delta t^2/12)$

and B is the sum of all the explicit terms.

Indroducing an intermidiate value ζ^{n+1*} :

$$(1-A\delta_{xx})\ \zeta^{n+1*} = B^{n,n-1}$$

$$(1-A\delta_{yy})\ \zeta^{n+1} = \zeta^{n+1*}$$

Two linear systems (one for each direction) result from the above procedure and are solved using Thomas method.

The importance of including the two correction terms it is obvious when Δx (or/and Δt) has large values (tsunami models)

In the case of the total reflection boundaries an iterative method have been used in order to include implicitly the Boundary Conditions. Explicit Boundary Conditions introduce easily in the split formula we use.

4.TSUNAMI PROPAGATION IN INSHORE ZONE

Output of the above models can be used as the input to the near shore simulation . In this region linear eq. 2.1. is not valid and hence eqs. 1.1 are used.

The propagation of a long wave in very shallow waters results a steepening of its front. This makes the deviations from hydrostatic pressure signi ficant. The non hydrostatic consideration is indroduced through the dispersion terms of eq. 1.1. In addition these terms balance the front steepening, due to the non-linear terms.

Without these terms eq. 1.1 reduce to S.W.E. which predicts breaking even in the case of a long wave propagation over a horizontal bottom, dispite the existence of the solitary wave.

The front steepening in shallow waters causes a breaking or undular bore. In the case of a breaking bore turbulence is generated on the front of the wave and is modelled through the dispersion terms $v_h\ (u_{xx} + u_{yy})$.

After the assumption of local equilibrium between production and dissipation of turbulence energy (Batjjes 1975, Th. Karambas et all. 1990) the

eddy viscosity coefficient v_h can be expressed as:

$$v_h = \beta\, s^{1/3} d\, (gd)^{1/2}$$ where s is the beach slope

where β is a coefficient of order O(1).

Applying the "dry bed" boundary condition (Xanthopoulos and Koutitas,-1976),which is very easily inrtoduced in the model , we are able to simulate the moving water front (run-up).

The approximation of partial derivatives in the numerical solution of the eq. 1.1 is made in a similar way as above , using also three time levels. Some instability problems appear when Δx is very small.A technique to overcome the instability is to evaluate the linear terms u_x and ζ_x at the time levels $(n-1)\Delta t$, $n\Delta t$, $(n+1)\Delta t$ and use them multiplied by different weighting factors at the different time steps:

$$(F_x)_i^n = \alpha(F_x)_i^{n+1} + (1-2\alpha)(F_x)_i^n + \alpha(F_x)_i^{n-1}$$ with α about 0.1

5.APPLICATIONS

1) Solitary and tsunami wave propagation (figure 1).

The wave travels over an horizontal bottom (d=2000 m) without any loss of its height ($L/\Delta x=20$).The model without the correction and Boussinesq terms fail to simulate accurately the long distence propagation ,generating also high frequency oscillations behind it (fig 1a).

The same test , but with a real tsunami as input and $L/\Delta x=5$, gives more satisfactory results for the present model (fig 1b, 1c).

2) Tsunami propagation In the Eastern Mediteranean sea (from Malta to Crete).

Figure 2 shows a bird's-eye view of a tsunami at its generation (West Coast of Greece) and two computed records.

3) Run-up of a solitary wave.

Figure 3 shows the amplitude evolution of a solitary wave, H/d =0.04, at different time instances as it climbs up the beach of 1/19.85 slope in comparison with Synolakis (1987) data.The model seems to simulate well the non-linear shoaling and run-up.

6.CONCLUSIONS

Two finite differences models has been developed in order to describe linear and non-linear long wave propagation. Both models are based on

Boussinesq equations. The first, the linear one, is suitable in deep sea while the non-linear in inshore zone.The output of the first is used as input to the second.

In both models correction terms has to be included in the F.D. integration in order to avoid numerical dispersion and dissipation.

Providing the non-linear model with a dispersion term (eddy viscisity concept) the simulation of turbulent bores is achieved.

Finally, applying the "dry bed" B.C., it is possible to describe the run-up of breaking and non-breaking waves on beaches.

REFERENCES

Abbot, M.B. McCowan, A.D. and Warren, I.R. (1984) "Accuracy of the short wave numerical models" ASCE, Journal of Hydraulic Engineering , vol. 110,No 10, pp. 1287,1301.

Battjes, J.A. (1975) "Modeling of Turbulence in the surf zone", Proc. Symp. Modeling Techniques, ASCE, pp. 1050-1061.

Imamura F. and Goto C. (1988) "Truncation error in numerical tsunami simulation by the finite difference method" Coastal Engineering in Japan vol. 31 ,No 2 JSCE, pp. 245-263.

Imamura F. and Shuto N. (1989) "Numerical simulation of the 1960 Chilean Tsunami" Proc. of the Japan-China Joint Seminar on Natural Hazard Mitigation, Kyoto, Japan, pp 515-524.

Karambas Th.,Koutitas C. (1990) "Mathematical modelling of short waves in surf zone", "Warer Waves Kinematics" , Kluwer Academic Publishers , pp 351,365.

Karambas Th., Krestenitis Y. and Koutitas C. (1990)" A numerical solution of Boussinesq equations in the inshore zone" Hydrosoft vol.3, No 1,pp 34-37.

Koutitas C. G.,Gousidou-Koutita M.,Papazachos V. (1986) "A microcomputer code for tsunami generation and propagation" Applied Ocean Research vol.8 , No 3, pp 156-163.

Papazachos, P., Koutitas, C.,et all. (1984),"Tsunami hazard in Greece and surrounding area", Res. Rept. Aristotle U. of Thessaloniki.

Peregrine, D.H. (1972) "Equations for water waves and approximations behind them", "Waves on Beaches and Resulting Sediment Transport", ed. R.E. Meyer, Academic Press.

Rosenberg, D.U. (1969) "Methods for the Solution of Differential Equations", Elsevier N.Y.

Synolakis, C. (1987) "The run-up of solitary waves", J. Fluid Mechanics, vol. 185, pp. 523-545.

Xanthopoulos T.,Koutitas C. (1976) "Numerical simulation of 2-D flood wave propagation due to dam failure", J. of Hydraulic Research, vol. 14,no 4.

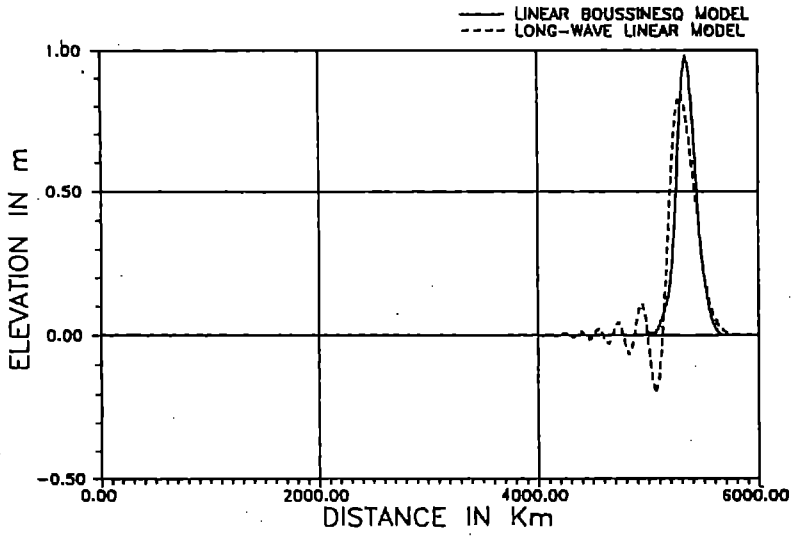
Ho/D=1/2000
LINEAR BOUSSINESQ MODEL
LONG-WAVE LINEAR MODEL
ELEVATION IN m
1.00
0.50
0.00
-0.50
0.00
2000.00
4000.00
6000.00
DISTANCE IN Km

(a)

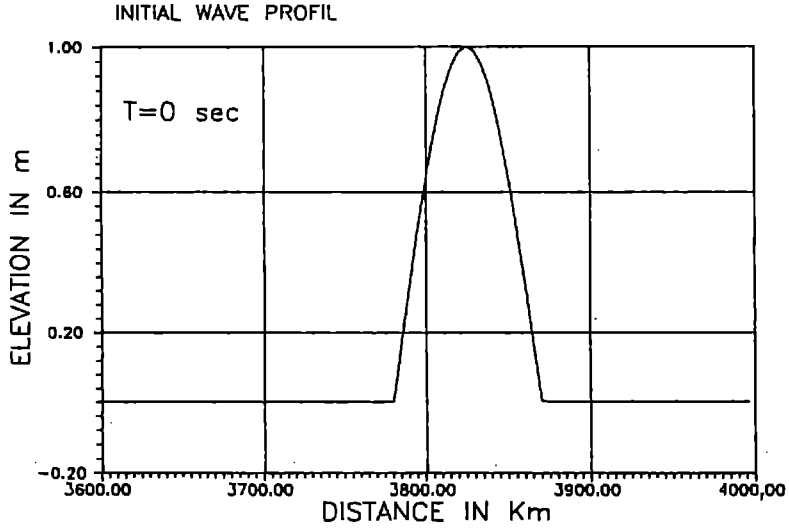
INITIAL WAVE PROFIL
T=0 sec
ELEVATION IN m
1.00
0.60
0.20
-0.20
3600.00
3700.00
3800.00
3900.00
4000.00
DISTANCE IN Km

(b)

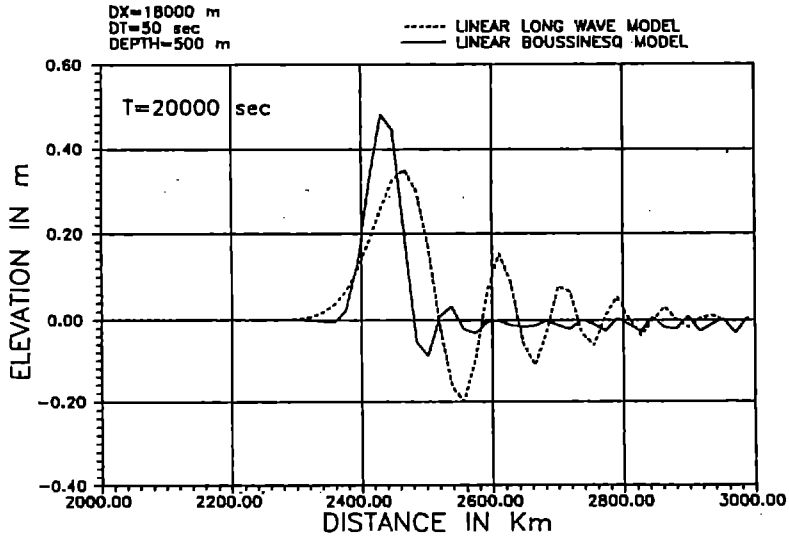
DX=18000 m
DT=50 sec
DEPTH=500 m
LINEAR LONG WAVE MODEL
LINEAR BOUSSINESQ MODEL
T=20000 sec
ELEVATION IN m
0.60
0.40
0.20
0.00
-0.20
-0.40
2000.00
2200.00
2400.00
2600.00
2800.00
3000.00
DISTANCE IN Km

(c)

FIGURE 1.

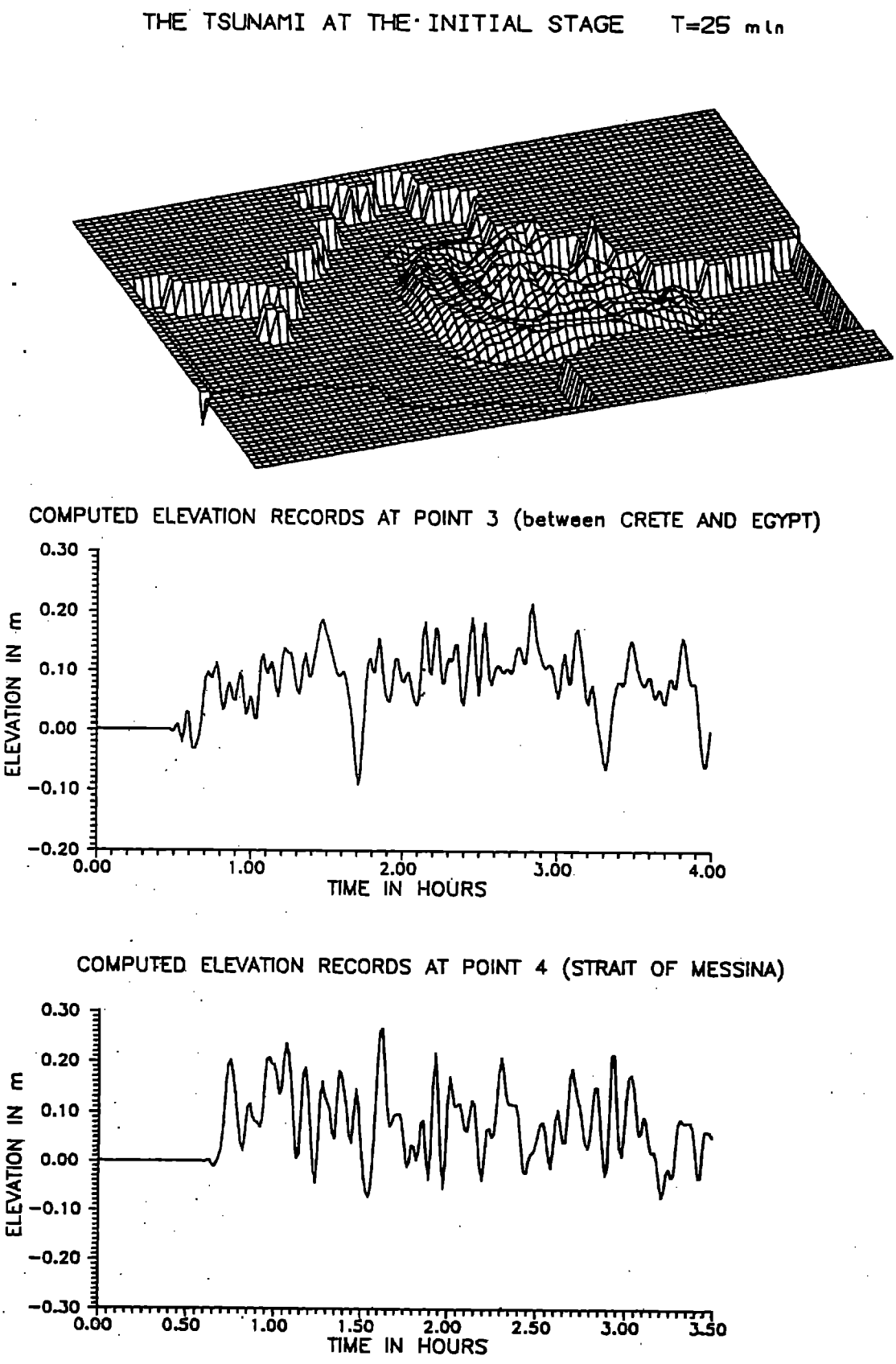
THE TSUNAMI AT THE INITIAL STAGE T=25 mln
COMPUTED ELEVATION RECORDS AT POINT 3 (between CRETE AND EGYPT)
ELEVATION IN m
0.30
0.20
0.10
0.00
-0.10
-0.20
0.00
1.00
2.00
3.00
4.00
TIME IN HOURS
COMPUTED ELEVATION RECORDS AT POINT 4 (STRAIT OF MESSINA)
ELEVATION IN m
0.30
0.20
0.10
0.00
-0.10
-0.20
-0.30
0.00
0.50
1.00
1.50
2.00
2.50
3.00
3.50
TIME IN HOURS

FIGURE 2.

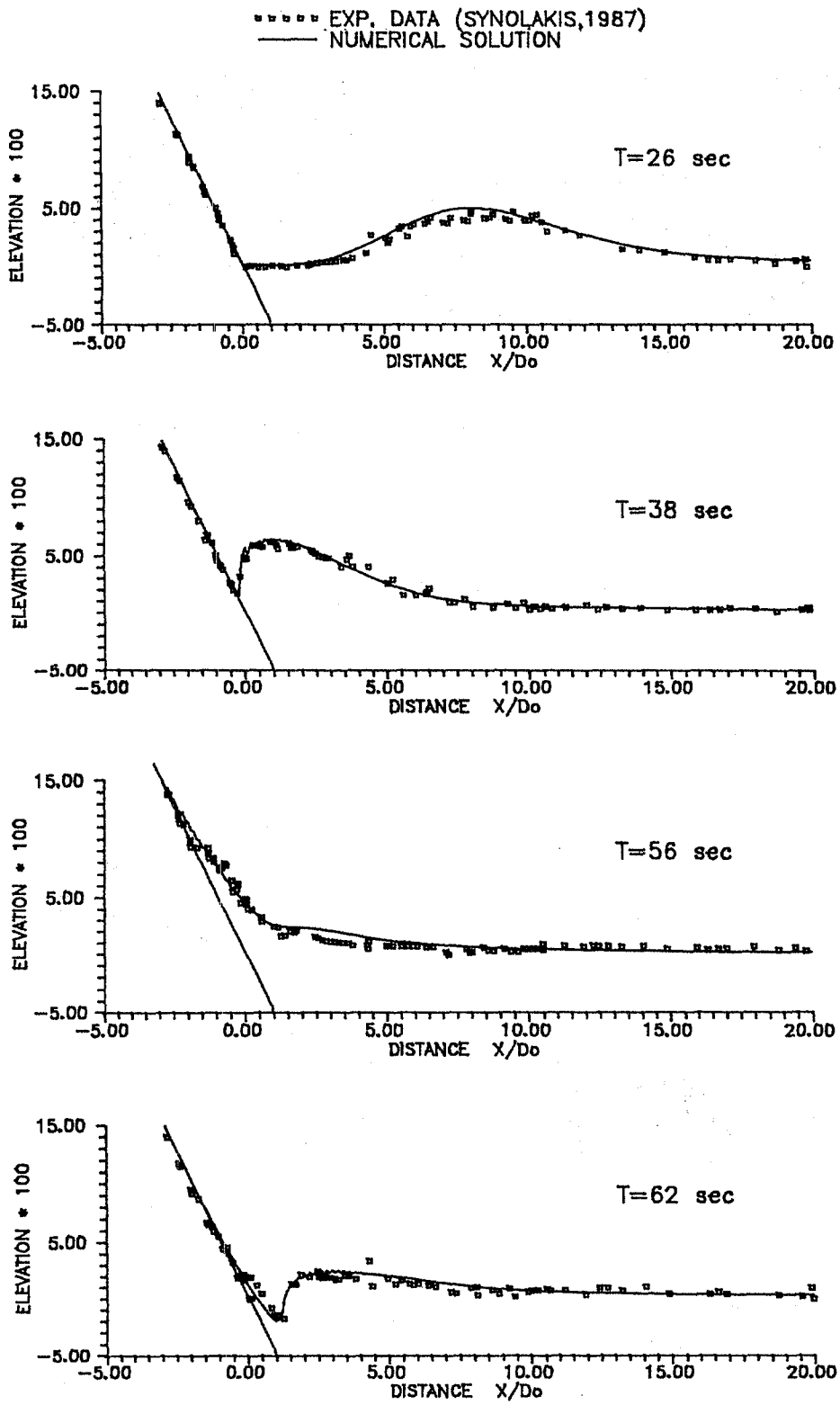
EXP. DATA (SYNOLAKIS,1987)
NUMERICAL SOLUTION
T=26 sec
T=38 sec
T=56 sec
T=62 sec
ELEVATION * 100
DISTANCE X/Do
15.00
5.00
-5.00
0.00
10.00
20.00

FIGURE 3.

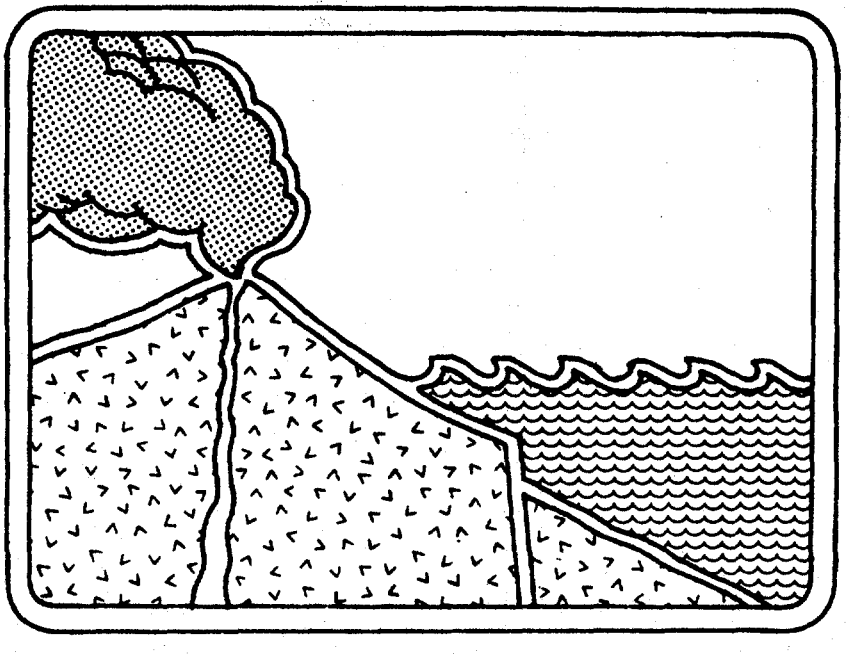

THE IDENTIFICATION OF TSUNAMI DEPOSITS IN COASTAL SEDIMENT SEQUENCES

A.G.DAWSON[1], I.D.L.FOSTER[1], S.SHI[1], D.E.SMITH[1] and D.LONG[2]

(1) Department of Geography, Coventry Polytechnic, Coventry, U.K., CV1 5FB.

(2) Marine Geology Research Programme, British Geological Survey, West Mains Road, Edinburgh, EH9 3LA.

ABSTRACT

The study of tsunamis has mostly been undertaken by physical oceanographers, geophysicists, seismologists, mathematicians and historians. Increasingly, however, geologists and geomorphologists also have an interest because many tsunamis deposit sediment. The study of sediments deposited by tsunamis is enormously important since it may enable scientists to identify past tsunamis that took place in pre–history, thus greatly extending our knowledge of the frequency and magnitude of past events. The study of sediments deposited by tsunamis in the past is also important since valuable information can be provided on former wave run–up. This information is much more precise than eye–witness accounts of tsunami run–up and is invaluable in the development of accurate numerical models of tsunamis. Despite the enormous potential of geological techniques in tsunami research, a major problem to be overcome, is the need to differentiate between coastal flood sediments deposited by tsunamis from those attributable to storm surges. In this paper, preliminary geological evidence from northern Scotland and the Scilly Isles, SW England is used to develop a model of tsunami coastal sedimentation.

1. INTRODUCTION

In many tsunami studies, scientists have used data on tsunami run–up to calibrate numerical models of both undersea fault–generated and submarine landslide–generated tsunamis. In most cases the values of run–up used have been based on eye–witness reports of past tsunami floods. Accordingly the study of tsunamis has attracted interest from physical oceanographers, geophysicists, mathematicians, seismologists and historians who have each provided data to explain the occurrence and mechanism of past tsunamis. Geologists and geomorphologists also have an important contribution to make towards the study of tsunamis - namely that the flooding of coasts during a tsunami is often associated with the deposition of marine sediments. It is maintained that the study of such sediments can provide scientists with much valuable information about the incidence and distribution of past tsunamis since evidence for these events can be directly observed through the study of sediments deposited during such floods. Consequently, much can be learned about the occurrence of tsunamis that not only took place prior to the historical time period but also those that have taken place in the recent past.

2. THE EFFECT OF TSUNAMIS ON COASTS

Tsunami waves behave as large water waves. As they approach a coastline, the individual waves become progressively deformed as water depth decreases. Wave deformation is a function of the ratio between the tsunami wavelength and water depth. Thus, owing to the long wavelengths normally associated with tsunami waves, disturbance of sea floor sediments due to the passage of a tsunami normally commences at water depths approximately equivalent to half the tsunami wavelength. The transition from laminar to turbulent water motion in the offshore zone is usually associated with the incorporation of considerable quantities of sea–floor sediment as suspended matter.

It has long been known that tsunamis deposit marine sediments on land. For example there have been numerous eye witness accounts of coastal sedimentation during individual tsunamis. In addition, there have been several reports of prehistoric tsunamis having deposited sediment in the coastal zone. In most cases, sand appears to have been deposited by the waves although on rarer occasions, boulders, coral and shell debris are reported to habe been laid down (Long et al., 1989a).

The extent of tsunami flooding along particular coastlines is indicative of the tsunami run–up above the level of the sea surface at the time the tsunami waves struck. In theory the altitude of the landward limit of sand deposited by the tsunami should record a minimum run–up altitude since the flood waters may have reached higher elevations yet did not deposit sediment. The upper limit of flood sediments therefore provides an approximate measure of former tsunami run–up, provided that it is also possible to estimate the position of the sea surface when a tsunami takes place (see below).

3. CHARACTERISTICS OF TSUNAMI SEDIMENTS

3.1 INTRODUCTION

At present several sand layers that have been observed in coastal and estuarine sediments have been attributed to tsunamis. Atwater (1986, 1988) has observed, for example, that several thin sand layers (each approximately 7cm thick) were deposited in the Puget lowland, Washington, due to tsunamis caused by offshore earthquakes during Late Holocene. Similarly Bourgeois and Reinhardt (1990) have described sand layers deposited by a major tsunami in Chile during 1960 (Atwater, pers. comm.).

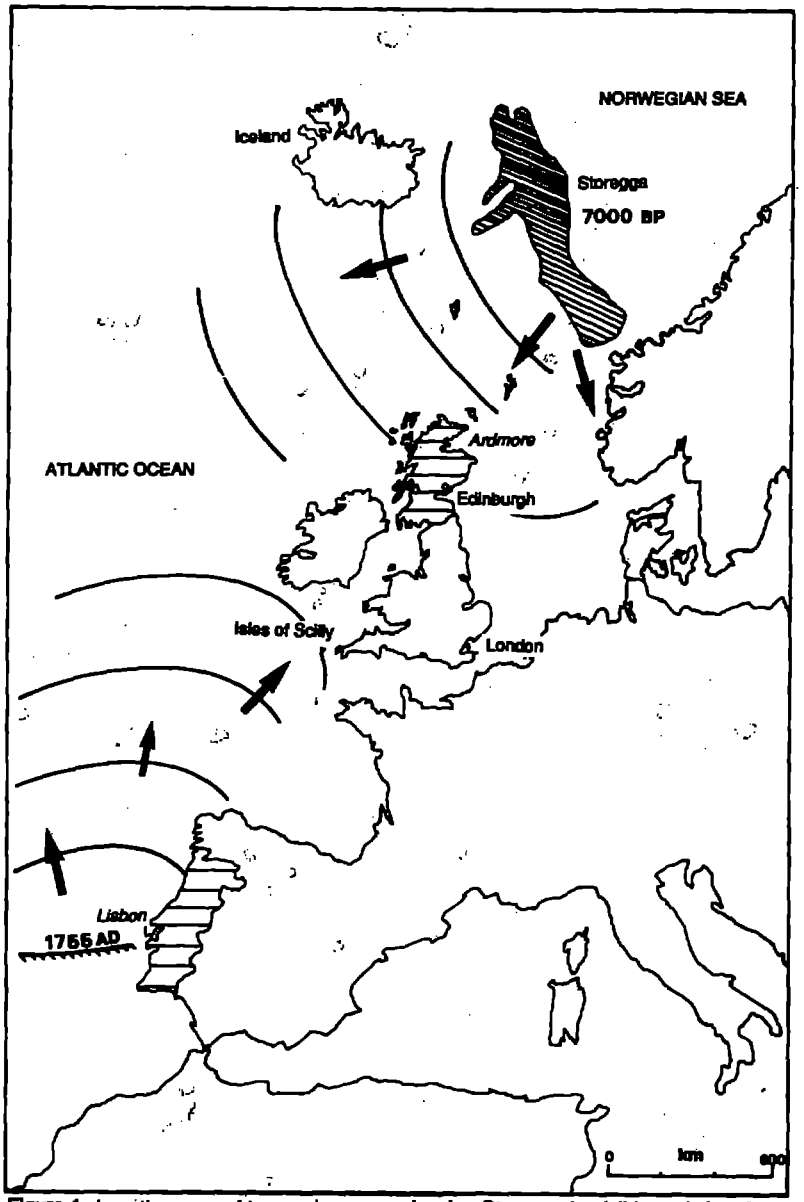

Figure 1. Location map of tsunami sources showing Storegga landslide and site of the Lisbon earthquake

However, the most detailed studies have been of sand layers in northern and eastern Scotland which are considered to have probably been deposited during a tsunami at approximately 7,000 BP. This tsunami was generated by one of the world's largest submarine landslides, the second Storegga Slide, that took place on the Norwegian continental slope (see Figure 1). Detailed accounts of this tsunami are published elsewhere (Dawson et al., 1988; Long et al., 1989a and 1989b). The highly detailed nature of this study has provided important information on the stratigraphy and sedimentology of tsunami sediments.

3.2 STRATIGRAPHY

The sand layer attributed to the Storegga tsunami generally consists of a widespread layer of grey, micaceous, silty fine sand. In some places, the lower part of the layer consists of coarse gravel overlain by sand. In general the sand layer is thickest seaward and decreases in thickness landwards as a tapering wedge that increases in altitude. The sand layer is deposited across pre–existing estuarine clay sediments as well as peat. In many places the base of the sand layer is marked by an erosional surface while, occasionally, small balls of peat, known as intraclasts, have been eroded from the underlying peat surface and incorporated within the deposit.

3.3 MICROFOSSILS

The sand layer often contains marine diatoms, the particular species of which depend upon water salinity, temperature and turbidity. In the Storegga sand layer, the most common marine diatom species is *Paralia sulcata* (Ehrenberg) Cleve, that often constitutes over 60% of the total diatom content. Other marine species present include Cocconeis scutellum Ehrenberg, *Diploneis* spp., *Grammatophera oceanica* (Ehrenberg) Grun and *Hyalodiscus stellinger* Bail (Smith et al., 1985). Many of the diatoms are broken and eroded, a factor that implies that the sand layer was deposited under high energy conditions. In theory some of the marine diatoms are likely to have been transported in suspension from the nearshore zone from water depths within the zone of tsunami wave deformation. However, individual diatom species can exist within quite considerable ranges of water depths and, as a result, it is not possible to attribute particular diatom species found within the tsunami deposit as having been transported from specific water depths offshore.

3.4 SEDIMENT CHARACTERISTICS

Initial observations suggested that the sand layer from Storegga tsunami was poorly sorted. However, the advent of analytical techniques for analysing very small samples has permitted particle size analysis at a very high resolution revealing pronounced vertical variations in particle size. From preliminary results, it appears that individual sediment cores are characterised by a series of fining–upward sediment sequences of several stacks of sediment superimposed upon one another (see Figure 2). This is further demonstrated by consideration of variations in the sorting and particle

sizes of contiguous samples at 1 cm intervals (see Figure 3). For example, a 52 cm thick sediment core of the sand layer from Ardmore, NE Scotland, exhibits a distinct clustering of values in approximate stratigraphic order indicative of deposition by a series of waves. This appears to indicate that separate tsunami waves are represented by distinct accumulations of sediment (see Figure 3). The most severe wave appears to be represented by the coarsest sediment accumulations and the least severe wave by an accumulation (stack) of relatively fine–grained sediment. Thus, particle size analysis of the sediment accumulations can provide information not only on the numbers of tsunami waves that struck a particular coastal area, but it might also provide information about the relative magnitude of the successive waves (see Figures 2 and 3).

Consideration of mareographs of past tsunamis demonstrates that there are often quite considerable variations in the timing of the largest wave in any tsunami inundation. In some cases the largest wave is the first while in others it may be the last (Wiegel, 1964). It would appear that detailed particle size analysis of tsunami sediments may well provide very detailed information on the hydrodynamic conditions of past tsunamis that, in turn, will be of immense value in the development of numerical models for particular tsunamis.

3.5 FORMATION HYPOTHESIS

The information described above provides certain clues about the hydrodynamic condition associated with the deposition of coastal sand accumulations during tsunamis. It enables an hypothesis of tsunami coastal deposition to be proposed that can be further tested in the future. During each tsunami flood wave, large accumulations of suspended sediment are transported landward by floodwaters across low–lying coastal areas. During the inrush of each wave of water, there is a corresponding downward percolation of flood water towards the groundwater table. As a result, the suspended sediment transported landward by the tsunami is deposited upon the ground surface. During sediment deposition the greatest thicknesses of sediment are deposited closest to the coast above the beach zone and there is a progressive landward decrease in sediment thickness. Thus, each phase of flood sediment deposition is associated with the formation of a wedge of sediment that tapers landward (see Figure 2). After each wave the coarsest sediment, due to its greater density, is deposited first and is rapidly followed by the deposition of finer–grained material. The occurrence of a major tsunami may therefore be associated with the superimposition of a series of sediment wedges, each of which is associated with a fining–upwards sedimentary unit.

4. DIFFERENTIATION BETWEEN TSUNAMI AND STORM SURGE SEDIMENTS: AN EXAMPLE FROM THE SCILLY ISLES, SW ENGLAND

4.1 INTRODUCTION

One of the biggest problems associated with episodes of past coastal flooding is the need to differentiate tsunamigenic and storm–surge events in coastal sedimentary records

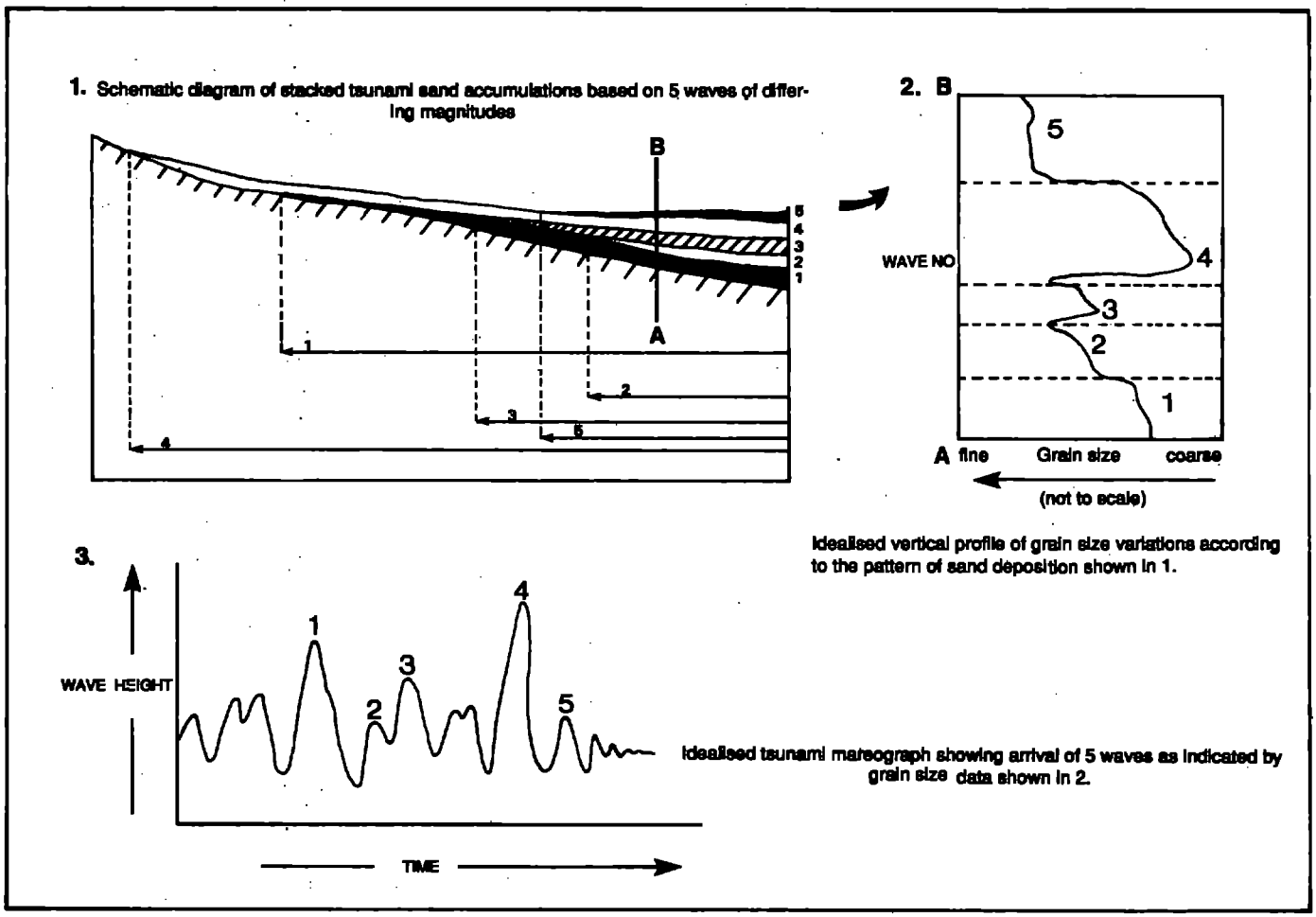

Figure 2. Tsunami reconstruction using sediment characteristics

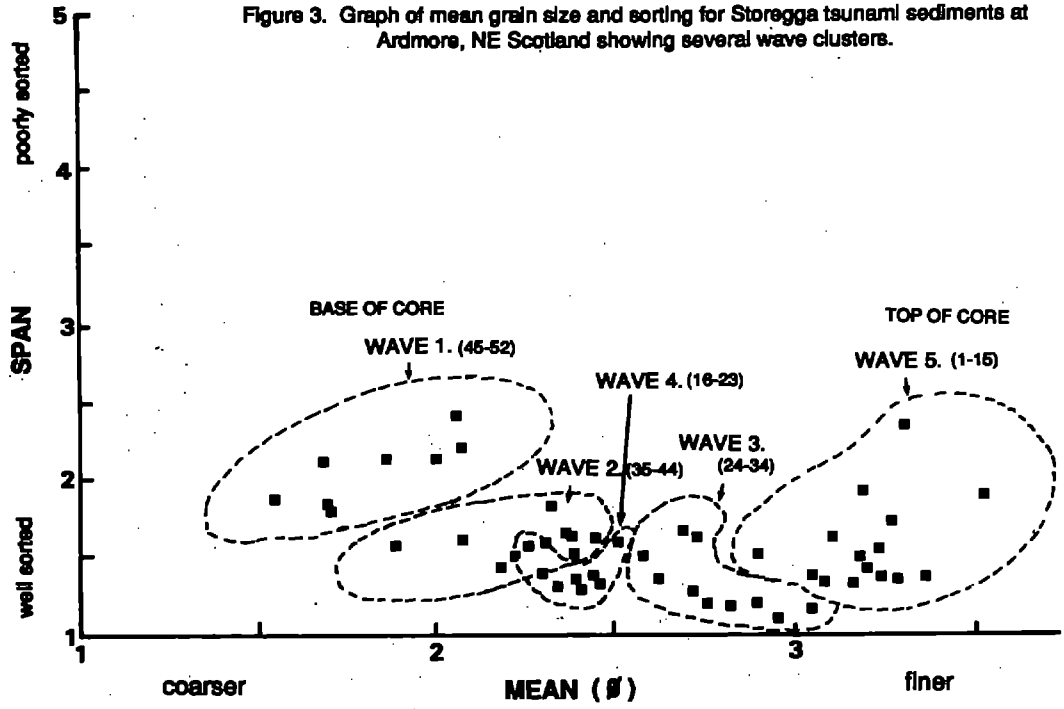

Figure 3. Graph of mean grain size and sorting for Storegga tsunami sediments at Ardmore, NE Scotland showing several wave clusters.

(Dawson et al., 1989). For example, do storm surges result in deposition of sediments and, if so, can these deposits be distinguished from those deposited by tsunamis? The problem is well illustrated by data from the Scilly Isles, SW England, an area known to have been affected both by storm surges and tsunamis during the last several hundred years.

The Scilly Isles comprise a small cluster of islands composed of granite which lie 40 km to the SW of Lands End (see Figure 1). On four of the islands occur five shallow coastal lagoons that lie at a height within 1 m of high spring tides. These lagoons are separated from the sea by windblown sands. During the summer of 1988, all five shallow lakes and their surrounding wetlands were cored using percussion coring techniques. Three of the five lagoons exhibit similar sedimentary sequences of alternating peat (or lacustrine deposits) and inorganic sand layers. The sequence is most clearly defined in Big Pool, St Agnes, the most southwesterly inhabited island of the group. Detailed analysis was undertaken within the sedimentary basin of this site with each of the six cores retrieved exhibiting a remarkable similarity in stratigraphy. The upper 30 to 45 cm were dominated by an upper peat (or lake sediment). Beneath this layer is a medium to fine sand between 15 and 40 cm in thickness. The sand layer is everywhere underlain by a layer of peat which, in turn, overlies a basal coarse sand. Calibrated radiocarbon dates using the probability distribution method for both the upper and lower 2 cm of the basal peat gave the following,

GU–2569	Bottom of basal peat	Probability 95.4%	(2o)	1019–1216 AD
GU–2570	Top of basal peat	Probability 95.4%	(2o)	1474–1672 AD

Consideration of the latter date implies that the upper sand was deposited by a marine flood towards the end of the 17th century or during the early to middle part of the 18th century. Caution should be exercised in the interpretation of these 14C dates, however, owing to the well–known Suess effect.

The marine origin of the upper sand layer is additionally supported by studies of grain size variations, surface morphological variations and by mineral magnetic analyses. These show that the upper sand is similar to local contemporary beach deposits (Albon, 1989). The sediments differ considerably, however, from sand dune deposits that occur nearby. For example, whereas the upper sand displays a unimodal particle size distribution, the dune sediments are characteristically bimodal with mean particle size values that are typically 120 micron finer than the upper sand. There is documentary evidence that severe coastal flooding took place in the Scilly Isles during the 18th century as a result of both storm surges and tsunamis (Borlase 1758, 1765).

4.2 STORM SURGES

Written evidence exists for a major storm surge in 1744 although earlier surges are known to have affected the area during the 1703 (Borlase, 1765). Heath (1750) described the events of the afternoon of the 26th September 1744, "...great stones were thrown by the sea into some houses standing next it...the off islands...had some of their lowlands overflowed, and some pools of their fresh water spoiled". Such situations are

not uncommon on Scilly, as witnessed by the storms of February 1990 when boulders up to 1 m in diameter were moved by waves 30 to 40 m inland. However, although most low lying areas were flooded, including Big Pool, there was no evidence of sand deposition in any of the sites re–examined after the flood during August 1990.

4.3 TSUNAMIS

It is possible that the sand layer have been due to the tsunami that followed the Lisbon earthquake of November 1st 1755. Documentary evidence is known for both Scilly Isles and West Cornwall for a series of flood oscillations that commenced around 2 pm on November 1st and which lasted several hours (Borlase, 1758, Tonkin and Tonkin, 1871) (see Figure 4). Indeed Borlase described the magnitude and frequency of the tsunami oscillations for Mounts Bay, Cornwall. Calculations of tidal fluctuations for November 1st, 1755 for the Scilly Isles, show that the time of high tide approximately coincided with the arrival of the first waves (Proudman Oceanographic Institute, pers. comm.) (see Figure 4), some five hours after the first shocks were reported on the Portuguese coast.

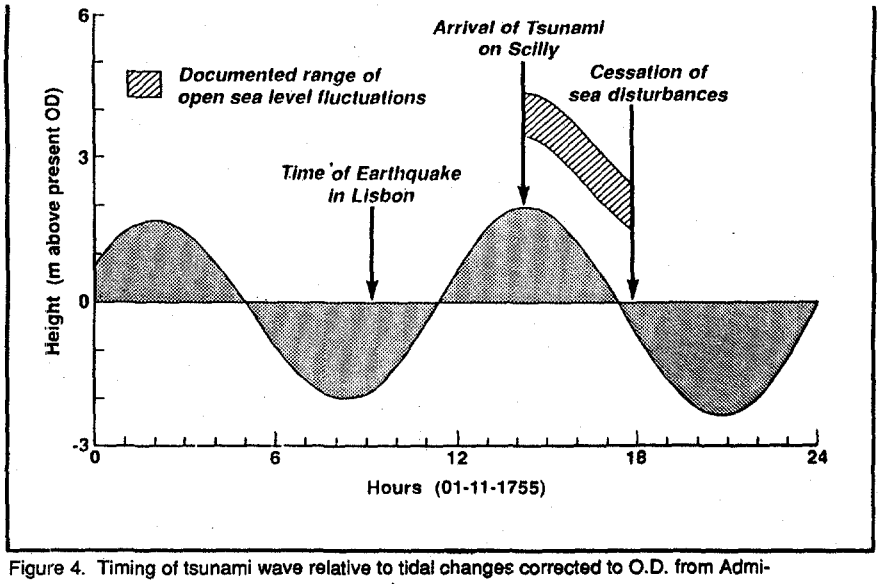

Figure 4. Timing of tsunami wave relative to tidal changes corrected to O.D. from Admiralty datum.

Calculations of the initial tsunami wave velocity suggest a value of 300 km hr^{-1}. Using water depths and travel distances from the earthquake epicentre to Scilly and gravity wave equation ($V = \sqrt{gd}$ where g = acceleration due to gravity and d is water depth), a travel time of 4 hr 47 min can be derived for the tsunami. This value is in close agreement with the documented observations for the time when the waves are reported to have first reached Scilly. It also implies that the waves would have approached the coast at an approximate velocity of 20 m s^{-1}.

The reconstructed tidal ranges, including adjustments for sea level change and present elevations OD are shown in Figure 4. Superimposed on the latter tidal range estimate is the observed range of wave heights observed by Borlase (1758). These show that sea levels during this period may have reached as high as +4.5 m OD during the tidal maximum. Borlase (1758) described the waves, "The first and second fluxes and

refluxes were not so violent as the third and fourth, at which time the Sea was as rapid as that of a mill–stream descending to an undershot wheel, and the rebounds of the sea continued in their full fury for fully to hours...alternately rising and falling, each retreat and advance nearly of the space of ten minutes, till five and a half hours after it began". Evidence that sand was deposited in Scilly during this time period is implied by the observations of Huxham (1755) at Plymouth who described the "...tearing up of mud and sand banks in a very alarming manner".

It therefore seems likely that Lisbon tsunami may well have been responsible for the sand layer deposited in the shallow lakes of Scilly. Further work is currently being undertaken on the Big Pool upper sand. The results tentatively suggest that there is a general sequence of fining upward in grain size on which are superimposed oscillations of alternating coarse–fine sequences that may well relate to individual waves reaching Big Pool.

5. DISCUSSION

At present, the balance of evidence seems to indicate that the upper sand unit at Big Pool, St Agnes was deposited as a result of the Lisbon tsunami. This does not imply, however, that storm surges do not cause coastal sediment deposition. However, the nature of sediment trasnsport and deposition during major storm surges is not understood. It has long been known, for example, that storm waves are generally destructive and lead to the removal seaward of large quantities of sediment (King, 1959). However, shingle and boulders are often transferred landward due to the enormous wave pressures that are focused on particular coastal areas.

Storm surges are fundamentally shorter–wave phenomena than tsunamis and appear to be associated with onshore deposition of coarse clastic detritus rather than large quantities of sand. It is possible that storm surges are characterised by destructive waves that cause severe beach erosion and the seaward removal of sediment. Tsunami waves, by contrast, are much longer–wave phenomena characterised by high magnitude constructive waves that cause widespread sediment deposition above high water mark.

ACKNOWLEDGEMENTS

Grateful thanks is given to A.Albon, K.Bardell, J.Fletcher, T.Jardine, R.Mothers and M.Pritchard for assistance with the Scilly Isles research and to R.A.Cullingford and C.Firth for valuable field research and advice. Thanks are expressed also to S.Dawson for cartographic assistance and for comments on an original draft of the text. D.Long publishes with permission of the Director, British Geological Survey (NERC).

REFERENCES

ALBON, A. 1989. An investigation into the coastal sedimentary sequences of Big Pool, Saint Agnes, Isles of Scilly (B.Sc. Dissertation, Coventry Polytechnic).

ATWATER, B.F. 1986. Evidence for great Holocene earthquakes along the outer coast of Washington State, Science, 236, 942–944.

ATWATER, B.F. 1988. Summary, as of 2 April 1987, of Radiocarbon ages on episodes of rapid coastal subsidence in westernmost Washington State, in C.F.SHEARER (ed.) "Minutes of the National earthquake prediction evaluation council, April 2nd and 3rd, 1987, Seattle, Washington", 228.

BORLASE, W. 1758. The Natural History of Cornwall (reprinted 1970; E and W Books, London).

BORLASE, W. 1765. Observations on the islands of Scilly (reprinted 1966; Frank Graham, Newcastle upon Tyne).

BOURGEOIS,J. and REINHARDT, M.A. 1989. Onshore erosion and deposition by the 1960 tsunami at the Rio Lingue estuary, South–central Chile, Eos, Transactions American Geophysical Union, 70, 1331.

DAWSON, A.G., LONG, D. and SMITH, D.E. 1989. The Storegga Slides: evidence from eastern Scotland for a possible tsunami, Marine Geology, 82, 271–276.

DAWSON, A.G., SMITH, D.E. and LONG, D. 1989. Early Flandrian tidal surges in the Tay estuary, Scotland, Journal of Quaternary Science, 4, 273–274.

HEATH, J. 1750. The Isles of Scilly (reprinted 1967; Frank Graham, Newcastle upon Tyne).

HUXHAM, J. 1755. Letter to Mr William Watson, FRS. Phil. Trans. Roy. Soc. London, 50, 371–373.

KING, C.A.M. 1959. Beaches and Coasts, Edward Arnold, London, 403 pp.

LONG, D., DAWSON, A.G. and SMITH, D.E. 1989a. Tsunami risk in northwestern Europe: a Holocene example, Terra Nova, 1, 6, 532–537.

LONG, D., DAWSON, A.G. and SMITH, D.E. 1989b. A Holocene tsunami deposit in eastern Scotland, Journal of Quaternary Science, 4, 61–66.

SMITH, D.E., CULLINGFORD, R.A. and HAGGART, B.A. 1985. A major Coastal Flood during the Holocene in Eastern Scotland, Eiszeitalter und Gegenwart, 35, 109–118.

TONKIN, J.C. and TONKIN, R.W. 1887. Guides to the Isles of Scilly, Penzance.

WIEGEL, R.L. 1964. Oceanographical Engineering, Prentice Hall Inc., 532pp.

TSUNAMI HAZARD ON THE SPANISH COASTS OF THE IBERIAN PENINSULA

MARIA LOURDES CAMPOS

Departamento de Geografia
y
Ordenación del Territorio
Universidad de Castilla-La Mancha
Cardenal Lorenzana, 1, 45002 Toledo, España.

ABSTRACT

Although tsunamis are not very frequent in the seas surrounding the Iberian Peninsula, some earthquakes with underwater epicenter generated tsunamis which have been observed on the Spanish coasts, both in the Mediterranean coastal area and in the Atlantic. Most of these tsunamis have been of a small size and associable with earthquakes with epicenter in the sea. Some events were related to landslides and turbidity currents. The most recent ones have been recorded by the tide-gauges of some Spanish harbours.

Nevertheless, there are also some reports of some tsunamis with a destructive nature in historical times, such as that produced by the well known Lisbon earthquake of 1755, which was the greatest and most destructive among the known tsunamis affecting the Spanish coasts. This tsunami caused waves higher than 18 m in the town of Cádiz, on the southwestern part of the peninsula, causing 1000 deaths as well as extensive flooding and destruction in Huelva and Cádiz.

The main tsunamigenic zone in the Atlantic Ocean is situated to SW of St Vicent cape in the Cádiz Gulf, where, among others, the historical tsunamis of 216 BC, 60 BC, 382, 1731 and 1755, and also the most recent of February 28th, 1969 took place. In western Mediterranean the most important tsunamigenic zone (though of lesser importance than the aforementioned one) is located close to the coast of Málaga, Murcia and Alicante, in the Alboran Sea and the northern part of Algeria. Special attention is given to the tsunamis generated by the Algerian earthquakes of 1954 and 1980 with epicenters inland, near the coast of Algeria and recorded by the tide-gauges of the Spanish harbours of Alicante, Málaga, Algeciras and also Ceuta, with an increase of 34 cm above the normal level of the sea in Alicante in the 1954 tsunami.

1. INTRODUCTION

Tsunami hazard on the Spanish coast is a kind of natural hazard that due to its small frequency has not been studied in Spain until recent times. However, it seems that interest about tsunami risk has increased recently especially in the area of the Gibraltar Strait, on account of a project of building a fixed link between Spain and Northern Africa.

Taking into account previous works of several authors on the seismicity and tectonics of the oceanic areas surrounding our peninsula, we will first of all identify historical tsunamis, on the basis of seismic catalogs and documentary sources, trying to locate the epicentral areas in order to define the limits of possible tsunamigenic zones. As to the tsunamis of the present time, tide-gauges recordings relative to the days of occurrence of some oceanic earthquakes sufficiently large that might have generated tsunamis, are analyzed. The parameters of the resulting tsunamis, if any, are also analyzed.

2. COASTAL AREAS EXPOSED TO TSUNAMI HAZARD IN SPAIN

The tsunamis that have damaged our coasts with larger or smaller intensity, have had their main source in the active seismic region of Azores-Gibraltar in the Atlantic Ocean, owing to the particular focal mechanism and parametral characteristics of the earthquakes having their epicenter there. The sector situated at the SW of St Vicent Cape in the Gulf of Cádiz is the main generating area. The earthquakes taking place 18° W towards the Azores Islands, according to available information, produce small-size tsunamis that are hardly observed in the Spanish coasts, though their effects can be felt in the Azores and Madeira Islands, and even on the coasts of Morocco (Sousa Moreira, 1968).

As shown in Table I concerning the known tsunamis in the Iberian peninsula, there are three coastal regions in Spain with different possibility of being struck by some tsunami. They are, from lesser to greater importance: the northern coast, Galicia and Cantabria; the Southern and Eastern Mediterranean coast, and the Atlantic coast. The Atlantic coast, from Lisbon to the Strait of Gibraltar, is the zone where tsunami hazard is higher, as 18 of the 34 listed tsunamis have been recorded there. In the second place there is the Mediterranean coast, especially from the Strait to Valencia in the SE (9 events in the table). In the last position, which means a very small risk indeed, we find the northern coast. In some points of Galicia (6 events in the table), small motions in the sea level have been observed generally as a consequence of the large tsunamis generated S and SW of St Vicent Cape in the Atlantic Ocean (for example the 1755 tsunami), although these tsunamis lose their energy in going round the Cape of Finisterre (see Figure 1).

3. ATLANTIC AND MEDITERRANEAN TSUNAMIGENIC ZONES

The main tsunamigenic zone is situated in the Atlantic Ocean between Azores and Gibraltar in the seismic alpine zone, SSW of St Vicent Cape in the Gorringe Bank. It is worth mentioning also some minor tsunamigenic zones, as those in the continental

margin at Galicia bank and in the abyssal plains (Sousa Moreira, 1988). In some previous works the author (Campos, 1988 and 1989) analyzes the possible tsunamigenic sources in the Azores-Gibraltar line, based on studies on focal mechanism solutions and on seismotectonics of the area made by several authors.

The atlantic seismicity is determined by the interaction involving American, Eurasian and African plates. The different kind of contacts among these is the reason for the seismicity parameters not being homogeneous. Three seismotectonic areas can be distinguished.

Zone A. From Mid-Atlantic ridge to 25°W. It is an area of expansion of the oceanic crust because of the Mid-Atlantic ridge, and it is unlikely that it would generate tsunamis, because earthquakes are of small magnitude and their focal mechanism solution is not associated with vertical displacement.

Zone B. From Gloria fault (24°) to 18°W. It is an area of friction where large-magnitude earthquakes occur, that however are associated with dextral horizontal displacements along a fault oriented E-W (Udias et al., 1985). This kind of displacement possibly generates small tsunamis that are not generally observed on the southwestern coast of the Iberian peninsula. However, their effects is felt in the Azores and Madeira Islands and also in Morocco. For example, the earthquakes of 8 May 1939 (M=7), of 25 November 1941 (M=8.3) and of 26 May 1975 generated small tsunamis which were observed in these islands as well as in Casablanca and Mogador. All these earthquakes show strike-slip focal mechanism solutions. The 1941 event was followed by a turbidity current that was probably generated by landslides on the sea bottom (Sousa Moreira, 1988).

Zone C. The Cádiz Gulf is the main source of tsunamis. There are earthquakes of small and large magnitude in this zone and the focal mechanism solution shows vertical displacements along a reverse fault, with stress axis nearly horizontal towards a N-S direction. This is the zone of the most intense interaction between the African and the Eurasian plates that undergo strong deformations in approaching and compressing. The most important tsunamis are generated in the zone that is located from 12° to 6°W along the parallel 36°N. In this area the Lisbon earthquake of 1755 had its epicenter as well as the one of 28 February 1969 (see Figure 1).

In the Mediterranean Sea tsunamis are much less frequent and their cuases are due to landslides and turbidity currents. Sometimes meteorological phenomena have been erroneously taken as tsunamis. Volcanic erutpions and earthquakes in the bottom of the sea and inland may also be responsible. The most important regions struck by tsunamis are the coasts of insular Greece, of Southern Italy and of the Western Adriatic Sea, in Eastern and Central Mediterranean respectively. On the contrary, in Western Mediterranean tsunamis are very scarce. On the Spanish Mediterranean coasts some small tsunamis of local character have been recorded; their main tsunamigenic zone is situated in the Alboran Sea and close to the coast of Málaga, Valencia and Alicante. In the Balearic Sea no tsunami has been recorded, although ample sea level oscillations

are recorded every year from June to September in several bays and harbours of the Balearic archipelago and of the northeastern peninsular coasts. These oscillations have periods in the order of 10 min and amplitudes of up to 2 m. Associated with these large sea level oscillations, atmospheric pressure fluctuations with similar periods and amplitudes around 1.5 hPa have been recorded (Ramis and Jansá, 1983; Jansá, 1986). For a harbour with exponential or flat bottom and a flat step shelf, it has been found that the oscillations can be explained as a resonant coupling between an atmospheric gravity wave, a coastally trapped edge wave and the oscillation modes of the harbour (Alonso et al., 1989). This phenomenon is known at Ciutadella, in the island of Menorca, as "rissaga" and in Catalonia as "seiche" or "seixe".

Seismicity in the interior of the Mediterranean Sea is quite scarce, though its edges are really active, particularly all the edges of the Aegean Sea. In Western and Central Mediterranean seismicity is characterized by small and intermediate magnitude earthquakes, the main seismic areas being the Alboran Sea, the southeastern edge od the Iberian peninsula, North of Africa and Sicily, with a greater seismicity. Seismotectonic studies show the prolongation of the Azores-Gibraltar fault through the North of Africa up to Sicily. The study of the focal mechanism solution of several earthquakes in North of Algeria (among them the one of Orleansville in 1954) shows a predominant thrust mechanism with southward dip angle. Due to the reasons mentioned above, the small earthquakes occurring in the Western Mediterranean do not generally produce tsunamis that can be observed on the Spanish shores, and those known in historical times, according to historic sources, are dubious (Galbis Rodriguez, 1932–1940). They seem to be related to seiches or earthquakes in the land near the coast (as those of Torrevieja in 1829), whose epicenter has not been located exactly.

Mediterranean tsunamis have basically a local character and do not propagate towards areas located far from their sources. Hence those observed in the Spanish Mediterranean coasts must have a very near source and not be caused by large earthquakes in the central or eastern parts of the Mediterranean. There is no record of the large Mediterranean tsunamis generated by earthquakes in Southern Italy obtained on the Spanish coasts. The mechanism that generates Mediterranean tsunamis is, therefore, closely related to landslides, rockfalls and turbidity currents in the submarine unconsolidated sediments, as a consequence of earthquakes on land, although the actual mechanism is still under discussion.

4. MAIN ATLANTIC AND MEDITERRANEAN TSUNAMIS

Of all the known tsunamis (Table I), one of the most important is that occurring on the 1st of November of 1755 as a consequence of the Lisbon earthquake, which caused great damage on the Southern Portuguese coasts, as well as on Southern Spain, Canary Islands and Northern Morocco. This tsunami has been studied by the author of this paper (Campos, 1989). It has been reported that the earthquake of Lisbon was followed by 18 tsunami waves. The arrival of the first wave took place at high tide, which resulted in a greater rising of the water. In some places it was also observed a water withdrawal from the shoreline in excess of 2 km (first manifestation of the tsunami). Violent waves repeated

for three times in many places (in Cádiz they totalled six times), while everywhere the water movements lasted for twenty-four hours. The maximum amplitude in Cádiz was 18–20 m and 11 m in Tarifa. The travel time estimated for the first arriving wave from the instant of the shock is around 30 min for the beaches of Huelva and about 65–75 min for Cádiz, which gives an average velocity of the wave propagation between 100 and 200 m/s. In Ayamonte the sea flooded all the small islands, inlets and beaches and even the streets of the town itself. A thousand people were estimated to have drowned and four hundred were buried, 250 in Redondela, 203 in Lepe and 66 fishermen died in Huelva. In Cádiz the water rose 3 m and came over the reef from the outside ocean into the bay. The Caleta was covered by water. The losses are estimated in 50 people and 24 in Conil (Royal Academy of History of Spain, 1756). In Figure 2 all coastal sites affected by the waves in the Iberian peninsula are shown.

Already in 881 it seems that the shoreline in Cádiz underwent considerable changes: in some places the sea withdrew, some islands disappeared as well as many towns on the southern and western shores. Another historical tsunami took place in 1731 in Cádiz as well: the sea water withdrew a league uncovering the old town of Gades and its temple of Heracles (Galbis Rodriguez, 1932–40).

The most recent tsunamis are those occurred on February 28th, 1969 and on May 26th, 1975. The 1969 tsunami in Cádiz arrived in low tide and its maximum amplitude was 28 cm with a main oscillation period between 16 and 20 min. Its average velocity was 98 m/s, the first wave having taken 85 min to reach the coast. The source of this tsunami is considered as being the same as the Lisbon tsunami. In Ceuta it was quite smaller with only 10 cm of maximum amplitude. The 1975 tsunami took 144 min to reach Cádiz and its source was in a more remote area around 17°W and some 1450 km away. Its average velocity was 132 m/s and its maximum amplitude 28 cm. It reached Ceuta 240 min after the shock with an average velocity of 95 m/s and just 45 cm of maximum amplitude. In both places it took place in high tide, which shows how small this tsunami has been (see Figure 3).

Among the Mediterranean tsunamis we must consider those observed in Alicante, Málaga, Algeciras and Ceuta as a consequence of the Algerian earthquakes in 1954 and 1980. The 1954 earthquake wich took place on September 9th in Orleansville and whose epicenter was located in land near the coast, was followed by a small tsunami produced by sliding movements generating also a turbidity current that broke submarine cables 40 to 70 miles away from the epicenter (Sousa Moreira, 1988). On the Alicante shores a rising over the normal tide level of 34 cm was observed. The tsunami took 50 min to reach Alicante and 180 min to reach Málaga. It was also observed in Ceuta and Algeciras. On October 10th, 1980 the earthquake in El Asnam with an almost identical epicenter produced oscillations around the tide levels in Alicante, Ceuta and Algeciras as well. In Alicante a greater amplitude was observed in the inner piers of the harbour (possibly related to seiches) than in the outer piers, reaching a maximum amplitude of 50 and 16 cm respectively. The waves arrived with a main oscillation period of 10-15 min in high tide. Its average velocity, 70-80 m/s, was low, possibly owing to shallowness.

TABLE I – Tsunamis associated with earthquakes and observed on the coasts of the Iberian peninsula. Sources: Catalog of Galbis Rodriguez (1932–1940); Sousa Moreira (1968) and Oceanographic Spanish Institute (1989)

Date	Epicenter		Mag	Observed in
	Latitude	Longitude		
216-218 BC	36 12′N	07 40′W	-	Cádiz
210 BC	36 00′N	10 30′W	-	Cádiz
209 BC	36 50′N	10 30′W	-	Cádiz
60 BC	36 00′N	10 00′W	-	Portugal and Galicia
365	36 50′N	04 40′W	-	Málaga and Andra
382	36 00′N	10 50′W	-	Portugal
881	36 00′N	08 00′W	7.5	Cádiz
26 Jan 1531	38 57′N	09 00′W	7.7	Lisbon and S.Portugal
09 Oct 1680	36 30′N	04 24′W	-	Málaga
27 Dec 1722	37 10′N	07 35′W	7.5	Algarve
1731	35 00′N	07 00′W	-	Cádiz
01 Nov 1755	37 00′N	10 00′W	8.5-9	Galicia, Lisbon, Algarve, Huelva, Cádiz, Morocco, Azores and Madeira
16 Nov 1755	37 00′N	10 00′W	-	Galicia and Lisbon
21 Dec 1755	37 00′N	10 00′W	-	Lisbon
29 Mar 1756	37 00′N	10 00′W	-	Lisbon
31 Mar 1761	37 00′N	10 00′W	6.5	Finisterre and Lisbon
21 Sep 1790	36 40′N	00 08′W	-	Cartagena
21 Jan 1804	36 42′N	03 00′W	-	Adra
02 Feb 1816	35 00′N	10 00′W	-	Portugal
21 Mar 1829	38 06′N	00 42′W	-	Torrevieja
23 Dec 1848	38 12′N	07 30′W	-	Portugal
06 Jan 1860	38 00′N	00 42′W	-	Torrevieja
05 Jun 1875	40 00′N	01 50′E	-	Valencia and Tarragona
15 Jan 1891	36 50′N	03 10′W	-	Algeria
16 Feb 1930	36 00′N	03 00′W	-	Algeria
08 May 1939	37 00′N	24 30′W	7	Azores
25 Nov 1941	37 25′N	19 01′W	8.2	Portugal and Azores
09 Sep 1954	36 17′N	01 28′E	7.3	Alicante, Málaga, Algeciras
28 Dec 1956	36 50′N	02 08′W	-	Almeria
28 Feb 1969	35 59′N	10 48′W	7.3	Portugal, Morocco, Azores, Galicia, Cádiz, Canary, Madeira
26 May 1975	35 54′N	17 36′W	6.7	Portugal, Morocco, Cádiz
10 Oct 1980	36 09′N	01 26′E	6.5	Alicante, Málaga, Algeciras

CONCLUSIONS

Tsunami hazard on Spanish shores is fortunately rather remote in spite of the historical disastrous tsunami 1755. Nevertheless if we take into account the similarity of the Lisbon earthquake with that occurred on February 28th, 1969, as far as focal mechanism and epicenter are concerned, we should consider the future production of a large tsunami in this area as possible if the earthquake magnitude surpasses 7-8. On the Mediterranean coasts the probabilities are far smaller.

Consequently a warning system for tsunamis should be established on the Cádiz Gulf, although the small lapse between the quake and the arrival of the waves raises some problems. An experimental installation of seismographs on the sea bottom in the area that was the source of the 1755 event is being carried out at present, as a means of trying to establish a possible warning system.

REFERENCES

Alonso, S., Tintore, J., Gomis, D. and Blade, I. (1989). Oscilaciones del nivel del mar de gran amplitud y ondas de talud en el Mediterráneo Occidental, Rev. de Geofísica, 45, 33–38.

Anonimo (1756). Noticia individual Que de la Academia de la Historia Del terremoto de 1° de Noviembre de 1755 Por orden Del Rey Nuestro Señor a quien la dedica, Manuscrito, Bibl. Academia de la Historia Madrid, R/25-5C, 91, pp 367.

Campos, M.L. and Sierra, J. (1988). Analisis de los tsunamis sentidos en las costas atlánticas del suroeste peninsular, VI Asamblea Nac. Geod. y Geof., IGN Madrid, pp 10 (in press).

Campos, M.L. (1989). Epicentral parameters of Lisbon Earthquake based on the study of the tsunami raised, Proc. Workshop on Historical Earthquakes in the Ibero-Maghrebian Region - Methodological approach and case studies, Lisboa, pp 16.

Campos, M.L. (1989). Sismicidad de la costa sudoccidental de España. Análisis y valoración geográfica de los posibles riesgos como consecuencia de los tsunamis en la zona, Tesis Doctoral, Edita Univ. Complutense de Madrid, pp 734.

Jansá, A. (1986). Respuesta marina a perturbaciones meso-meteorológicas: la "rissaga" de 21 de Junio de 1984 en Ciutadella (Menorca), Rev. de Meteorología, Junio, 5–29.

Ramis, C. and Jansá, A. (1983). Condiciones meteorológicas simultáneas a la aparición de oscilaciones del nivel del mar de amplitud extraordinaria en el Mediterráneo occidental, Rev. de Geofísica, 39, 35–42.

Sousa Moreira, V. (1968). Tsunamis observados en Portugal, Serv. Meteorol. Nac., Publ. GEO, 143, Lisboa, pp 17.

Sousa Moreira, V. (1988). Historical and recent tsunamis in the European Area, Science of Tsunami Hazards, 6, 37–42.

Udias, A., Buforn, E. and Muñoz, D. (1985). Mecanismo de los terremotos y tectónica, Ed. Univ. Complutense de Madrid, Madrid, pp 232.

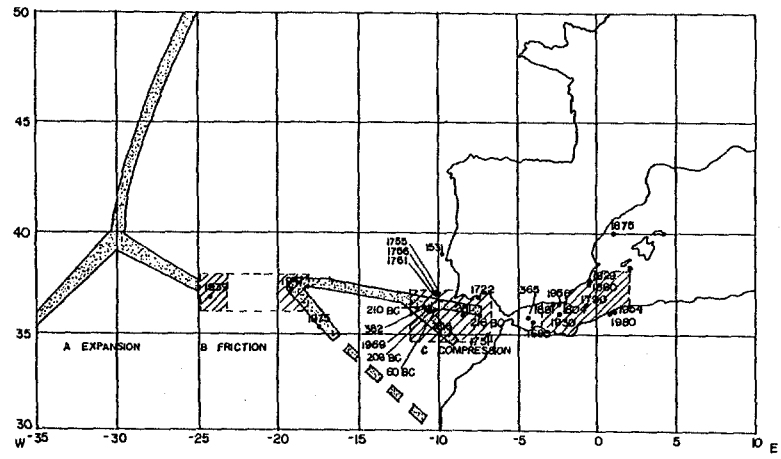

Figure 1.- Epicenters of oceanic earthquakes producing tsunamis in the Atlantic Ocean & Mediterranean Sea, between 35°W & 5°E

Tsunamigenic zones

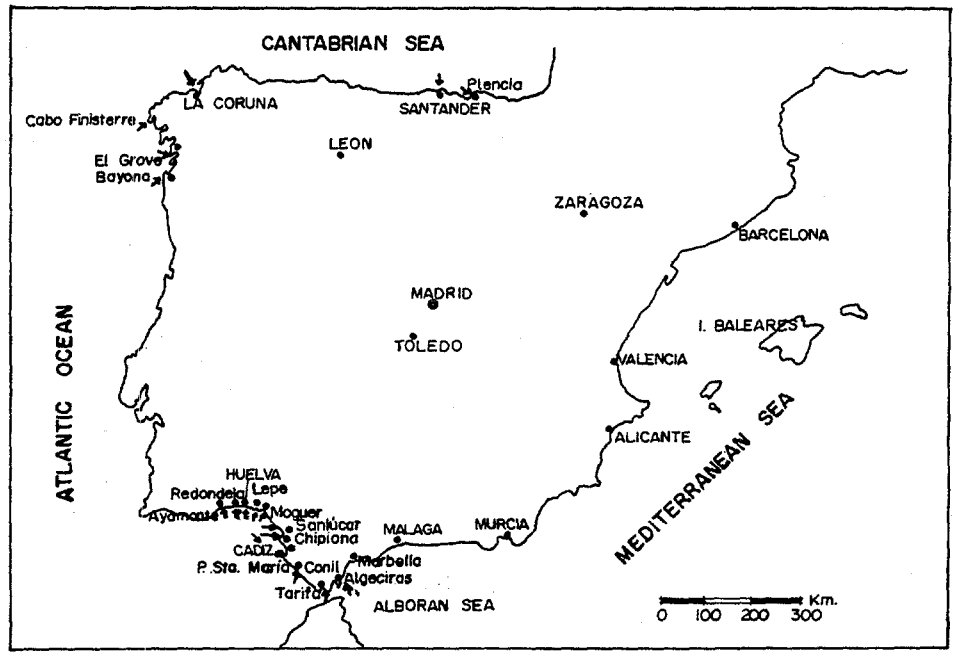

Figure 2.- Spanish sites affected by the Tsunami of the 1 st November 1755. (Source: Royal Academy of History 1756)

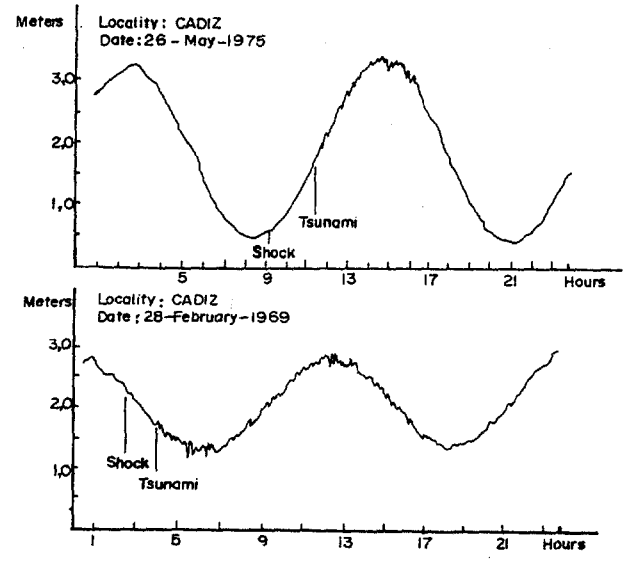

Figure 3.- Cadiz's mareograms of the Tsunamis of 1975 & 1969. (Source: Oceanographic Spanish Institute 1989)

A Cumulative Subject Index to The Science of Tsunami Hazards, The Journal of the Tsunami Society

George D. Curtis,
Publisher

All contributions to the Journal, including this issue, have been categorized under one or more subjects. Except for the current issue, subjects were assigned after review of the paper; for this issue authors adhered to the request to provide subjects and keywords.

The index is maintained in a database program, which includes up to four keywords for future or special retrieval usage. Subjects were limited to nine, but will be expanded in the future if warranted. Authors are invited to suggest differing or additional subject listings for their papers for the next index.

A cumulative chronological index was published in Volume 7, No. 2.

In the listings which follow, the first author, year, volume, and number are given. In a future issues, a complete author index will be provided and if space permits, an updated chronological and subject index will be included.

Science of Tsunami Hazards
The International Journal of
The Tsunami Society
Subject Index

Title	Author	Reference
COASTAL		
A Tsunami Avoidable Susceptability Index	Morgan, J.	2:1, 1984
Fractal Dimension and Length of an Irregular Coastline: Application to the St. Lawrence Estuary	El-Sabh, M. I.	3:1, 1985
Tsunami Flood Level Predictions for American Samoa	Houston, J. R.	3:1, 1985
Height Distribution of the Tsunami Generated by the Nihonkai-Chubu Earthquake	Kajiure, K.	4:1, 1986
Hydromatic Nature of Disasters by the Tsunamis of the Japan Earthquake of May 1984	Iwasaki, T.	4:2, 1986
Comparison of Observed and Numerically Calculated Heights of the 1983 Japan Sea Tsunami	Tsuji, Y.	4:2, 1986
On Audible Tsunami on the Coast	Nakamura, S.	6:1, 1988
Maximum Tsunami Amplitudes and Associated Currents on the Coast of British Columbia	Dunbar, D.	7:1, 1989
Numerical Simulation of Slide Generated Water Waves	Harbitz, C.	9:1, 1991
The Identification of Tsunami Deposits in Coastal Sediment Sequences	Dawson, A. G.	9:1, 1991
EARTHQUAKE		
Tsunamigenic Earthquakes in China 1831 B.C. to 1980 A.D.	Qinghai, Z.	4:3, 1986
Sanak-Kodiak Tsunami of 1788	Soloviev, S. L.	8:1, 1990
PROPAGATION		
Cylindrical Solitons Passing Through a Focus	Pelinovsky, E.	1:1, 1982
Non-linear and Dispersive Effects for Tsunami Waves in the Open Ocean	Mirchina, N. R.	1:1, 1982
The Influence of the Earth's Rotation on the Energy Characteristics of Tsunami Waves	Volt, S. S.	4:1, 1986
Numerical Simulation of the Tsunami of June 23, 1946	Murty, T. S.	4:1, 1986
Effect of Bathymetric Roughness Upon Tsunami Travel Time	Holloway, G.	4:3, 1986
Propagation of Tsunami Waves Generated by Elliptical Sources	Galkin, V. M.	4:3, 1986
The Foreslope Hills of the Eraser Delta: Implications for Tsunamis in Georgia Strait	Hamilton, T. S.	5:1, 1987
Calculations of Tsunami Travel Time Charts in the Pacific Ocean--Models, Algorithms, Techniques, Results	Shokin, Y. I.	5:2, 1987
Mathematical Simulation of Tsunami Excitation by Dislocations of Ocean Bottom	Dotsenko, S. F.	6:1, 1988

Title	Author	Reference
RUNUP		
Tsunami Flood Level Predictions for American Samoa	Houston, J. R.	3:1, 1985
Comparison of Observed and Numerically Calculated Heights of the 1983 Japan Sea Tsunami	Tsuji, Y.	4:2, 1986
A Study of Numerical Techniques on Tsunami Propagation and Runup	Shuto, N.	4:2, 1986
Design and Development of a Coastal Tsunami Gauge	Curtis, G. D.	4:3, 1986
Numerical Tsunami Flooding Study-	Mader, C. L.	8:2, 1990
Modelling of Tsunami Generation and Runup	Bundgaard, H. I.	9:1, 1991
SEISMIC		
Hurst Phenomenon in Tsunamigenic Earthquake Data	Murty, T. S.	2:1, 1984
National Geophysical Data Center Databases Supporting Investigations of Geological Hazards	Lockridge, P. A.	2:1, 1984
Tsunamis and Earthquake Mechanisms in the Island Arc Regions	Chubarov, L. V.	3:1, 1985
Tsunamigenic Earthquakes in the Pacific and the Japan Sea	Koyama, J.	4:2, 1986
Activity of Tsunamigenic Earthquakes Around the Pacific	Iida, K.	4:3, 1986
Generation, Wave Form, and Local Impact of the September 19, 1985 Mexican Tsunami	Farrera, S. F.	5:1, 1987
The Novel Seismic Source Mechanism of the 7 May 1986 Tsunami	Adams, W. M.	5:1, 1987
Rapid Sizing of Potentially Tsunamigenic Earthquakes at Regional Distances in Alaska	Whitmore, P. M.	5:2, 1987
Coastal Algerian Earthquakes: A Potential Risk of Tsunamis in Western Mediterranean?	Chaouche, A. Y.	9:1, 1991
Theoretical and Experimental Tsunamigenic Models to Study Inland Active Geostructures	Finzi-Contini, G.	9:1, 1991
SOURCE		
Parameters of Tsunami Waves in the Source	Mirchina, N. P.	1:1, 1982
Propagation of Tsunami Waves Generated by Elliptical Sources	Galkin, V. M.	4:3, 1986
Coastal Algerian Earthquakes: A Potential Risk of Tsunamis in Western Mediterranean?	Chaouche, A. Y.	9:1, 1991

Title	Author	Reference
GENERAL		
The All-Union Meeting on Tsunamis in Yuzhno-Sakhalinsk	Soloviev, S. L.	2:1, 1984
Probable Aleutian Source of the Tsunami Observed in August 1872 in Hawaii, Oregon, and California	Cox, D. C.	2:2, 1984
A Working Vocabulary for Tsunami Study	Adams, W. M.	3:1, 1985
All-Union Conference on Tsunami Problems in Gorky	Soloviev, S. L.	4:2, 1986
Spectral Analysis of Mareograms from Urup Tsunamis of 13 and 20 October 1963	Soloviev, S. L.	5:1, 1987
Some Tsunami Memories	Zetler, B. D.	6:1, 1988
Memoriam to Sergei Sergeevich Voit (1920-1987)	Soloviev, S. L.	7:1, 1989
Survey of Research Studies and Technological Development of Tsunami in USSR in 1987-1989	Soloviev, S. L.	8:1, 1990
Fourteenth International Tsunami Symposium Novosibirsk, USSR, July 31-August 3, 1989	Bernard, E. N.	8:1, 1990
Cumulative Index	Curtis, G.	9:1, 1991
HAZARD		
Landslides and Mudflows in a Young Volcanic Hawaiian Type Structure	Dupon, J. F.	2:1, 1984
Design and Development of an Intelligent Digital System for Computer-Aided Decision-Making During Natural Hazards	Adams, W. M.	2:2, 1984
A Tsunami Preparedness Assessment for Alaska	Carte, G. W.	2:2, 1984
Needs and Developments in Tsunami Monitoring	Curtis, G. D.	3:1, 1985
Hydromatic Nature of Disasters by the Tsunamis of the Japan Earthquake of May 1984	Iwasaki, T.	4:2, 1986
Generation, Wave Form, and Local Impact of the September, 19, 1985 Mexican Tsunami	Farrera, S. F.	5:1, 1987
The Foreslope Hills of the Eraser Delta: Implications for Tsunamis in Georgia Strait	Hamilton, T. S.	5:1, 1987
Introduction: Tsunamis Generated by Earthquake and Volcanic Eruptions	Tinti, S.	6:1, 1988
Data for Investigating Tsunami Activity in the Mediterranean Sea	Antonopoulos, J.	8:1, 1990
A Preliminary Evaluation of the Tsunami Hazards in the Moroccan Coasts	El Alami, S. O.	9:1, 1991
Tsunami Hazard on the Spanish Coasts of the Iberian Peninsula	Campos, M. L.	9:1, 1991
Tsunami Potential in Southern Italy	Tinti, S.	9:1, 1991
HEIGHT		
Height Distribution of the Tsunami Generated by the Nihonkai-Chubu Earthquake	Kajiure, K.	4:1, 1986

Title	Author	Reference
HISTORY		
National Geophysical Data Center Databases Supporting Investigations of Geological Hazards	Lockridge, P. A.	2:1, 1984
Extreme Values of Tsunami Magnitudes	Koyama, J.	4:1, 1986
The Great Waves by Douglas Myles	Mader, C. L.	4:2, 1986
Tsunamigenic Earthquakes in China 1831 B. C. to 1980 A. D.	Qinghai, Z.	4:3, 1986
Tsunami! Hawaii's Own Dramatic Stories and the Facts About the Giant Waves by Walt Dudley and Min Lee	Curtis, G. D.	5:2, 1987
Introduction: Tsunamis Generated by Earthquake and Volcanic Eruptions	Tinti, S.	6:1, 1988
A Review of the Historical 1627 Tsunami in the Southern Adriatic	Guidoboni, E.	6:1, 1988
Revision of the Tsunamis Occurred in 1783 in Calabria and Sicily (Italy)	Tinti, S.	6:1, 1988
The Tsunami Generated From Eruption of the Volcano of Santorin in the Bronze Age	Pararas-Carayannis, G.	6:1, 1988
Historical and Recent Tsunamis in the European Area	Moreira, V. S.	6:1, 1988
The Largest Historical Tsunamis in the Northern Adriatic Sea: A Critical Review	Guidoboni, E.	7:1, 1989
Data for Investigating Tsunami Activity in the Mediterranean Sea	Antonopoulos, J.	8:1, 1990
Sanak-Kodiak Tsunami of 1788	Soloviev, S. L.	8:1, 1990
A Preliminary Evaluation of the Tsunami Hazards in the Moroccan Coasts	El Alami, S. O	9:1, 1991
The Identification of Tsunami Deposits in Coastal Sediment Sequences	Dawson, A. G.	9:1, 1991
MAGNITUDE		
Hurst Phenomenon in Tsunamigenic Earthquake Data	Murty, T. S.	2:1, 1984
Use of the Abe Magnitude Scale by the Tsunami Warning System	Blackford, M. E.	2:1, 1984
Tsunamis and Earthquake Mechanisms in the Island Arc Regions	Chubarov, L. V.	3:1, 1985
Extreme Values of Tsunami Magnitudes	Koyama, J.	4:1, 1986
Tsunamigenic Earthquakes in the Pacific and the Japan Sea	Koyama, J.	4:2, 1986
The Novel Seismic Source Mechanism of the 7 May 1986 Tsunami	Adams, W. M.	5:1, 1987

Title	Author	Reference
Modelling of Tsunami Generation and Runup	Bundgaard, H. I.	9:1, 1991
Theoretical and Experimental Tsunamigenic Models to Study Inland Active Geostructures	Finzi-Contini, G.	9:1, 1991
WARNING		
Design and Development of an Intelligent Digital System for Computer-Aided Decision-Making During Natural Hazards	Adams, W. M.	2:2, 1984
A Tsunami Preparedness Assessment for Alaska	Carte, G. W.	2:2, 1984
The Alaska Tsunami Warning Center's Responsibilities and Operations	Sokolowski, T.	3:1, 1985
Real-time Monitoring and Modelling for Tsunami Threat Evaluation	Curtis, G. D.	5:1, 1987
Rapid Sizing of Potentially Tsunamigenic Earthquakes at Regional Distances in Alaska	Whitmore, P. M.	5:2, 1987
Basic Improvement of Tsunami Warning Systems of Previous Experiences	Adams, W. M.	6:1, 1988
Tsunami Hazard on the Spanish Coasts of the Iberian Peninsula	Campos, M. L.	9:1, 1991
WAVES		
Storm Surges--Meteorological Ocean Tide by T. S. Murty	Adams, W. M.	4:1, 1986
Wave Force of Tsunami Bore on a Vertical Wall	Togashi, H.	4:1, 1986
An Explanation of Characteristics Distribution of the Tsunami Maximum Inundation Heights Observes at Small Islands	Abe, K.	4:3, 1986
Numerical Tsunami Flooding Study-1	Mader, C. L.	8:2, 1990
Numerical Model on Tsunami Propagation	Karambas, T. V.	9:1, 1991
Maximum Tsunami Amplitudes and Associated Currents on the Coast of British Columbia	Dunbar, D.	7:1, 1989
MODEL		
A Model of the 1975 Hawaii Tsunami	Mader, C. L.	1:1, 1982
Numerical Modelling of Tsunami Flooding	Adams, W. M.	1:1, 1982
A Numerical Tracking of the 1883 Krakatoa Tsunami	Nakamura, S.	2:1, 1984
Developing of a Tsunami-Flooding Model Having Versatile Formulation of Moving Boundary Conditions	Lewis, C. H.	Monograph, 1983
Importance of Local Contemporary Reports of Effects of Historical Tsunamis in Tsunami Risk Analysis	Cox, D. C.	2:2, 1984
A Landslide Model for the 1975 Hawaii Tsunami	Mader, C. L.	2:2, 1984
Verification, Calibration and Quality Assurance for Tsunami Models	Adams, W. M.	2:2, 1984
Tsunami Flood Level Predictions for American Samoa	Houston, J. R.	3:1, 1985

Title	Author	Reference
Numerical Simulation of the Tsunami of June 23, 1946	Murty, T. S.	4:1, 198
Storm Surges--Meteorological Ocean Tide by T. S. Murty	Adams, W. M.	4:1, 198
Wave Force of Tsunami Bore on a Vertical Wall	Togashi, H.	4:1, 198
A Study of Numerical Techniques on Tsunami Propagation and Runup	Shuto, N.	4:2, 198
An Explanation of Characteristics Distribution of the Tsunami Maximum Inundation Heights Observed at Small Islands	Abe, K.	4:3, 198
Real-time Monitoring and Modelling for Tsunami Threat Evaluation	Curtis, G. D.	5:1, 198
Numerical Computation of Tsunami Runup by the Upstream Derivative Method	Kowalik, Z.	5:2, 198
Numerical Modelling of Water Waves by Charles L. Mader	Murty, T. S.	5:2, 198
Mathematical Simulation of Tsunami Excitation by Dislocations of Ocean Bottom	Dotsenko, S. F.	6:1, 198
Tsunami Induced Oscillations in Corinthos Bay Measurements and 1-D vs. 2-D Mathematical Models	Koutitas, C.	6:1, 198
Numerical Simulation of Tsunami Amplitudes on the Coast of British Columbia Due to Local Earthquakes	Ng, M.	8:2, 199
Numerical Tsunami Flooding Study-1	Mader, C. L.	8:2, 1990
Travel Time Charts for the Caribbean	Weissent, T. P.	8:2, 1990
Modelling of Tsunami Generation and Runup	Bundgaard, H. I.	9:1, 1991
Numerical Model on Tsunami Propagation	Karambas, T. V.	9:1, 1991
Numerical Simulation of Slide Generated Water Waves	Harbitz, C.	9:1, 1991
MONITORING		
Establishment and Operation of a Tsunami Monitoring Program	Curtis, G. D.	1:1, 1982
Needs and Developments in Tsunami Monitoring	Curtis, G. D.	3:1, 1985
New Tsunami Recorders at Wake Island	Van Dorn, W. G.	4:1, 1986
Design and Development of a Coastal Tsunami Gauge	Curtis, G. D.	4:3, 1986
Real-time Monitoring and Modelling for Tsunami Threat Evaluation	Curtis, G. D.	5:1, 1987
On Audible Tsunami on the Coast	Nakamura, S.	6:1, 1988

THE TSUNAMI SOCIETY

SCIENCE OF TSUNAMI HAZARDS

Publication Format for Camera-Ready Copy and Information for Authors:

1. Typing area shown by border.

2. One-column text.

3 All text must be typed single-space. Indent 5 spaces to start a new paragraph.

4. Page numbers in lower right hand corner in pencil or blue marker.

5. Top half of first page to contain the title in capitals, followed by the authors and author affiliation, centered on page.

6. Bottom half of first page to contain the abstract with the heading ABSTRACT centered on page.

7. Author must also enclose a separate sheet containing:
   - name and mailing address of senior author
   - one or two suggested index subjects
   - three to five keywords for cataloging
   - statement of any other submittal, publication, or presentation

8. Send original and a copy, with above information, to:

Dr. Tad Murty, Editor
Institute of Ocean Sciences
Box 6000
Sidney, B.C., V8L 4B2
CANADA

10" or 25 cm

7½" or 19 cm

APPLICATION FOR MEMBERSHIP

THE TSUNAMI SOCIETY
P.O. Box 8523
Honolulu, Hawaii 96815, USA

I desire admission into the Tsunami Society as: (Check appropriate box.)

☐ Student ☐ Member ☐ Institutional Member

Name _____ Signature _____

Address _____ Phone No. _____

_____

Zip Code _____ Country _____

Employed by _____

Address _____

Title of your position _____

FEE: Student $5.00 Member $25.00 Institution $100.00

Fee includes a subscription to the society journal: SCIENCE OF TSUNAMI HAZARDS.

Send dues for one year with application. Membership shall date from 1 January of the year in which the applicant joins. Membership of an applicant applying on or after October 1 will begin with 1 January of the succeeding calendar year and his first dues payment will be applied to that year.